ROYAL SOCIETY
OF CHEMISTRY

REVIEW

Check for updates

Triphenylene as a versatile scaffold for advanced functional materials

Ehsan Ullah Mughal, [ID] *[a] Nafeesa Naeem, [ID] [a] Ayza Jabeen,[a] Farwa Zainab,[a] Amina Sadiq[b] and Kenneth E. Maly [ID] *[c]

Triphenylenes are a class of polycyclic aromatic hydrocarbon that have been attracting increasing attention owing to their widespread applications in areas such as liquid crystals, organic electronics, photovoltaics, light emitting diodes, and catalysts. The utility of triphenylenes stems from their flatness, rigidity, and aromatic nature. This review provides an exploration of triphenylene derivatives, with an emphasis on recent advancements in their synthesis, properties, and multifaceted applications. Highlighting their synthetic strategies, we discuss both classical methods and modern approaches, including metal-catalyzed reactions and photochemical techniques, which have enabled the development of a wide range of substituted triphenylenes, as well as their dimers, trimers, twinned molecules, and oligomers. The electronic structure of triphenylene, characterized by a delocalized π-electron system, underpins its remarkable charge transport properties. In terms of applications, triphenylene-based liquid crystals are particularly notable for forming columnar mesophases with highly ordered structures, facilitating advantageous macroscopic molecular orientation. These properties underscore its potential for next-generation functional materials across diverse domains, including organic electronics, photovoltaics, light-emitting diodes, and catalysis. By integrating insights into its properties and future potential, this review aims to provide a valuable resource for researchers investigating triphenylene and its derivatives.

1. Introduction

Triphenylene **1** (Fig. 1), also known as isochrysene, 1,2,3,4-dibenzonaphthalene, and 9,10-benzophenanthrene,[1] is a polycyclic aromatic hydrocarbon that is of interest in organic chemistry and materials science. It is a planar, aromatic, symmetrical hydrocarbon having molecular formula $C_{18}H_{12}$. It was first isolated from the pyrolytic decomposition products of benzene by Schultz, who named the compound "triphenylene".[1] The most detailed review to date was authored by Buess and Lawson, published approximately six decades ago, which provided extensive insights into the compound's structure, synthetic routes, chemical reactivity, and potential applications.[1] The X-ray crystal structure of triphenylene was first determined by Banerjee and Guha in 1937, revealing its planar molecular structure and orthorhombic crystal lattice.[2] Triphenylene itself packs in a herringbone motif featuring offset π-stacking and C–H···π interactions,[2] the intermolecular packing can be influenced by adding substituents to the ring.[3] The stability of triphenylene compared to its isomers; chrysene,

benzo[a]anthracene, benzo[c]phenanthrene, and tetracene can be explained in terms of the Clar sextet rule, which is used to evaluate the aromatic stability of polycyclic aromatic hydrocarbons (PAHs).[4] According to this rule, stability increases with the number of distinct benzene-like aromatic sextets (fully delocalized π-electrons within a six-membered ring) that can be drawn in the structure without overlapping π-electrons.[5] Triphenylene can accommodate three Clar sextets, each located in one of its outer benzene rings, without any overlap of π-electrons. The presence of additional Clar sextets in triphenylene results in greater aromatic stabilization compared to its isomers, highlighting its enhanced thermodynamic stability.[6] It has twelve positions for substitution, peripheral sites including 2, 3, 6, 7, 10 and 11 are most common (Fig. 1). Triphenylene
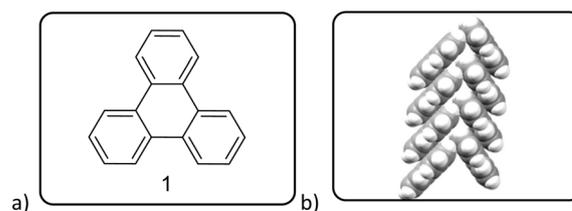
[a]Department of Chemistry, University of Gujrat, Gujrat-50700, Pakistan. E-mail: ehsan.ullah@uog.edu.pk

[b]Department of Chemistry, Govt. College Women University, Sialkot-51300, Pakistan

[c]Department of Chemistry and Biochemistry, Wilfrid Laurier University, Waterloo, Ontario N2L 3C5, Canada. E-mail: kmaly@wlu.ca

Fig. 1 (a) Structural representation of triphenylene scaffold **1** 2D structure,[9] (b) Herringbone packing arrangement of triphenylene molecules in the crystal lattice. Reproduced from ref. 9 with permission from International Union of Crystallography, copyright 1963.

molecules exhibit exceptional stacking behavior, primarily governed by their planar aromatic structure and the nature of peripheral functional groups. These functional groups extend laterally from the core, forming lateral chains that influence intermolecular interactions and molecular organization. The type of intermolecular interactions induced by these substituents includes π–π stacking and van der Waals forces, both of which play a crucial role in the formation of well-ordered columnar assemblies. Alkoxy (–OR) groups, while electron-donating and often leading to electron-rich aromatic systems, can actually reduce the strength of π–π stacking interactions due to increased electronic repulsion between π-systems. However, in many liquid crystals, the observed columnar stacking is believed to arise from micro segregation between the rigid aromatic cores and the flexible alkyl or alkoxy chains, promoting phase-separated self-assembly and stabilizing columnar mesophases.[7,8]

The lateral chains also improve solubility and influence molecular packing, directly impacting the material's charge transport and optoelectronic properties. These attributes make triphenylene a versatile scaffold for applications in organic electronics, photovoltaics, and advanced functional materials.

Triphenylene's geometry, comprised of one central benzene ring and three nonadjacent benzene rings,[10] has led to a vast range of properties and uses such as luminescence,[11] 1D charge migration,[12] 1D energy migration,[13] liquid crystalline nature,[14,15] ferroelectric switching,[16] self-assembling nature,[17] organic light-emitting-diodes,[18] liquid crystal display (LCD) application,[19] catalysis,[20] as chemo-sensors for the detection of ions[21] and as transporting materials in solar cells.[22] The polycyclic compound and its derivatives due to their various applications have been the major factor behind the progress of electronics, materials science, and nanotechnology.[23,24] The crystalline structure of triphenylene that is well-defined supports its capability to create stable and highly conductive films, which makes it a strong candidate for the development of next-generation optoelectronics and organic electronics where efficient charge transport is the result of ordered molecular packing.[25,26] The extended π-system and peripheral substituents also allow it to act as a molecular receptor, interacting with the guests.[27,28]

The transfer of charge between molecules has been enhanced thanks to the 2D planar geometry and also the π-conjugated system.[29,30] Moreover, triphenylene's physicochemical properties are crucial for its practical applications. Triphenylene is usually characterized by low solubility in polar solvents, such as water[31] because of its strong aromatic interactions and non-polar character; thus, it creates various difficulties especially in methods that require solution-based processing or monitoring the environment through aqueous sensors.[32,33] The solubility, however, can be made to increase substantially by attaching various functional groups at the edge like alkyl chains, alkoxy groups, and other polar substituents.[34]

Triphenylene derivatives are extensively studied in the context of discotic liquid crystals (DLCs). The core structure of most DLCs is made up of three characteristics: flatness, rigidity, and an aromatic character.[14,35] Flexible chains are then attached to the core, which act as its outer layers. A large number of

symmetrical and unsymmetrical derivatives have been studied and these compounds frequently self-assemble to form columnar mesophases.[36] In addition to this, they also focused on the "twinned" and "oligomeric" triphenylene structures to add more value and function.[37,38] The connection of the discotic units with a flexible spacer of the right length leads to the forming of this columnar mesophase, while a rigid space results in the nematic phase.[39,40]

The methods outlined in previous reviews[41,42] focus on synthetic methods applicable to triphenylene derivatives. Nevertheless, the current review consists of a new view of triphenylene and its functionalized derivatives, pointing out synthetic paths, structural characteristics, and wide applications. In this case, classical and modern synthetic methods are considered, and the latest developments are presented as a means to produce the exact functionalization and create derivatives with customized properties.

This review also highlights the applications of triphenylene derivatives. Applications in liquid crystals and organic electronics rely on the electronic properties and self-assembly of triphenylenes, while sensing applications rely on their photophysical properties. Furthermore, their rigid structure and 3-fold symmetry make these compounds well-suited as molecular scaffolds for other functional materials.

2. Syntheses of triphenylene derivatives

2.1. A historical approach

Several synthetic strategies were developed for triphenylene synthesis. The earliest synthesis was devised by Mannich, when cyclohexanone was treated with methyl alcoholic sulfuric acid, relatively small yield of dodecahydrotriphenylene was obtained which was then dehydrogenated with selenium to obtain triphenylene.[43] Since its initial discovery, extensive research has been conducted on the structure and synthesis of triphenylene and its derivatives. The first review of triphenylenes focused on their synthesis, reactivity, and properties, was written by Buess and Lawson in 1960.[1] Forty years later, Perez and Guitian surveyed multiple methods to synthesize substituted triphenylene and their benzo-derivatives.[41] This review aims to consolidate and summarize the significant body of work in these areas, offering an overview of the advances made in understanding and utilizing this versatile class of compounds. Terphenyl is the most frequently used precursor for the synthesis of triphenylenes, using methods including oxidative cyclization,[44] photocyclization,[45] Cu-mediated Ullman coupling reaction or palladium catalyzed cross-coupling reaction employing aryl boronic acids.[46] Starting from biphenyl, traditional methods include Diels Alder cycloaddition,[47] oxidative cyclization,[48] palladium-catalyzed coupling. These methods suffer from drawbacks such as over-oxidation, aggressive reagents and low solubility of oxidants; regioselectivity problems, harsh conditions and limited substrate scope.

While some of the traditional synthetic approaches to triphenylene derivatives remain in use, the development of
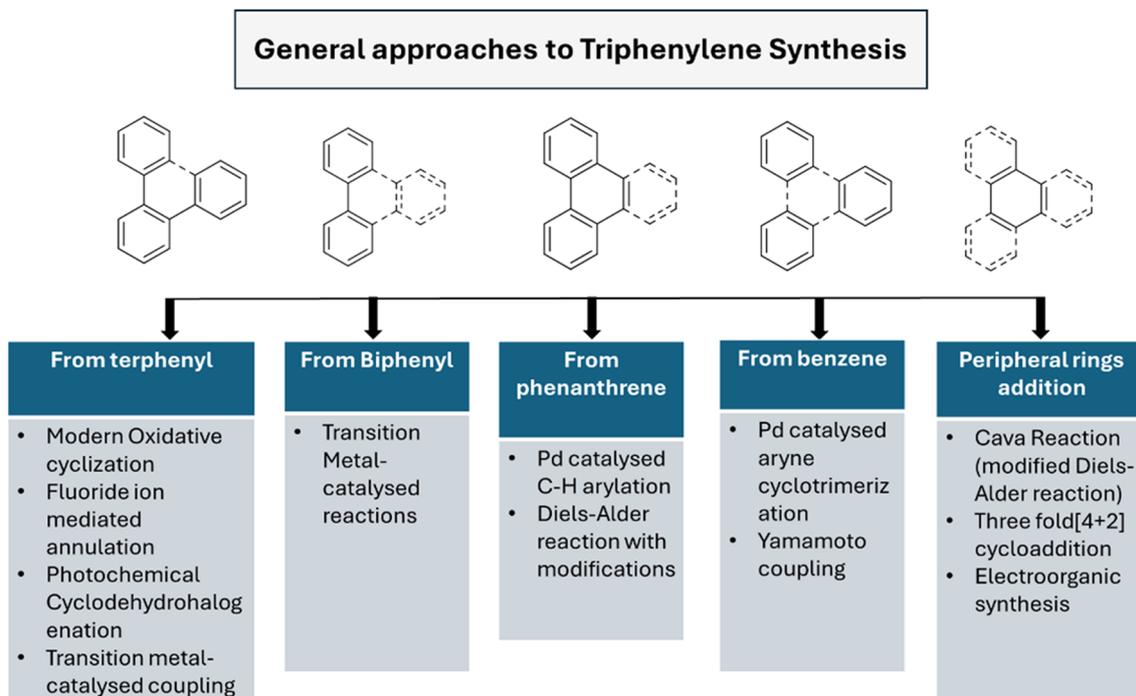
Fig. 2 Conventional and modern methods to convert different precursors into triphenylene.

synthetic methods has led to new approaches to this class of compounds. As shown in Fig. 2, these methods generally involve constructing triphenylenes from simpler aromatic precursors, offering several different ways to access triphenylenes.

2.2. Modern approaches (2005–2024)

2.2.1. From terphenyl compounds. The synthesis of triphenylene from terphenyl compounds typically involves the cyclization of the central phenyl ring to form the extended aromatic core. This transformation is conventionally achieved using oxidative coupling or dehydrogenation reactions, often by strong oxidizing agents such as ferric chloride ($FeCl_3$) or copper salts under high-temperature conditions (Fig. 3).[49] These classical oxidative cyclizations are collectively known as the Scholl

Fig. 3 Conventional and modern methods of triphenylene synthesis from o-terphenyl.

reaction, which promotes C–C bond formation through intramolecular oxidative cyclodehydrogenation. While $FeCl_3$ and $MoCl_5$ are commonly used oxidants[50] for the classical Scholl reaction, alternative oxidative cyclization conditions, such as DDQ (2,3-dichloro-5,6-dicyano-1,4-benzoquinone) with methanesulfonic acid,[51] have also been employed to achieve efficient ring closure.[52]

Recent approaches involve modern oxidative cyclization strategies with improved functional group compatibility and milder reaction conditions. Dehydrogenative cyclization and oxidative cyclodehydrogenation are synonymous terms that describe oxidative ring-closing accompanied by dehydrogenation. These reactions offer unique advantages depending on the desired application. Some other innovative synthetic approaches are fluoride ion-mediated annulation,[53] oxidative biaryl coupling using Cerium Ammonium Nitrate (CAN),[54] photochemical cyclodehydrohalogenation.[55]

One of the milder approaches to triphenylenes by Rathore and coworkers involves oxidative cyclodehydrogenation using DDQ (3) in the presence of methanesulfonic acid (Scheme 1).[51] This method is a variant of the classical Scholl reaction, which promote C–C bond formation through oxidative cyclization of o-terphenyls and hexaarylbenzenes.[56,57] In this method, o-terphenyl **2** in dichloromethane/methanesulfonic acid was treated with 1 equiv. of DDQ at 0 °C under argon. The reaction turned from green to dark brown within minutes, and after aqueous workup, triphenylene **5** was obtained in quantitative yield.[51] The method is milder than traditional $FeCl_3$-based protocols and allows easy recovery of the reduced DDQ byproduct via bicarbonate extraction, making it both efficient and practical.
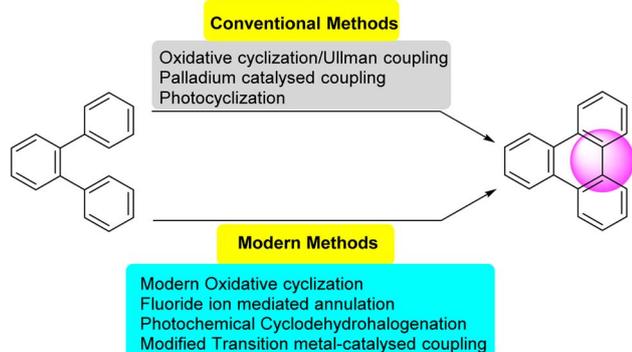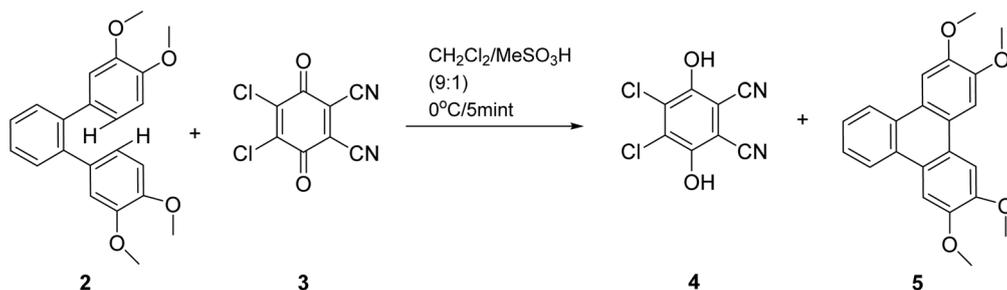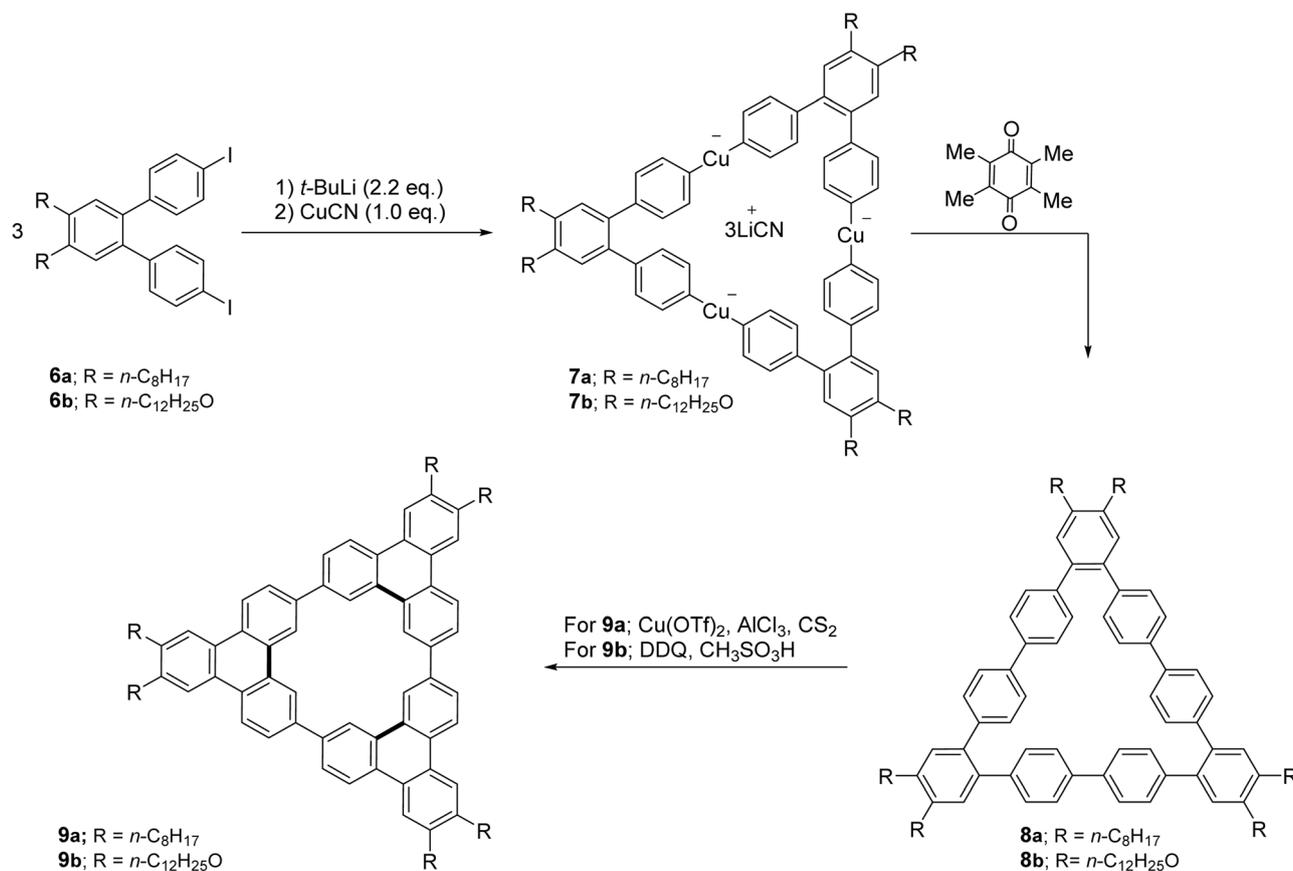
Scheme 1 Oxidative cyclodehydrogenation using DDQ and methanesulfonic acid. Reproduced from ref. 51 with permission from American Chemical Society, copyright 2010.

Several research groups extended oxidative cyclization strategies to complex macrocyclic frameworks. For example, cyclic nonaphenylenes **8** and dodecaphenylenes can be prepared by electron transfer oxidation of Lipshutz cuprates with duroquinone.[58] Subsequent dehydrogenative cyclization by treating with $Cu(OTf)_2$ and $AlCl_3$ in CS_2 with 73% yield or by using DDQ and CH_3SO_3H in dichloromethane can yield the corresponding triphenylene macrocycle **9** as illustrated in Scheme 2.[59] These carbocyclic conjugated molecules **9** with long alkyl and alkoxy chains exhibit amphiphilic properties, phase separation, and supramolecular self-aggregation, allowing them to self-associate into oligomers in both solution and the solid state. Their shape-persistent π-frames make them highly suitable for designing advanced organic materials.

Oxidative biaryl coupling using ceric ammonium nitrate (CAN) is the facile, safer and mild method to synthesize substituted triphenylene and their derivatives as compared to strategies using other oxidants such as $FeCl_3$, $CuCl_2$ or $Cu(OTf)_2$ with $AlCl_3$ in CS_2, $MoCl_5$ with or without $TiCl_4$ in CH_2Cl_2.[60,61] Gupta and coworkers demonstrated Scholl reactions employing CAN which can act as an oxidant as well as Lewis acid can convert various *o*-terphenyls to triphenylene (Scheme 3).[54] This CAN mediated Scholl reaction showed tolerance for a broad range of functional groups and heteroaromatic system gave good to excellent yield.


Scheme 2 Synthesis of cyclic triphenylene trimers (**9a–b**) by dehydrogenative cyclization. Reproduced from ref. 59 with permission from John Wiley and Sons, copyright 2013.
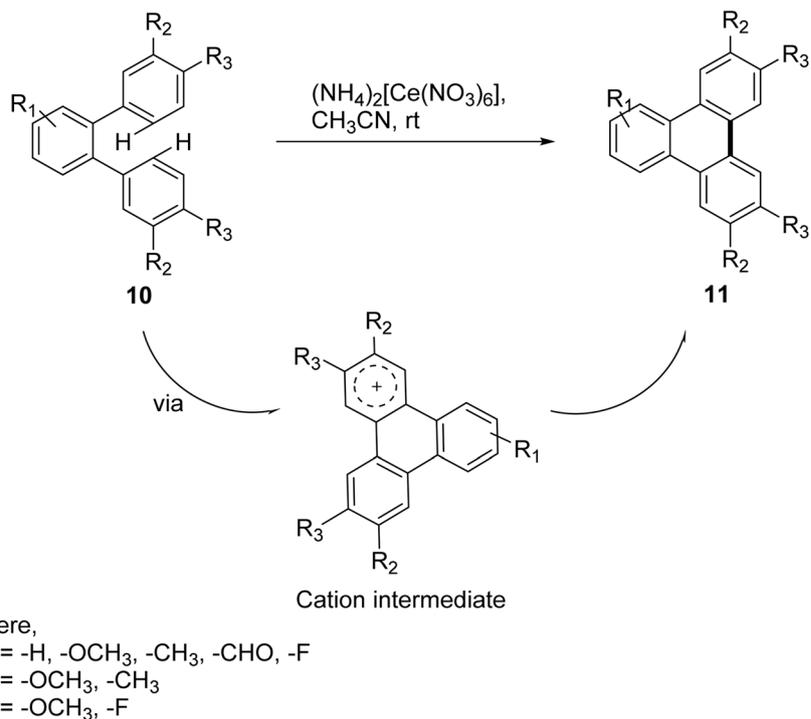
Scheme 3 Oxidative biaryl coupling of *o*-terphenyl to form **11**. Reproduced from ref. 54 with permission from Royal Society of Chemistry, copyright 2018.

In contrast, Kumar and coworkers at first reported the cyclization of terphenyl to triphenylene without using any oxidizing agent.[53] By using Suzuki–Miyaura coupling reaction, terphenyl derivatives **13** possessing *tert*-butyldimethylsilyl (OTBS) groups were synthesized (Scheme 4). Irreversible cyclization of terphenyl yields substituted triphenylene **14** induced
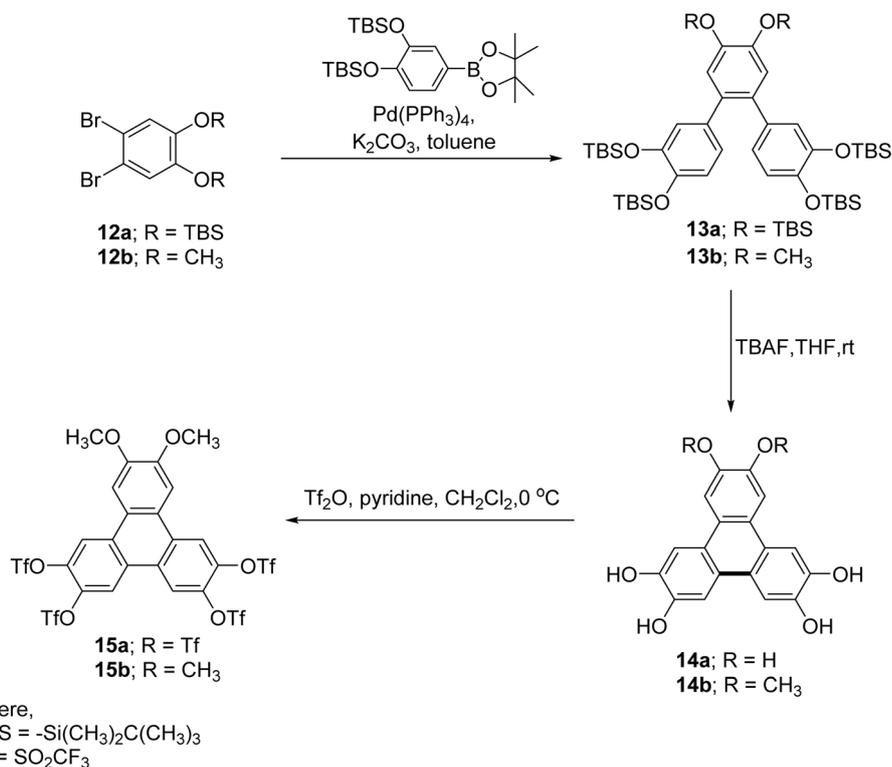
Scheme 4 Tetrahydroxy triphenylene **14** synthesis. Reproduced from ref. 53 permission from Royal Society of Chemistry, copyright 2013.
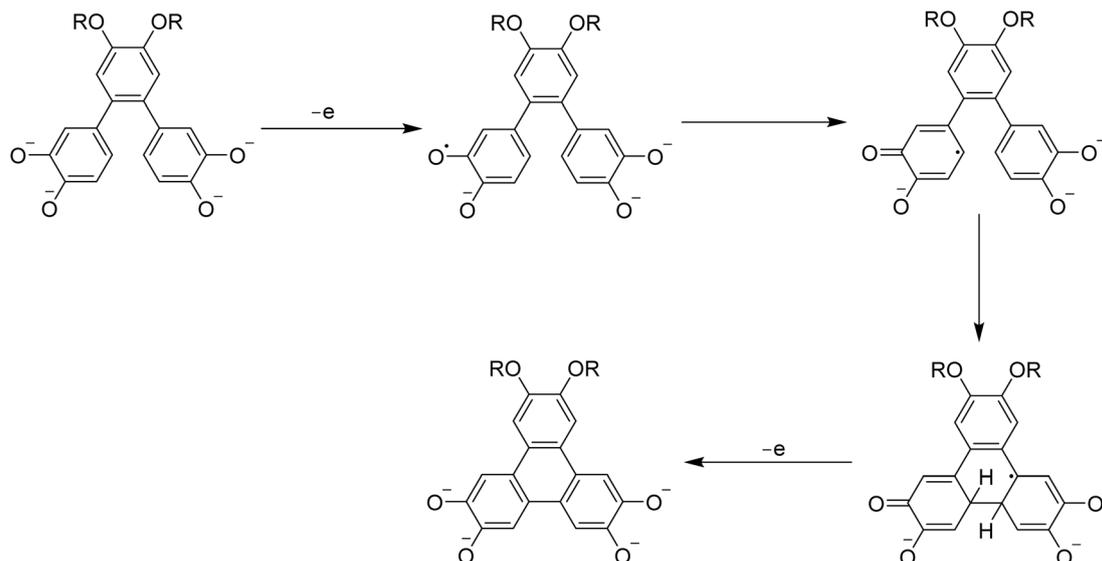
Scheme 5 Proposed mechanism for cyclization of terphenyl to triphenylene. Reproduced from ref. 53 permission from Royal Society of Chemistry, copyright 2013.

by fluoride ion along with deprotection of OTBS groups.[53] Mechanistically, the intermediate undergoes nucleophilic attack at the *ortho*-position of an adjacent aryl ring, promoting cyclization through an electrophilic rearrangement (Scheme 5). The reaction concludes with aromatization, yielding the triphenylene core with enhanced π-conjugation and planarity. This method provides a mild, oxidant-free approach for the selective formation of triphenylene derivatives with controlled substitution patterns. Thus methoxy-substituted *o*-terphenyl (**13a, b**) are successfully annulated to tetrahydroxy triphenylene derivatives (**14a, b**).

The fluoride-mediated triphenylene synthesis reported by Kumar was sensitive to substituents and was unsuccessful when methoxy groups were replaced by longer chains.[62] These factors combined likely led to decreased reaction efficiency when scaled up. As an alternative approach, they reacted the *o*-terphenyl compound **16** with DDQ in a mixture of dichloromethane/TFA by 10 : 1 to produce **17**, followed by deprotection of the TBS groups using KF and HBr to furnish 2,3-bis(hexyloxy)-6,7,10,11-tetrahydroxy triphenylene **18** in good yield (Scheme 6).

Photocyclization reactions have been widely employed in the synthesis of PAHs. In 1964, Mallory introduced the use of iodine

as a catalyst for the photochemical cyclization of stilbenes leading to the synthesis of phenanthrene.[63] This photocyclization approach has also been applied to the synthesis of triphenylenes.[45,64] The reaction is thought to proceed by a photochemical electrocyclic ring-closing reaction, followed by dehydrogenation. As such, an oxidant is required for the reaction. Building upon this, alternative photocyclization strategies have emerged in which halogenated terphenyls undergo elimination of HX after photocyclization. These methods avoid the need for an oxidant to form the fused aromatic system. For example, photochemical dyclodehydrochlorination (CDHC) of chloro-substituted terphenyl gives triphenylene in good yield.[65] Similarly, photocyclodehydrofluorination (PCDHF) involves photocyclization, followed by elimination of HF to produce triphenylenes. For example. Li and coworkers used fluorinated precursors and *o*-terphenyls in a PCDHF reaction to prepare fluorinated alkoxytriphenylene **24** which can be used as discotic liquid crystal (Scheme 7).[55] Crucial intermediate *o*-terphenyl was prepared by fluorinated biphenyl **19** (2,3,4,5,6-pentafluoro-2'-iodo-4',5'-dimethoxy-1',1'-biphenyl) and phenylboronic acid **20**, using Suzuki reaction. *o*-terphenyl underwent the PCDHF reaction to yield 1,2,3,4-tetrafluoro-6,7,10,11-tetraalkoxytriphenylene **22**. Deprotection of alkoxy group was
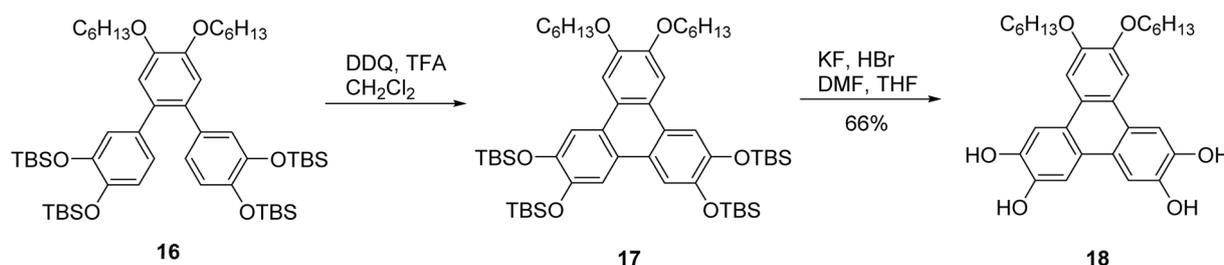
Scheme 6 Hexyloxy substituted tetrahydroxytriphenylene **18** derivatives. Reproduced from ref. 62 with permission from Royal Society of Chemistry, copyright 2014.

© 2026 The Author(s). Published by the Royal Society of Chemistry
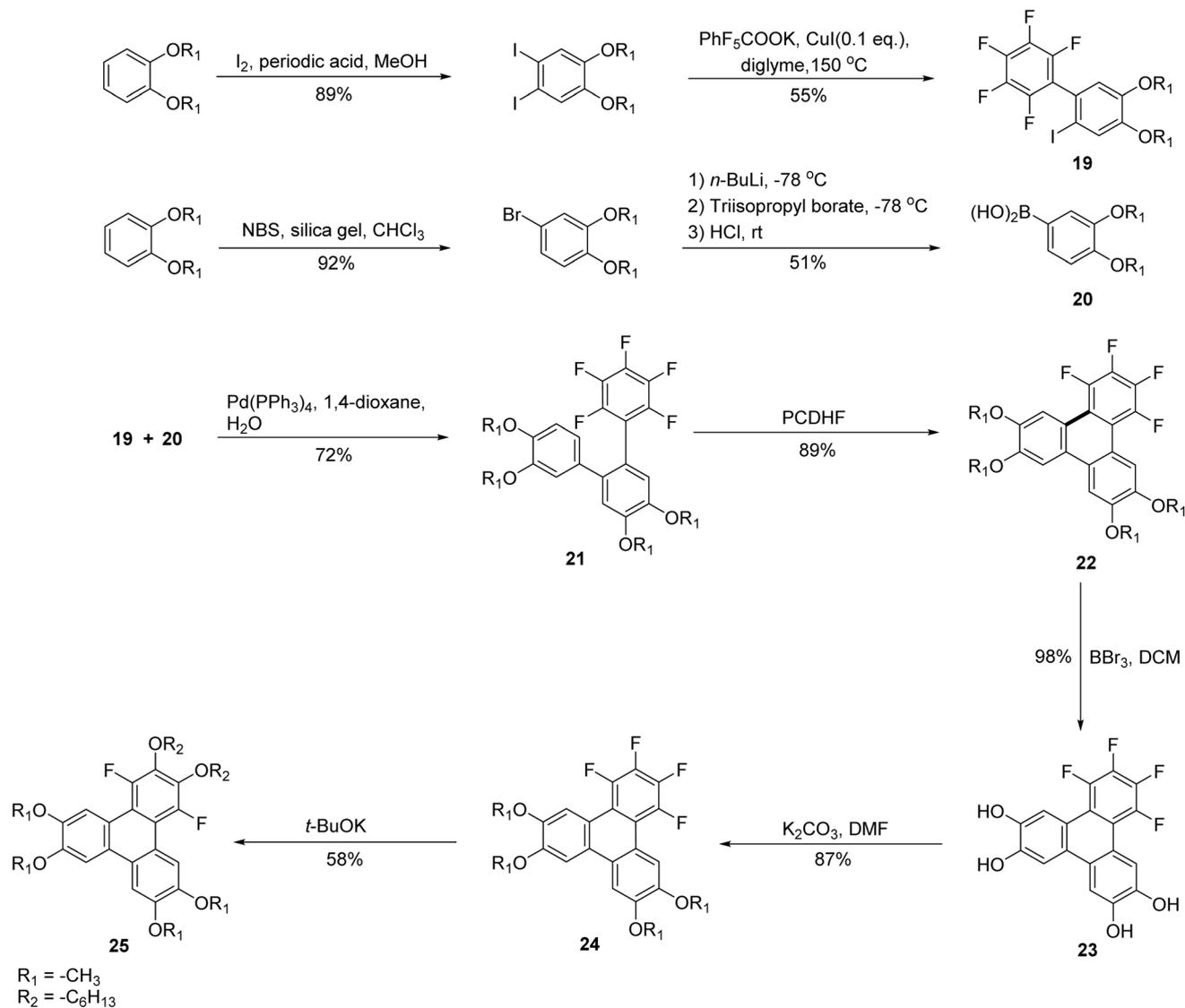
Scheme 7 Synthesis of fluorinated hexakisalkoxytriphenylene **25** discotic liquid crystals. Reproduced from ref. 55 with permission from Royal Society of Chemistry under a Creative Commons Attribution-NonCommercial 3.0 Unported Licence., copyright 2022.

done by BBr_3 and dichloromethane to yield **23**. It was then treated with alkyl halide and potassium carbonate to yield **24** which subsequently underwent S_NAr to produce **25** where fluorine atoms were replaced by alkoxy groups. This technique provided opportunity to control core fluorine and a alkoxy groups readily at different positions.[55] Remarkably, metal-free synthetic strategies have recently emerged as viable alternatives for constructing fluorinated triphenylene derivatives. For instance, Zhou and co-workers reported an efficient S_NAr-based, transition-metal-free approach to structurally related triphenylene systems, highlighting the growing potential of sustainable methodologies in this field.[66]

Morin and colleagues demonstrated that phenylsulfonates can serve as efficient photolabile groups for generating aryl radicals under light irradiation.[67] These radicals then undergo intramolecular cyclization to form a range of triphenylene derivatives. Notably, the phenylsulfonate group proved to be both versatile and stable, and it remained compatible with Suzuki cross-coupling reactions illustrated in Scheme 8. In Path-I to assess the efficiency of the phenylsulfonate group as a photocleavable moiety, a simple *o*-terphenyl was prepared. Starting from precursor **26**, **27** was obtained *via* condensation with phenol under basic conditions. Subsequent Suzuki–Miyaura coupling with a boronic ester yielded compound **28** in 70%, confirming the phenylsulfonate group's stability under cross-coupling conditions, an essential feature for constructing larger PAHs. Path-II was adopted to overcome the steric hindrance caused by phenylsulfonate group by introducing this group after the Suzuki–Miyaura coupling. The *o*-terphenyl core **30** was synthesized *via* selective coupling in 88% yield, followed by the introduction of a fluorosulfonyl group using a modified Willis method (35% yield). Subsequent condensation with various *p*-substituted phenols (*e.g.*, NH_2, F, NO_2, CN) gave good to excellent yields.[67]
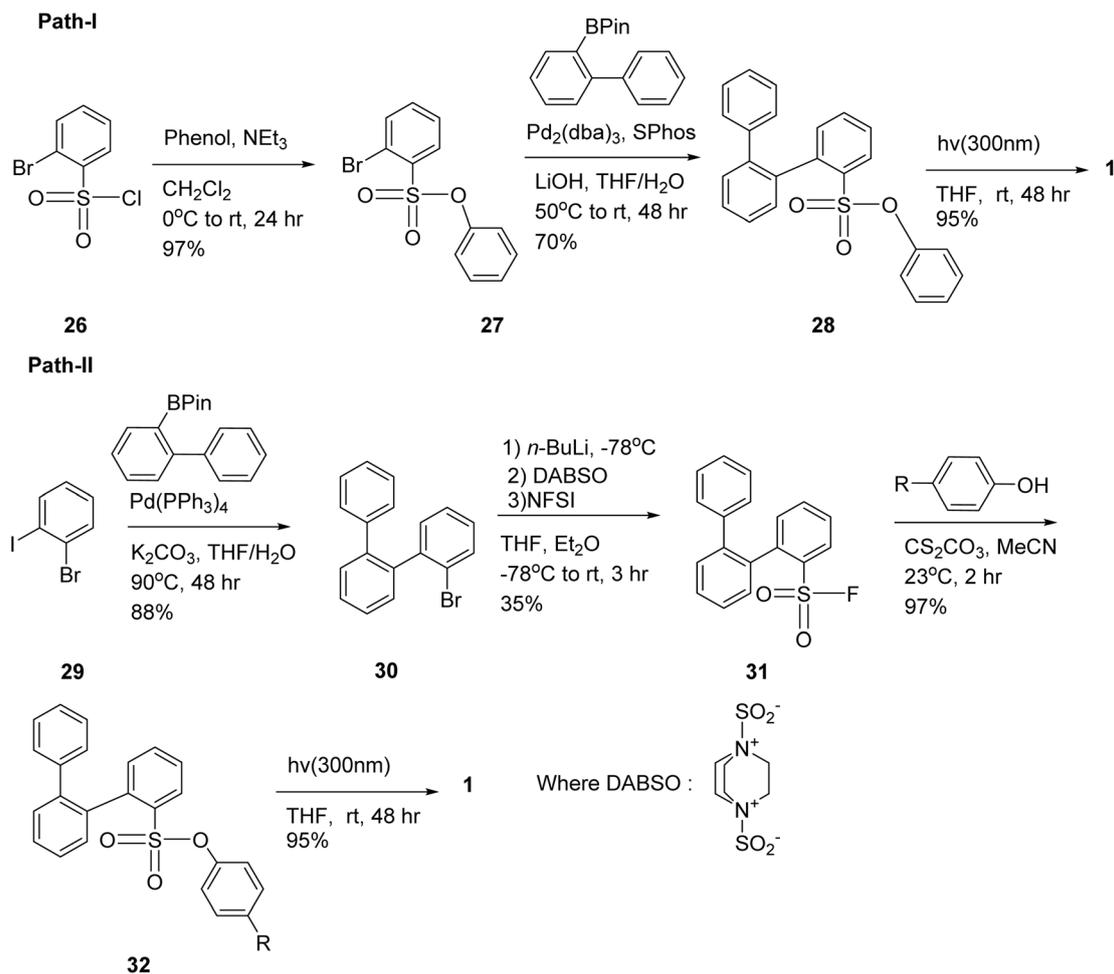
Scheme 8 (Path-I): Synthetic pathway for the preparation of triphenylene from chlorosulfonyl derivatives. (Path-II): An alternative strategy involving the preparation of fluorosulfonyl derivatives as precursors. Reproduced from ref. 67 with permission from Royal Society of Chemistry under a Creative Commons Attribution-NonCommercial 3.0 Unported Licence., copyright 2024.

An alternative strategy for triphenylene synthesis involves the use of transition metal-catalyzed cross-coupling reactions, followed by intramolecular oxidative cyclodehydrogenation to form the fused aromatic core. For instance, *o*-terphenylene derivative **35** was synthesized using a Pd(PPh$_3$)$_4$ catalyzed Suzuki reaction, highlighting the versatility of palladium catalysis in introducing various substituents.[68] Ultimately, the intramolecular Scholl cyclodehydrogenation emerged as a pivotal step, enabling the synthesis of a diverse array of polar triphenylene derivatives with potential applications in materials science and organic electronics as illustrated in Scheme 9.

2.2.2. Synthesis from biphenyl compounds. The synthesis of triphenylene from biphenyl derivatives provides an alternative route to triphenylene derivatives. The conventional methods often involve oxidative cyclization, in which biphenyl derivatives react with oxidizing agents such as FeCl$_3$ or AlCl$_3$,
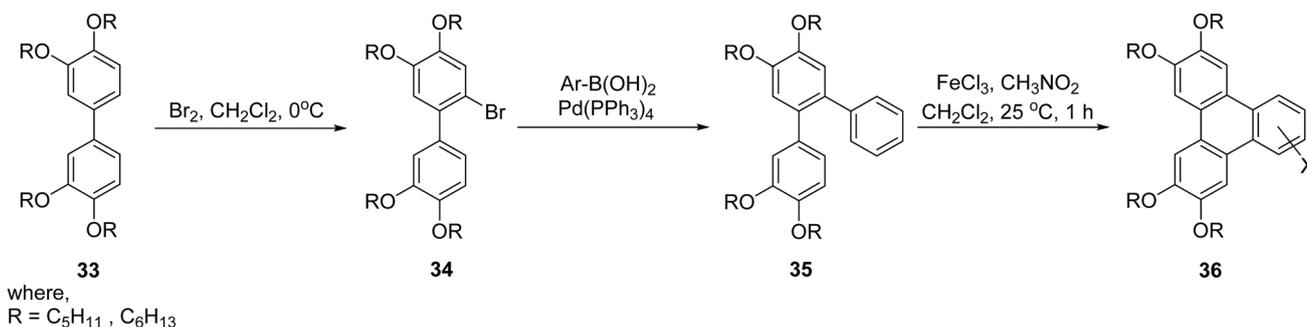
Scheme 9 Synthesis of polar triphenylene **36** derivatives. Reproduced from ref. 68 with permission from Elsevier, copyright 2017.

Conventional Methods

Traditional Pd-catalysed coupling
Diels-Alder cycloaddition
Oxidative cyclization

Modern Methods
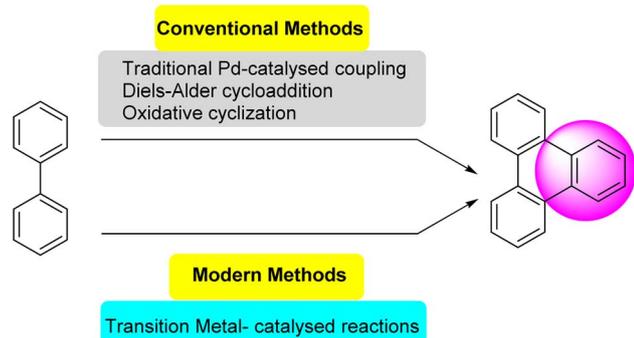
Transition Metal- catalysed reactions

Fig. 4 Traditional and advanced methods to convert biphenyl to triphenylene.

leading to the formation of the extra aromatic ring *via* dehydrogenation and the intramolecular coupling.[48] These methods allow for precise control over functionalization and can integrate various substituents during or after the cyclization process. Additionally, photochemical cyclization, and Scholl reactions are employed to achieve highly efficient and regioselective synthesis, especially for functionalized derivatives of triphenylene (Fig. 4).

Recent advances in triphenylene synthesis have introduced several efficient methods. Palladium-catalyzed C–H arylation,[69] oxidative coupling, and phenyl-addition/dehydrocyclization (PAC) are among the notable approaches.

Transition metal-catalyzed annulation strategies have emerged as important tools for the construction of aryl–aryl bonds, which can be used effectively for the preparation of triphenylene derivatives. For example, Liu and coworkers reported an aryne based palladium-catalyzed annulative π-extension involving a biphenyl derivative.[70] The reaction involves formation of a benzyne intermediate, which reacts with an aryl palladium species, leading to cyclization. They reacted 2-iodo-4′-methylbiphenyl **37** with 2 equivalents of *o*-(trimethylsilyl) phenyl triflate **38**, 5 mol% of Pd(dba)₂, 5 mol% of P(*o*-tolyl)₃, and 3 equivalents of CsF in a solvent mixture of 2 mL MeCN and 2 mL toluene at 110 °C for 24 hours, yielding the annulation product **39** in 38%. Optimization revealed that the controlled generation of benzyne from **38** using CsF is essential for the reaction's success (Scheme 10). Increasing the toluene content in the solvent mixture gradually improved the yield by slowing the benzyne formation.

In contrast, Pan and coworkers developed a non-aryne, direct arylation approach for synthesizing triphenylene through the palladium-catalyzed coupling of 2-iodobiphenyls **40** and iodobenzenes.[69] This reaction entails palladium-catalyzed dual activations of C–H bonds and double palladium-catalyzed carbon–carbon bond formation (Scheme 11). A wide range of unsymmetrically functionalized triphenylenes (**42**) can be produced using this approach from readily available substrates as illustrated.

The catalytic cycle (Scheme 12) for the synthesis of triphenylene begins with the oxidative addition of 2-iodobiphenyl to Pd(0), forming complex **A**. This is followed by intramolecular C–H activation to produce palladacycle **B**. Subsequent oxidative addition of iodobenzene to **B** results in Pd(ɪᴠ) complex **C**, which undergoes reductive elimination to form Pd(ɪɪ) complex **E**. An alternative pathway may involve the transmetalation-type exchange of aryl ligands between **B** and a phenylpalladium(ɪɪ) species, yielding dinuclear arylpalladium complex **D**, which upon reductive elimination also leads to complex **E**.[69]

One of the drawbacks of some of these non-aryne based approaches catalyzed by palladium complexes is that they typically require laborious pre-functionalization steps.[71,72] So, a new one-step mixture of functionalized triphenylene frameworks *via* Pd-catalyzed 2- or 4-fold C–H arylation of inactivated benzene derivatives and readily available arene substrate was described by Mathew and coworkers.[73] This synthesis employs pivanilide, a Pd₂(dba)₃ catalytic system along with cyclic diaryliodonium salts **44** as *p*-extending agents, enabling siteselective inter- and intramolecular tandem arylation sequences (Scheme 13) with proposed 2-fold C–H arylation mechanism (Scheme 14). The resulting *N*-substituted triphenylene is of interest for using a field-effect transistor sensor for the fast, subtle, and reversible detection of alcohol vapor. The *N*-substituted triphenylenes synesized are integrated into an alcohol field-effect transistor (FET) sensor, which demonstrates a swift and reversible response.

The previously reported tandem arylation route using coordinating moiety-bearing arenes to synthesize triphenylene (Scheme 13) as a completely benzenoid PAH building unit suffered as few drawbacks. This route aided by preinstalled directing groups (DGs), restricts access to the parent framework.[74] Lee *et al.* later introduced the inaugural non-directed, DGs free and one to two step Pd-catalyzed aromatic extension method for constructing triphenylene frameworks using basic arenes.[75] Palladium-catalyzed 2-fold C–H arylation enables consecutive C–C linkage processes, leading to the formation of fully benzenoid triphenylene structures employing cyclic diaryliodonium salts in Scheme 15.

5% Pd(dba)₂, 5% p(o-tolyl)₃, 3.0 CsF
MeCN : toluene, 110 °C, 24 h

38%

37 **38** **39**
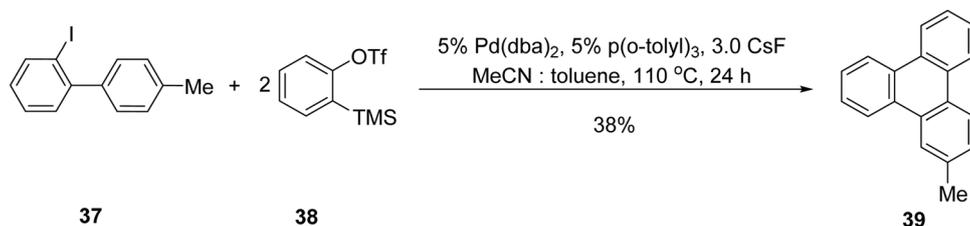
Scheme 10 Pd-catalyzed annulation of benzyne. Reproduced from ref. 70 with permission from American Chemical Society, copyright 2005.
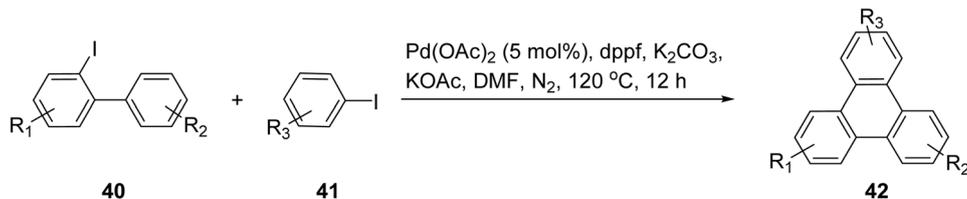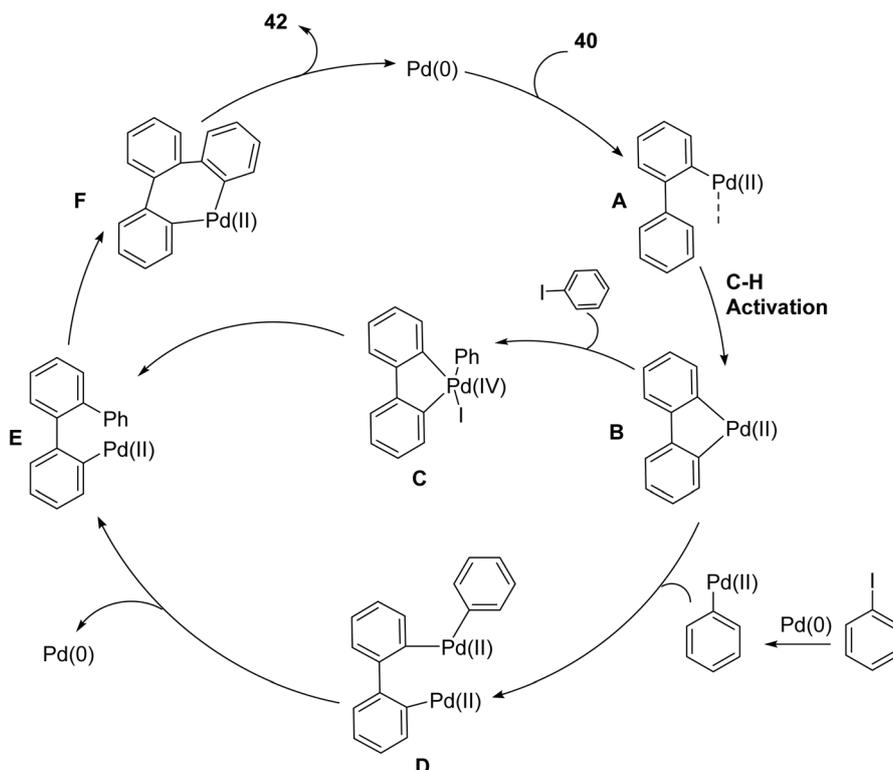
Scheme 11 Palladium catalyzed C–H arylation. Reproduced from ref. 69 with permission from American Chemical Society, copyright 2016.

Yang and coworkers developed a regioselective approach to synthesize unsymmetrical triphenylene using *o*-bromobenzoic acid and aryl iodides *via* palladium/norbornene catalyzed coupling reaction.[76] Moreover, they showed the synthesis of a number of triphenylenes through a palladium-catalyzed C–H arylation reaction between *o*-bromobenzoic acids **49** and 2-iodobiphenyls **48** without the need for norbornene and benzoquinone as mentioned in Scheme 16.

In 2018, Xu and co-workers reported an efficient palladium-catalyzed Suzuki–Miyaura coupling strategy for the synthesis of

functionalized triphenylene derivatives **53** using arylboronic acids **51** and 2,2′-dibromobiphenyl **52** precursors (Scheme 17).[77] This approach combines cross-coupling with intramolecular C–H activation, enabling a cascade annulation process that leads directly to triphenylene frameworks. Elevated reaction temperatures were found to significantly enhance cyclization efficiency, thereby facilitating the formation of asymmetrically substituted triphenylenes in a single synthetic sequence. A wide range of *p*-substituted arylboronic acids, including those bearing methyl, fluoro, chloro, cyano, and ester functionalities,
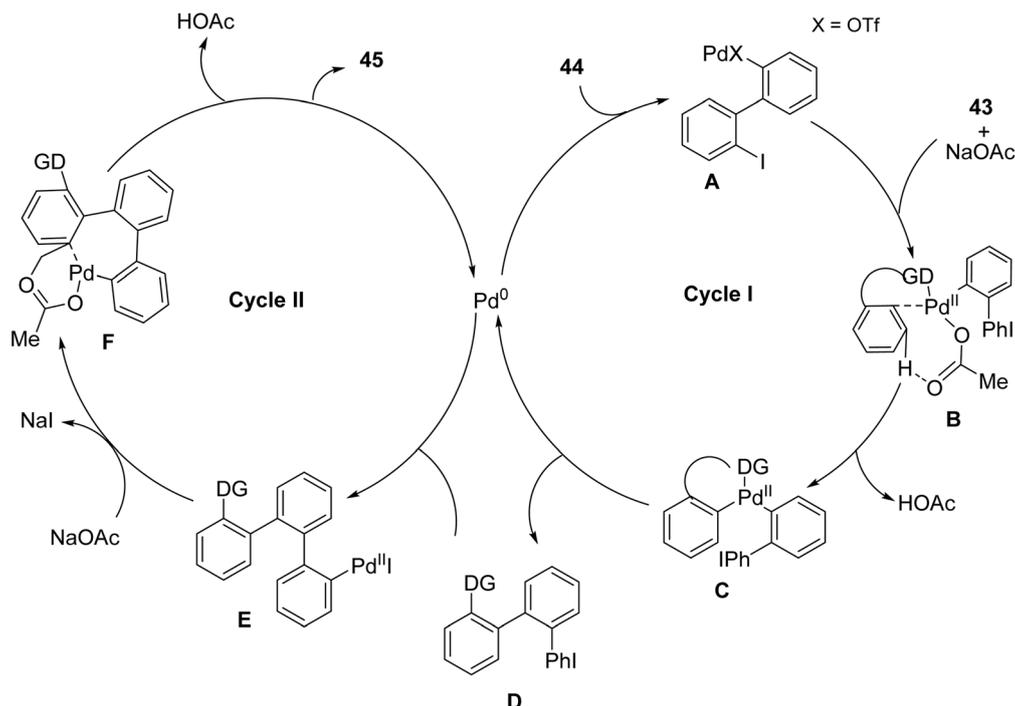
Scheme 12 Proposed mechanism for Pd-catalyzed C–H arylation. Reproduced from ref. 69 with permission from American Chemical Society, copyright 2016.
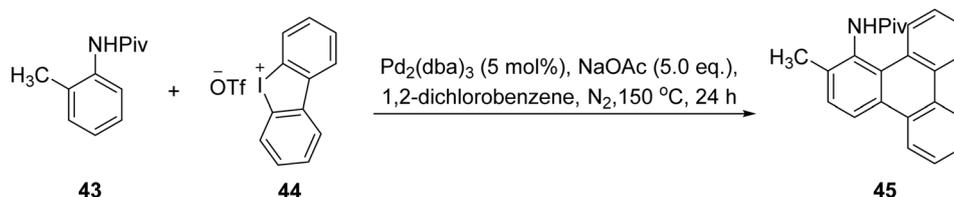
Scheme 13 2-Fold C–H arylation for building triphenylene. Reproduced from ref. 73 with permission from John Wiley & Sons, copyright 2017.

Scheme 14 2-Fold C–H arylation mechanism. Reproduced from ref. 73 with permission from John Wiley & Sons, copyright 2017.

participated smoothly in the transformation, affording the desired products in high yields. In addition, boronic acids containing electron-withdrawing groups displayed pronounced regioselectivity during the annulation step. Hence, this methodology offers high atom efficiency, reduced synthetic cost, and excellent control over regioselectivity, making it a powerful strategy for constructing polycyclic aromatic systems through consecutive C–C bond formation and ring fusion.

In 2018, Zhao and co-workers reported an efficient copper-catalyzed strategy for the synthesis of asymmetrically substituted triphenylene derivatives **56** *via* oxidative annulation of electron-rich biphenyl precursors **54**, mainly 3,3′,4,4′-

Scheme 15 Single arylation followed by double arylation. Reproduced from ref. 75 with permission from American Chemical Society, copyright 2019.

tetraalkoxybiphenyls, with diaryliodonium salts **55** that tolerate halogen substituents (Scheme 18).[78] The transformation proceeds through successive C–H activation steps and exhibits broad functional-group compatibility, including aryl iodonium reagents bearing bromine, chlorine, and fluorine substituents. Aryl iodonium salts containing electron-donating groups proved particularly effective, delivering comparable yields while retaining halogen functionalities suitable for further post-synthetic cross-coupling modifications. Mechanistic investigations indicate that the high chemoselectivity originates from the preferential activation of electron-rich biphenyl substrates, as electron-deficient biphenyls and unsubstituted biphenyls failed to undergo cyclization under the same conditions. Although operationally straightforward and synthetically valuable, the methodology is currently limited to alkoxy-substituted biphenyl frameworks and catechol-derived aryl partners, which restricts its broader applicability to more diverse aromatic systems.

In addition to the classical oxidative trimerization, Yamamoto coupling, and the more recent photo-cyclo-de-hydrofluorination (PCDHF) protocols, the field has witnessed rapid progress in nucleophilic aromatic substitution of poly-fluoroarenes (S_NArF) as a powerful route to fluorinated tri-phenylene scaffolds and discotic mesogens. Polyfluorinated arenes such as hexafluorobenzene (C_6F_6), octa-fluoronaphthalene ($C_{10}F_8$), and decafluorobiphenyl ($C_{12}F_{10}$–$C_{12}F_{10}$) possess highly activated C–F bonds capable of undergoing regioselective substitution with organolithium nucleophiles, enabling controlled construction of π-extended and heavily fluorinated aromatic architectures.

In this work,[79] the fluorinated precursors **59** (1,2,3,4-tetrafluoro-6,7,10,11-tetraalkoxytriphenylene) and **58**
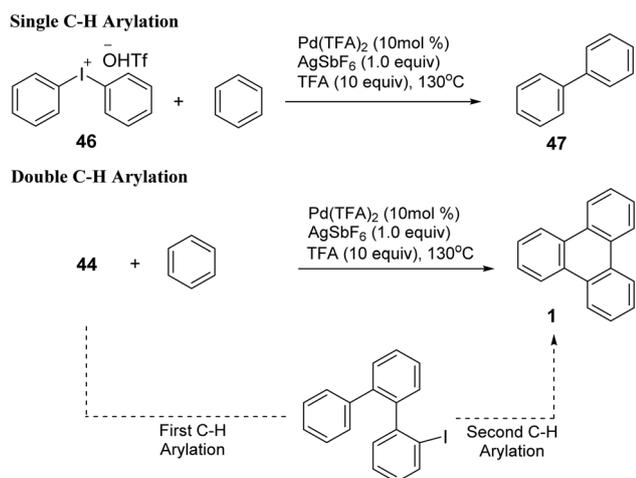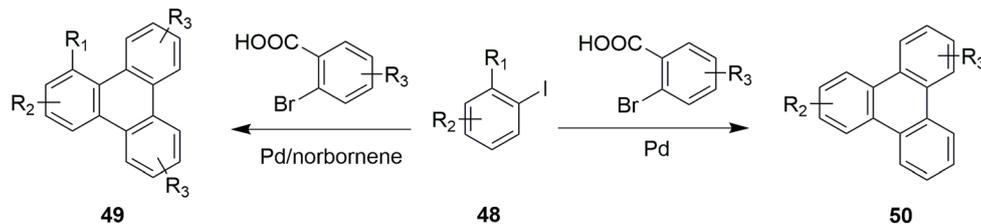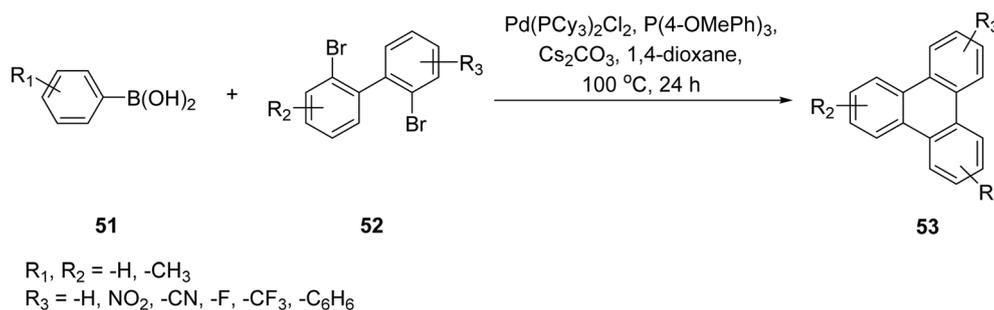
Scheme 16 Palladium catalyzed C–H arylation for triphenylene synthesis. Reproduced from ref. 76 with permission from American Chemical Society, copyright 2018.

Scheme 17 Construction of triphenylene frameworks *via* palladium-catalyzed Suzuki–Miyaura cross-coupling of arylboronic acids and 2,2′-dibromobiphenyl building blocks. Reproduced from ref. 77 with permission from Elsevier, copyright 2019.

(9,10,11,12,13,14-hexafluoro-2,3,6,7-tetraalkoxybenzo[*f*]tetra-phene), each functionalized with four racemic 3,7-di-methyloctyloxy chains, were subjected to reactions with a series of aryl-lithium reagents (ArLi; Ar = naphthalen-1-yl or -2-yl (NA/NB), benzothiophen-2-yl (BT), triphenylen-2-yl (TP), pyren-1-yl (PY), and tetraphenylethylenyl (TPE)). These transformations afforded the corresponding monosubstituted derivatives, **61** (trifluorotriphenylene-based) and **60** (pentafluorobenzo[*f*]tetraphene-based) (Scheme 19). Single-crystal X-ray diffraction analyses of three chain-free model derivatives revealed characteristic F···H contacts and antiparallel π–π stacking, providing structural evidence that supports and confirms the aryl substitution sites. The mesomorphic behaviour of these fluorinated pseudo-discotic systems was examined using polarized optical microscopy, differential scanning calorimetry, and small- and wide-angle X-ray scattering (SAXS/WAXS).

One of the major contributions in this area is the development of F-discotic liquid crystal (F-DLC) frameworks obtained from S$_N$ArF reactions between polyfluoroarenes and biphenyl-dilithium or aryl-lithium reagents, as demonstrated by Zhang *et al.*[66] The method provides efficient access to multi-fluorinated discogens displaying enhanced mesomorphic stability, strong π–π interactions, and tunable dielectric properties. In this study,[66] a rapid synthesis of a series of 1,2,3,4-tetrafluoro-6,7,10,11-tetraalkoxytriphenylenes **65** (4F-TP$_n$, n = 3–14) and 9,10,11,12,13,14-hexafluoro-2,3,6,7-tetraalkoxybenzo[*f*]tetra-phenes **64** (6F-BTP$_n$, n = 6–16) was achieved *via* S$_N$FAr of perfluoroarenes, following a slightly modified literature procedure. The key precursors, 2,2′-dilithio-1,1′-biphenyl derivatives **62** with varied alkoxy chain lengths, were reacted with hexa-fluorobenzene (C$_6$F$_6$) and octafluoronaphthalene (C$_{10}$F$_8$) to afford the Janus-like 4F-TP$_n$ **65** and 6F-BTP$_n$ **64** compounds in good yields (Scheme 20). Starting from inexpensive and readily available 5-bromosalicylaldehyde, 4F-TP$_n$ **65** were synthesized in four steps, with overall yields ranging from 25–53%. Upon warming to room temperature, 1.2 equivalents of the respective
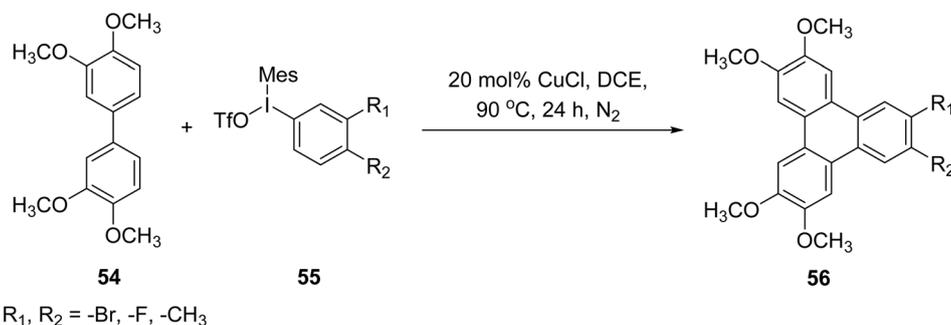
Scheme 18 Copper-catalyzed C–H arylation route to unsymmetrical triphenylenes. Reproduced from ref. 78 with permission from American Chemical Society, copyright 2018.
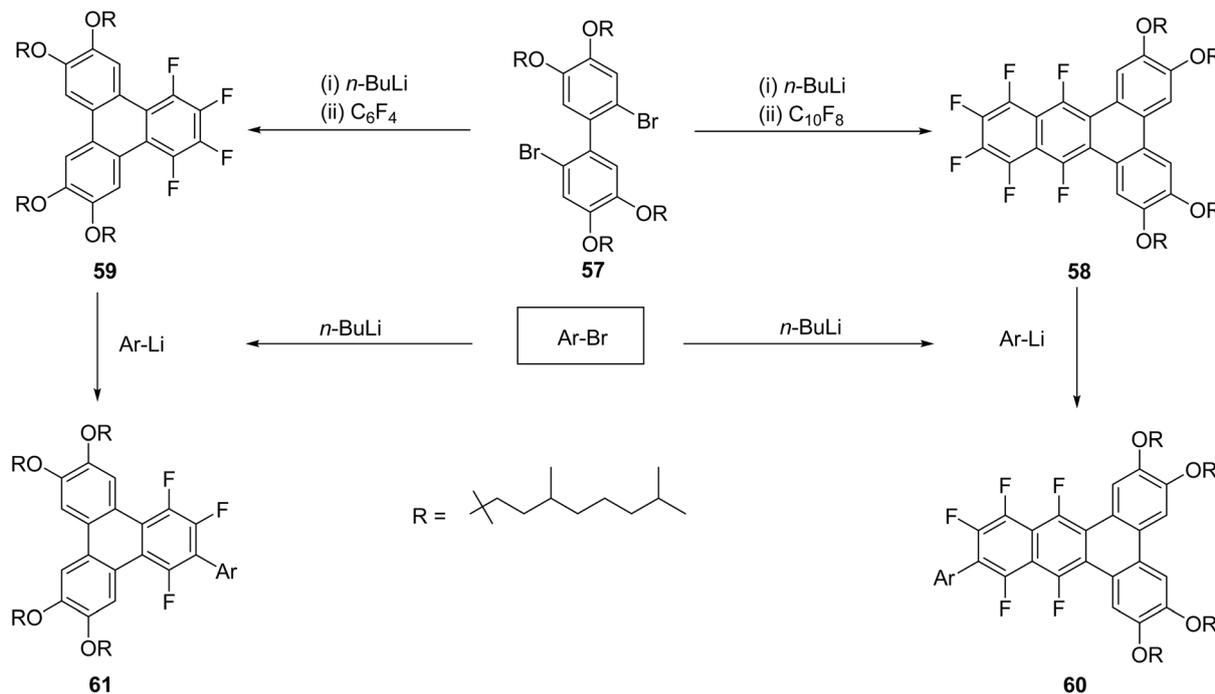
Scheme 19 Synthesis of tri- and penta-fluorotriphenylenes. Reproduced from ref. 79 with permission from American Chemical Society, copyright 2025.

perfluoroarene were added, yielding the target Janus compounds. The yields for this second, double-annulation step was notably lower (approximately 15% for 2F-TBTP$_n$ **67** and 40% for 4F-TBTC$_6$ **66**) compared to the initial single S$_N$FAr reactions (65–83% for 4F-TP$_n$ and 53–73% for 6F-BTP$_n$), likely due to steric hindrance around the triphenylene core and the reduced solubility of the tribenzotetraphene products. Nonetheless, these yields are expected to be amenable to optimization in future studies.

Subsequent studies further expanded this chemistry to a variety of aryl-fluoroarene discotic systems (Ar-FDLCs), showing that selective substitution patterns could be achieved by adjusting the stoichiometry of the lithiated reagents and the electronic configuration of the polyfluoroarene substrates. These developments were articulated in ref. 80 and later refined to yield structurally diverse F-DLCs with controllable optical textures.[81]

Non-covalent interactions between arenes and fluoroarenes have emerged as a valuable tool for constructing both flexible and rigid supramolecular architectures, and they are now increasingly applied in the design of liquid-crystalline materials.[82] These interactions arise from the strong electronegativity of fluorine, which significantly alters the electronic distribution and dipole moment of the fluorinated aromatic units. In this context, two families of fluorinated triphenylene derivatives equipped with four peripheral alkyl chains of different lengths were synthesized through S$_N$ArF of polyfluoroarenes.[80] The first family consists of the homologous 2-phenyl-1,3,4-trifluorotriphenylenes **71** (PH$_n$, R = C$_n$H$_{2n+1}$, n = 3–12), obtained in approximately 60–90% yield by reacting lipophilic 2,2′-dilithiobiphenyl reagents with pentafluorobiphenyl (C$_6$F$_5$–

C$_6$H$_5$). Using analogous conditions, a second set of 2-aryl-1,3,4-trifluorotriphenylene derivatives bearing larger aromatic substituents—such as naphthyl (1- or 2-isomers), benzothiophen-2-yl, triphenylen-2-yl, pyren-1-yl, and tetraphenylethenyl groups—was prepared in moderate to high yields (Scheme 21). A key outcome of this study is the systematic observation of columnar mesophases across all fluorinated derivatives. Compound such as **71** consistently generate columnar hexagonal (Col$_{hex}$) mesophases as well, although the breadth and stability of these phases strongly depend on the bulk and geometry of the appended aromatic units. These findings highlight the decisive role of aromatic fluorination and the strength of arene–fluoroarene interactions in promoting columnar ordering by favoring face-to-face assembly of electron-rich and electron-poor aromatic frameworks.[80]

Two positional isomeric families of triphenylene derivatives featuring "inverted" alkoxy-chain substitution patterns were prepared: 7,10-dialkoxy-1,2,3,4-tetrafluoro-6,11-dimethoxytriphenylenes and 6,11-dialkoxy-1,2,3,4-tetrafluoro-7,10-dimethoxytriphenylenes, designated as p-TPF$_n$ (**81**) and m-TPF$_n$ (**76**), respectively. In addition, the corresponding non-fluorinated isomers, 3,6-dibutoxy-2,7-dimethoxytriphenylene (p-TP4; **80**) and 2,7-dibutoxy-3,6-dimethoxytriphenylene (m-TP4; **75**), were synthesized (Scheme 22). All compounds were obtained in good overall yields through a three-step sequence based on transition-metal-free nucleophilic aromatic substitution of fluoroarenes. The reactions involved the coupling of suitably substituted 2,2′-dilithiobiphenyl intermediates with either perfluorobenzene (C$_6$F$_6$) to generate the fluorinated series p-TPF$_n$ (**81**) and m-TPF$_n$ (**76**), or o-difluorobenzene (C$_6$H$_4$F$_2$) to afford the non-fluorinated analogues p-TP4 (**80**) and
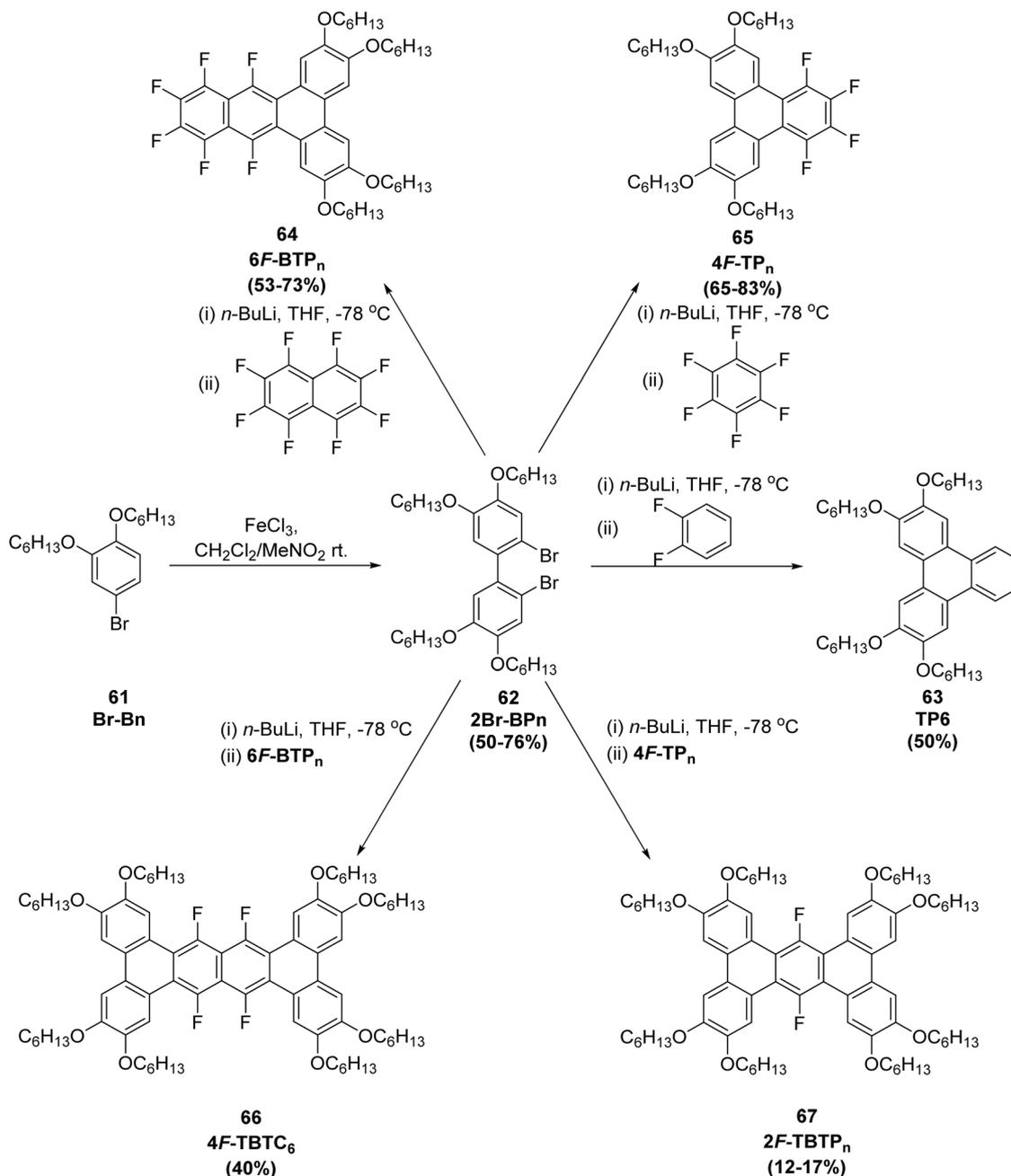
Scheme 20 General synthetic route for Janus-type and π-extended discotic fluorinated polyaromatic hydrocarbons (F-PAHs). Reproduced from ref. 66 with permission from John Wiley & Sons, copyright 2023.

m-TP4 (**75**). Furthermore, the fluorinated derivatives adopt closely packed columnar stacking arrangements, an organization that is typically favorable for the formation of columnar liquid-crystalline phases.[81]

2.2.3. Synthesis from phenanthrene derivatives. The transformation of phenanthrene into triphenylene represents a valuable synthetic strategy for constructing fully conjugated PAHs. This approach is particularly significant because triphenylenes are more highly conjugated than phenanthrenes, so it effectively expands π-conjugation and enhances electronic and optical properties. Conventional methods (Fig. 5) used for

this conversion include Diels Alder reactions,[83] photo-cyclization[84] cationic cyclization.[85]

Guitian and coworkers devised a route to achieve tri-phenylene that passes through 1-triphenylenol, employing a Diels–Alder cycloaddition of 9,10-phenanthryne, which was derived from precursor **82**, with furan to yield compound **83**.[86] Subsequent acidic treatment of **83** resulted in a quantitative yield of 1-triphenylenol **84**. A subsequent one-pot synthesis using hexamethyldisilazane (HMDS) in refluxing THF, trapped by *n*-BuLi and Tf₂O afforded triflate. Treatment of this triflate with 5 mol% of Pd₂(dba)₃ and dimethyl acetylene di-carboxylate (DMAD) yielded polycyclic arene **86**, subsequent
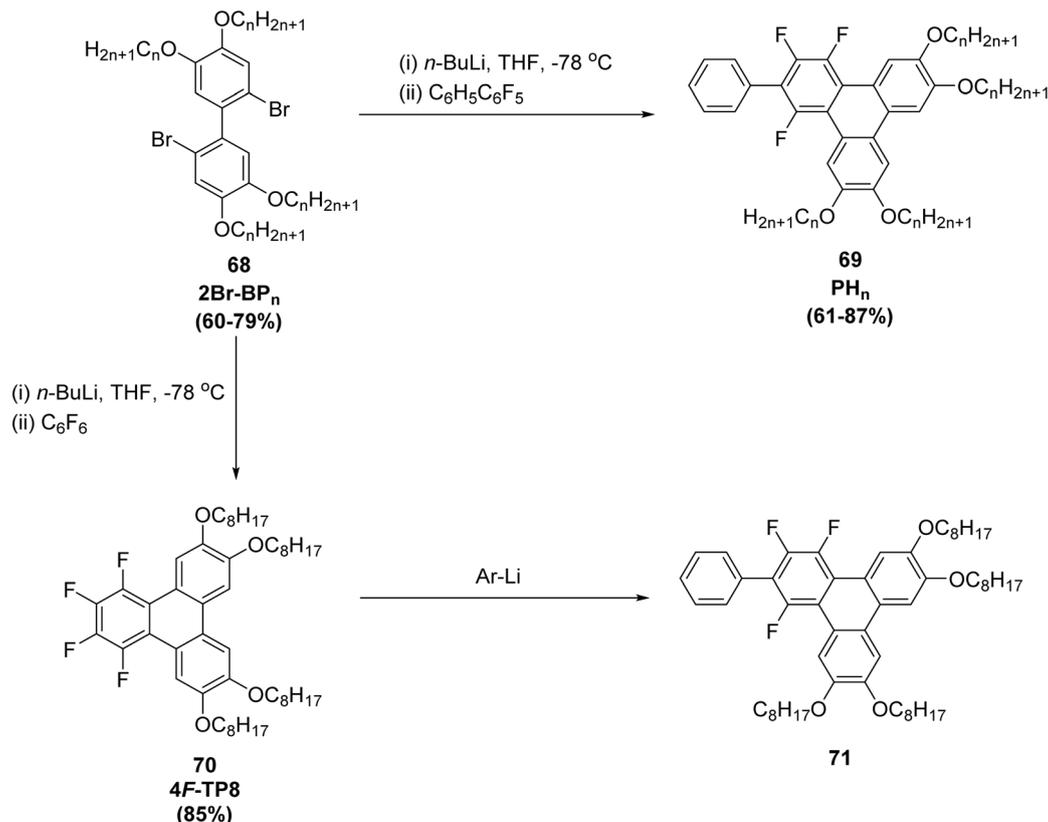
Scheme 21 Synthesis of 2-aryl-1,3,4-trifluorotriphenylene derivatives. Reproduced from ref. 80 with permission from Royal Society of Chemistry, copyright 2023.

from reaction of one aryne and two alkynes, this method allows for subsequent transformations using arynes in Scheme 23.

Junji and coworkers demonstrated that fluorinated phenanthrenes could be used to generate arynes *via* metalation and elimination of fluoride.[87] Diels–Alder reactions of these arynes with isobenzofurans **88** yielded the respective cycloadducts, which underwent reductive aromatization in an SnCl$_2$/HBr system, resulting in benzotriphenylenes **91**. For example, in the presence of **88**, treatment of bromo(fluoro)phenanthrene with butyllithium at −90 °C allowed for Li–Br exchange followed by LiF elimination, generating the phenanthryne **90**. Upon warming to room temperature, **90** was obtained in 55% yield, along with fluorophenanthrene in 24% yield. In this process, phenanthryne underwent a Diels–Alder reaction with isobenzofuran **88**. Reductive aromatization of this adduct to benzotriphenylene **91**, took place under basic conditions from **90** (Scheme 24).

Sterically congested large triphenylenes can be accessed *via* Diels Alder reaction of phencyclones with alkynes, as method demonstrated by Perez and coworkers.[88] Cycloaddition of alkyne **93** with cyclopentadienone **92** could lead to the formation of iodotriphenylene **94**, after cheletropic extrusion of CO (Scheme 25). Compound **94** was formed in a remarkable 73% yield, and was subsequently used to obtain sterically congested PAHs. Later, Müllen and coworkers extended the use of this method to prepare triangular triphenylene macrocycles (*e.g.* **98**),

the phencyclones were produced from the corresponding phenanthrene diones.[89] The Diels Alder reaction of alkynes with phencyclone **97** was followed by a nickel-mediated coupling reaction (Scheme 26).

Guitian and coworkers reported the production of aryne **101** ensued by treating triflate **99** with tetrabutylammonium fluoride (TBAF) in the presence of cyclopentadienone **92**. Subsequent refluxing of this mixture in tetrachloroethane for 3 hours resulted in a 44% yield of benzotriphenylenol **100**.[90] This achievement is noteworthy given the presence of an unprotected hydroxyl group, which could potentially react with the extremely electrophilic aryne. It appears that the intermediate formed from the Diels–Alder reaction of aryne **101** and dienone undergoes an *in situ* transformation, ultimately yielding compound **100** through CO extrusion as described earlier (Scheme 27).

2.2.4. Synthesis from benzene derivatives by cyclotrimerization. This method for triphenylene synthesis proceeds by formal trimerization of three benzene rings. Among the most common conventional approaches is oxidative trimerization using FeCl$_3$.[91] However, this approach is limited to electron-rich substrates. Transition metal mediated synthesis of triphenylene was discovered when 1,2-dibromobenzene was treated with Ni(cod)$_2$/PPh$_3$.[92] Mannich reported H$_2$SO$_4$-catalyzed trimerization of cyclohexanone leading to triphenylenes.[93] More recently, other approaches such as palladium-catalyzed aryne
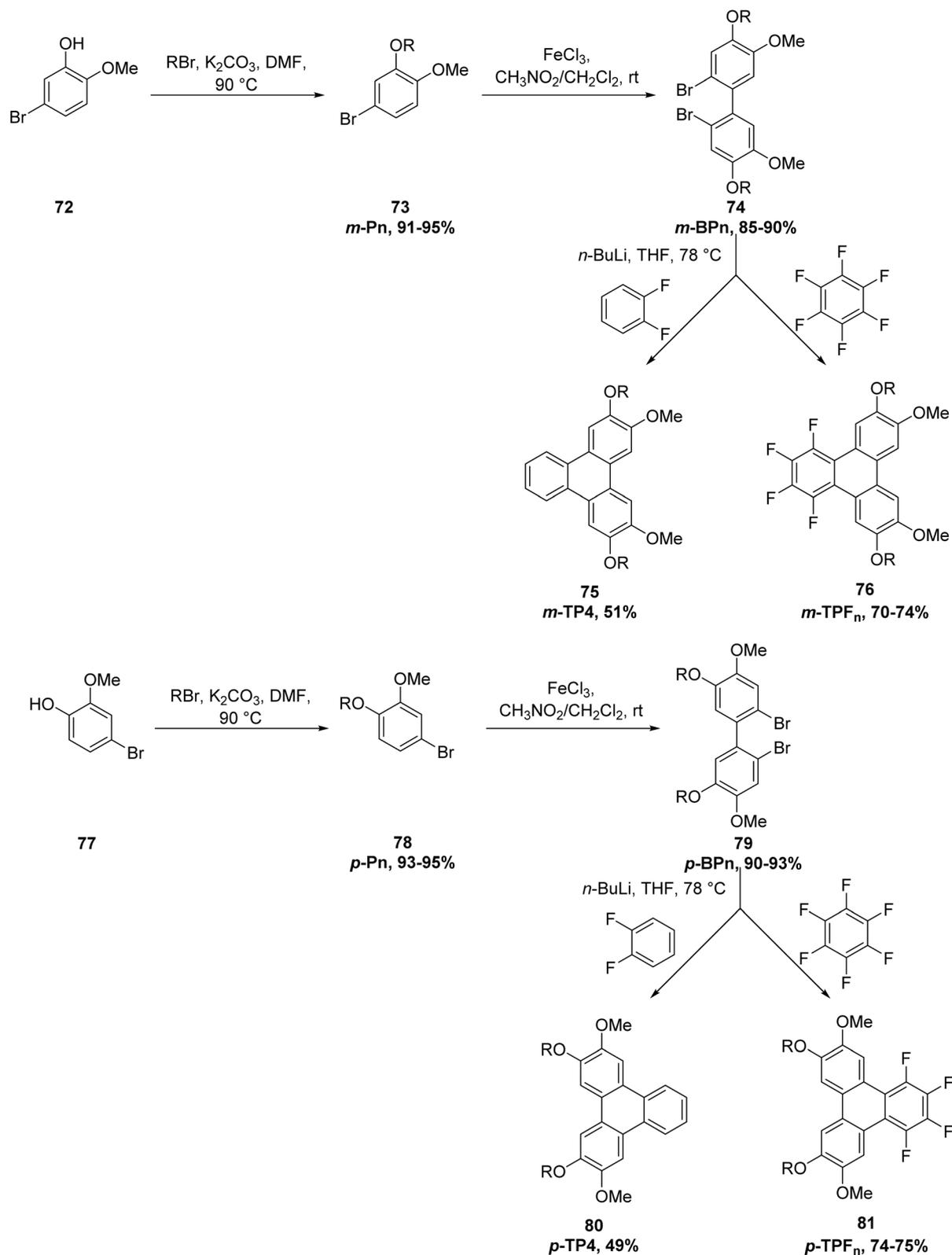
Scheme 22 Synthetic route for the synthesis of Janus-like TP discogens, *p*-TPFn, *m*-TPFn, *p*-TP4 and *m*-TP4 (and intermediates); R = C_nH_{2n+1}, with n = 4, 6, 8, 10. Reproduced from ref. 81 with permission from John Wiley & Sons, copyright 2024.

Conventional Methods

Diels-Alder reaction
Photocyclization
Cationic cylization
Wittig reaction

Modern Methods

Pd catalysed C-H arylation
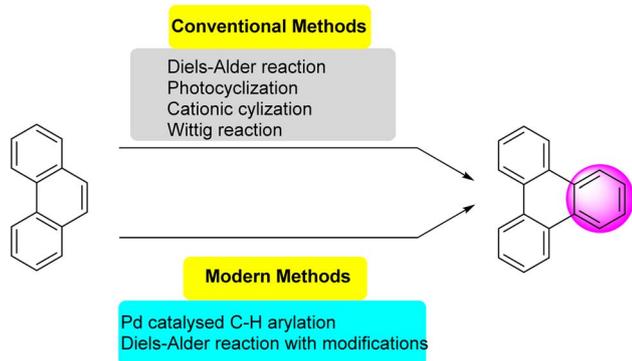Diels-Alder reaction with modifications

Fig. 5 Triphenylene frameworks synthesis from phenanthrene moiety.

cyclotrimerization and nickel-mediated Yamamoto coupling have been developed (Fig. 6).

Peña and coworkers performed the catalytic trimerization of arynes that involves carefully selecting the catalyst and the method for aryne generation **103** using mild reaction conditions. Treating tirmethylsilylaryl triflate **102** with 2 equivalents of anhydrous CsF in the presence of catalytic [Pd(PPh$_3$)$_4$] in acetonitrile at room temperature resulted in fluoride-induced elimination of TMS and triflate, followed by aryne trimerization, yielding 83% triphenylene derivatives **104** with yields up to 83% (Scheme 28).[74]

Galow and colleagues extended Peña's aryne cyclotrimerization to access sterically hindered triphenylenes.[94] They reported 1,4,5,8,9,12-hexamethyltriphenylene **107** synthesis by using o-trimethylsilylaryl triflate bearing multiple methyl groups. Addition of cesium fluoride in the presence of a palladium catalyst resulted in the formation of **106** (Scheme 29). X-ray crystallography indicates that it adopts a highly distorted C$_2$ geometry, featuring a 53.30° end-to-end twist, due to increased steric interference from the methyl groups.

In a similar approach, Guitian and coworkers synthesized 1-methoxytriphenylene through a palladium-catalyzed [2 + 2 + 2] cycloaddition involving mixed arynes that is one molecule of 3-methoxybenzyne and two molecules of benzyne.[86] This process yields seven potential products due to homo- and hetero-cyclotrimerization of the arynes. The distribution of these products appears to be influenced by the reagent ratio, the rate of aryne–palladium complex formation, and the subsequent transformation rates. Optimal conditions for obtaining a high yield of **111** involve using a 1 : 4 molar ratio of aryl precursors **108** and benzene triflate with CsF in the presence of 10 mol% of Pd(PPh$_3$)$_4$ (Scheme 30).

In contrast to Peña's work, Liu and coworkers devised Pd-catalyzed reaction to generate triphenylenes by reaction of two arynes with an iodobenzene.[70] For example, reaction of ethyl 4-iodobenzoate **112** and triflate **113** afforded the target triphenylene **114** in a 50% yield, as illustrated in Scheme 31. The two possible pathways were proposed, in one, the Pd(0) species undergoes oxidative cyclization with the aryne to form a palladacycle, followed by C–H activation and reductive elimination. Alternatively, Pd(0) may first insert into the aryl iodide bond, giving an aryl–Pd intermediate that subsequently engages with the aryne. This reaction allowed access to low symmetry triphenylenes where one of the outer rings bears different substituents. However, the reaction necessitated the use of an excess of aryne, which resulted in aryne cyclotrimerization to give **115** as a byproduct.

Since aryne cyclotrimerization often results in low yields and requires the synthesis of aryne precursors, an alternative approach consists of nickel-mediated Yamamoto coupling. Schroeder et al. showcased the nickel-mediated Yamamoto coupling of o-dibromoarenes **116** as a succinct and efficient method for synthesizing electron-deficient substituted triphenylene derivatives **117** which could not be prepared using Scholl reaction or palladium-catalyzed cyclotrimerization.[95]
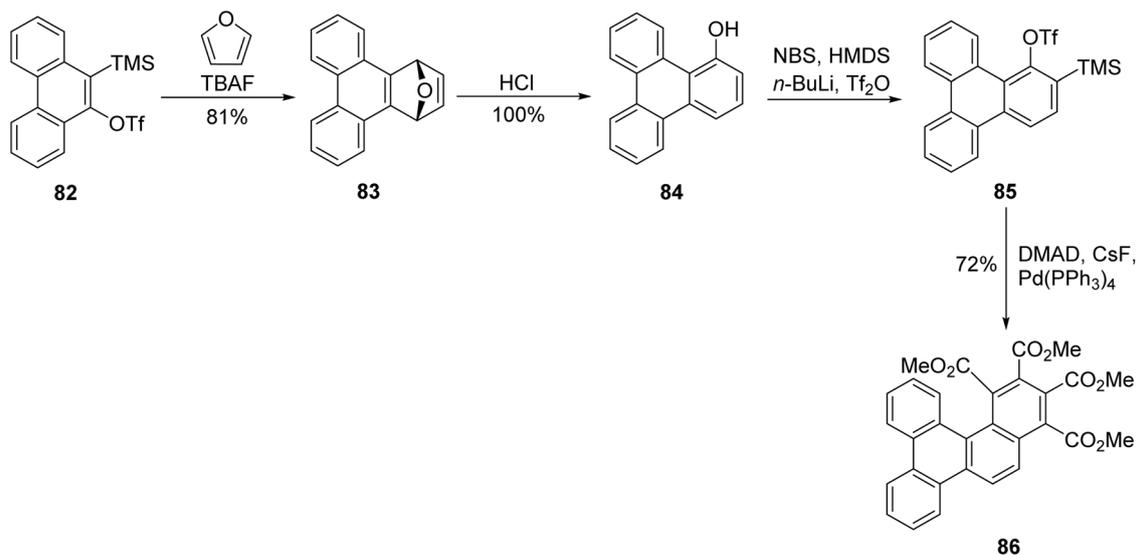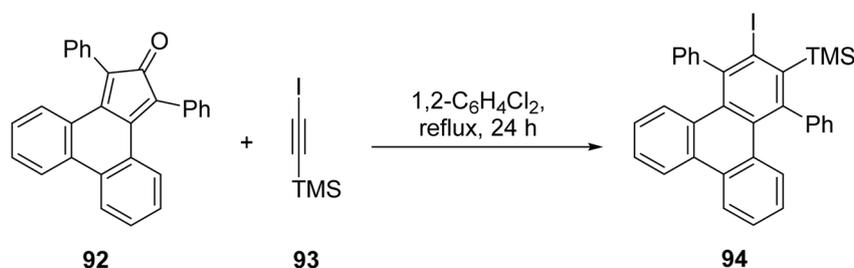
Scheme 23 Trimerization of 3,4-phenanthryne to yield sterically congested trimer. Reproduced from ref. 86 with permission from American Chemical Society, copyright 2008.
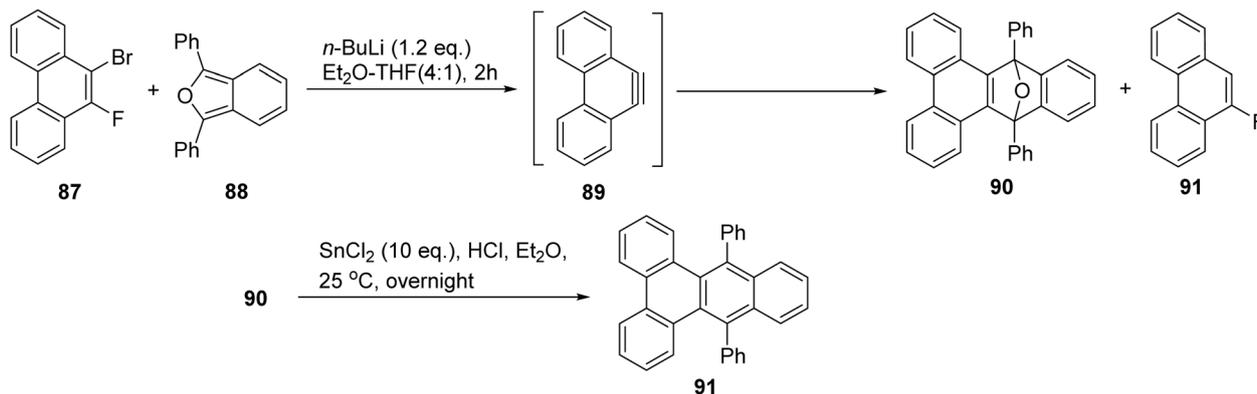
Scheme 24 Diels Alder reaction between extended arynes and isobenzofuran. Reproduced from ref. 87 with permission from John Wiley & Sons, copyright 2020.

Scheme 25 Synthesis of 1,4-diphenyl-2,3-triphenyene. Reproduced from ref. 88 with permission from Royal Society of Chemistry, copyright 2013.

Homocoupling of aryl bromides in the presence of bis(1,5-cyclooctadiene)nickel(0) forms new aryl–aryl bond thus cyclotrimerization occurs to form 3-fold symmetric triphenylene (Scheme 32). Yamamoto coupling results with various *o*-dibromoarenes are also given in Scheme 32. Remarkably, Rudiger and coworkers also demonstrated the use of Yamamoto coupling as a convenient alternative to aryne based methods by the synthesis of cyclotrinaphthylenes in a good yield.[96] It is also effective in preparing the compounds, which are crucial for organic semiconductor applications due to their ability to form columnar liquid crystalline phases with extended π-stacked arrays.[97]

Furthermore, Schroeder and coworkers also illustrated the applicability of this method in preparation of electron-deficient mesogens bearing imide groups.[95] They synthesized triphenylene trisimide **121** and its thionated counterpart **122**, enabling a comparative analysis of their mesomorphic properties. 4,5-Dibromo-*o*-xylene **118** was oxidized to anhydride **119** which reacts with octyl amine in the presence of Ni(OAc)$_2$ to give imide (Scheme 33). Polarized optical microscopy and differential scanning calorimetry studies reveal that compound **120** exhibits a columnar mesophase with high clearing point.

Electrochemical methods provide a metal-free and environmentally friendly route for the oxidative trimerization of catechol derivatives to synthesize triphenylene and its ketal-protected intermediates. Unlike conventional approaches that rely on high-valent metal salts (*e.g.*, FeCl$_3$, MoCl$_5$), electrochemical oxidation avoids metal waste, reduces reagent costs, and minimizes side reactions such as ketal cleavage.[98] The compound 2,3,6,7,10,11-hexahydroxytriphenylene **124**, is widely utilized as a building block in supramolecular chemistry. Regenbrecht and coworkers demonstrated its efficient synthesis through a galvanostatic anodic oxidation process.[99] This method involves the oxidation of catechol ketals **123**, followed by acidic hydrolysis to yield the desired product with high purity and optical clarity. The electrolysis was feasible under practical galvanostatic conditions using platinum sheets as electrode materials and propylene carbonate (PC) and tetra-butylammonium tetrafluoroborate (TBABF$_4$) as electrolyte in Scheme 34. Precipitation of non-polar triphenylene is favoured in the polar electrolyte. PC is inexpensive and not hazardous to environment so this procedure effectively improved access to triphenylene derivatives.

2.2.5. Benzannulation-based synthesis. The one-pot formation of peripheral rings presents an effective alternative for constructing triphenylenes that are otherwise challenging to synthesize (Fig. 7). For example, a series of electron-deficient triphenylene and trinaphthylene carboximides were synthesized by Wu and coworkers.[100] Electron deficient phthalimides cannot undergo intermolecular oxidative cyclodehydrogenation reactions due to lack of electron density required for cyclization So, they effectively utilized the Diels–Alder cycloaddition reaction of the highly reactive radialene with maleimide **126** to synthesize carboximides **127**. Radialene, having elevated chemical reactivity towards dienophiles, was produced *in situ* by treating hexakis(bromomethyl)benzene **125** with NaI in DMF,
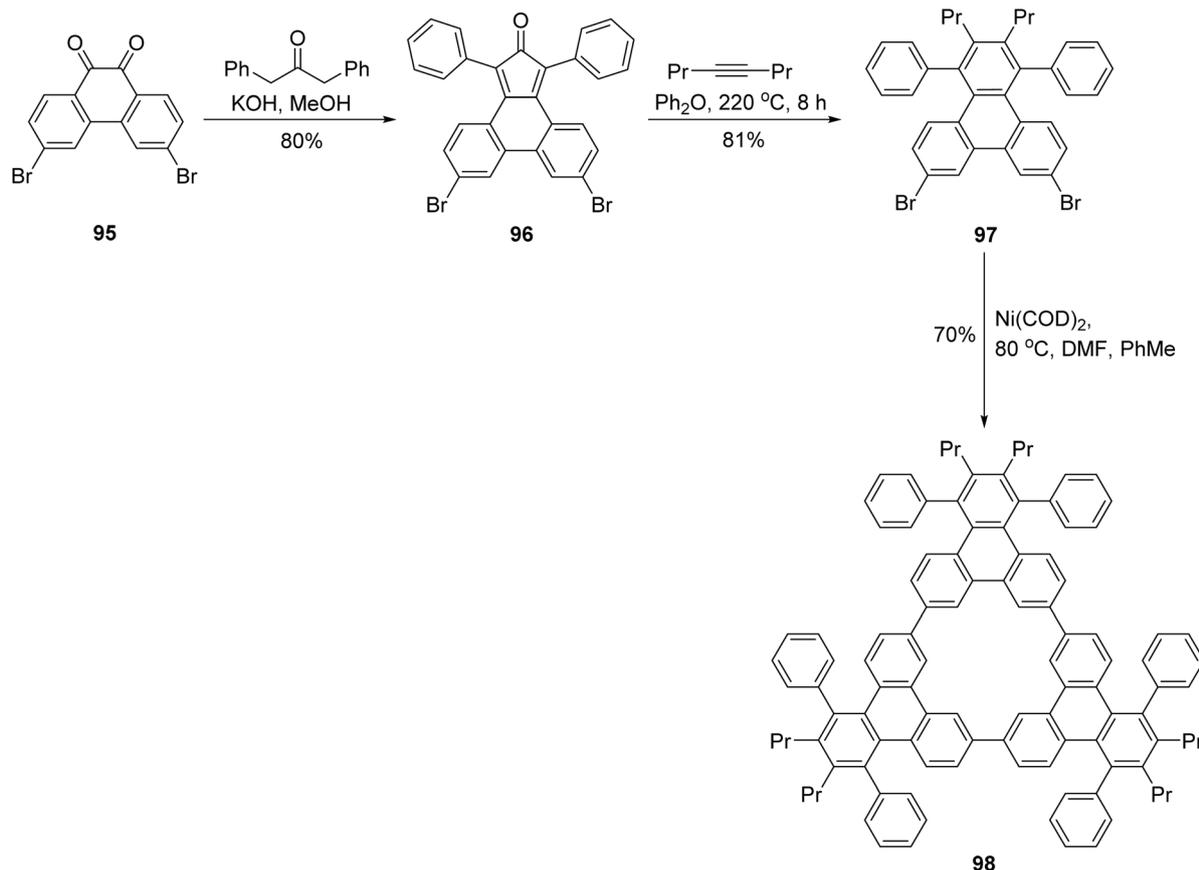
Scheme 26 Synthesis of triphenylene molecular triangle. Reproduced from ref. 89 with permission from John Wiley & Sons, copyright 2011.

followed by Diels–Alder cycloaddition with maleimides. The resulting addition products were then aromatized initially through reaction with bromine, followed by treatment with triethylamine, yielding **125** in yields ranging from 12% to 18% (Scheme 35). Despite the relatively modest yields, this marks the first applied mixture of dicarboxylic imide-substituted triphenylenes. This synthetic strategy could be extended to produce more extended starphenes in the future.

Osawa and coworkers used a similar approach to prepare triphenylene hexaesters.[101] Initially, hexamethylbenzene **129** underwent benzylic bromination, yielding hexakis(bromomethyl)benzene **125** in quantitative yield. The subsequent Cava reaction of **125** with dimethyl acetylenedicarboxylate (DMAD) in the presence of sodium iodide resulted in the formation of hexahydrotriphenylene with a modest

yield of 14% (Scheme 36). This product was further oxidized with MnO_2 to afford **129** in high yield (95%). The drawbacks of this approach are that the hexamethylbenzene starting material is relatively costly, and that the Cava reaction is low-yielding.

The S_NArF approach has also been applied to the synthesis of fluorinated triphenylenes, including the preparation of 4F-substituted triphenylene (4F-TP) via the reaction of triphenylene bromide/lithium intermediates with Ar–F substrates, reported by Donnio et al. (2024) in ref. 102. This strategy enables late-stage fluorination and modular diversification of the triphenylene core, which is not readily achievable through classical oxidative cyclization or metal-mediated coupling routes. In this study,[102] a series of aryl- and fluoroaryl-functionalized triphenylenes (Ar-TP; **131** and FAr-TP; **132**) were prepared using two complementary methods: Suzuki–Miyaura cross-coupling
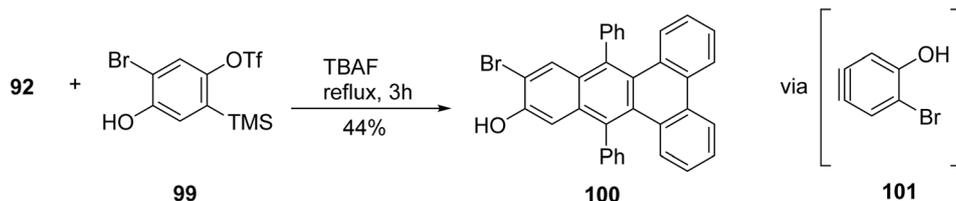
Scheme 27 Diels Alder reaction between unprotected hydroxyl containing triflate and dienone. Reproduced from ref. 90 with permission from John Wiley & Sons, copyright 2011.
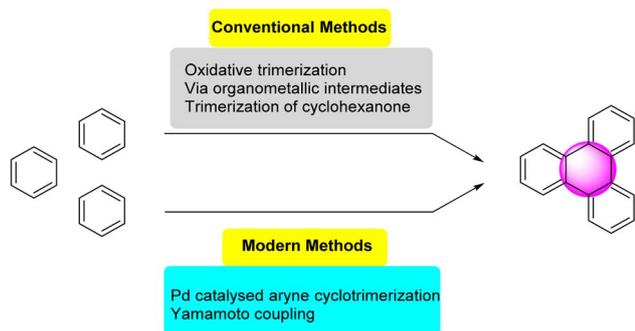
**Fig. 6** Assembling of benzene units to form triphenylene.

for arylation and S_NAr of perfluoroarenes for fluoroarylation (Scheme 37). Both strategies originate from the common precursor 2-bromo-3,6,7,10,11-pentakis(hexyloxy)triphenylene (Br-TP; **130**). Some derivatives even display columnar order at room temperature and exhibit higher thermal stability than the benchmark 2,3,6,7,10,11-hexakis(hexyloxy)triphenylene. Structural variations significantly influence mesomorphic behavior. Increasing the size and rigidity of the side aryl substituents—from phenyl (P-TP) to naphthyl (N-TP), and further to biphenyl (BP-TP)—leads to higher clearing temperatures and broader mesophase stability. Fluorination of the peripheral aryl groups produces a similar effect: derivatives bearing a greater number of fluorine atoms show enhanced Col_{hex} stability, consistent with stronger arene–fluoroarene interactions that reinforce columnar stacking.

Additional expansions of the methodology include Suzuki-type transformations on fluoroarene systems described in ref. 103, and the construction of Ar-FDLC materials designed for optoelectronic applications, as showcased in ref. 79, where fluoroarene-based mesogens were successfully integrated into LED architectures.

This work describes the synthesis of two structurally related families of π-conjugated aromatic derivatives constructed from a simple triphenylene scaffold and subsequently investigates their mesomorphic and optical behavior.[103] This study aims to achieve two goals. The first is to elucidate how fluorination of the peripheral aryl ring influences both molecular self-assembly and photophysical behavior by systematically comparing Fn with their partially fluorinated PH_n and non-fluorinated BTP_n analogues—an essential step for tailoring structure–property relationships for targeted applications (Scheme 38). The second objective is to demonstrate that the terminal fluoroarene unit **135** serves as a versatile synthetic handle, enabling the construction of new π-extended architectures that would otherwise be difficult to obtain using conventional methods. Together, these aspects underscore the potential of this approach to contribute both to the development of advanced functional materials and to the expansion of synthetic methodologies in aromatic π-systems.

Collectively, these reports establish S_NArF-driven fluoroarene chemistry as a rapidly emerging platform for generating structurally diverse and functionally rich triphenylene derivatives. The combination of predictable regioselectivity, high functional-group tolerance, and compatibility with polyfluorinated π-systems has enabled access to new molecular designs that were previously synthetically inaccessible. These advances underscore the need for a comprehensive updated review that integrates Yamamoto coupling, PCDHF chemistry, and S_NArF methodologies into a unified understanding of contemporary triphenylene synthesis.
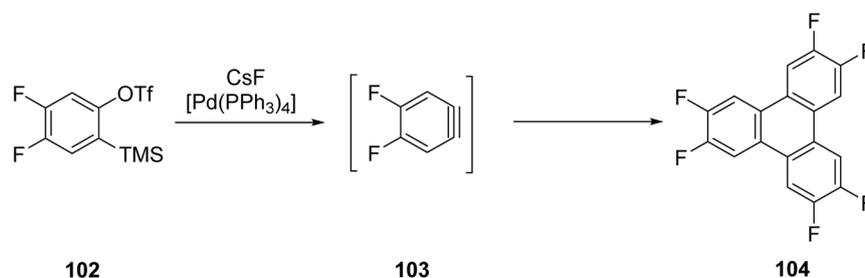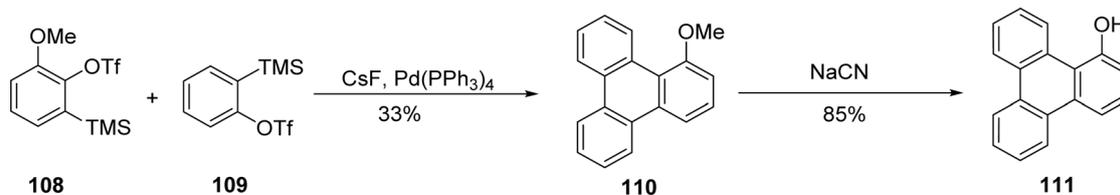

Scheme 28 Earliest Palladium catalyzed cyclotrimerization of arynes. Reproduced from ref. 74 with permission from John Wiley & Sons, copyright 1998.
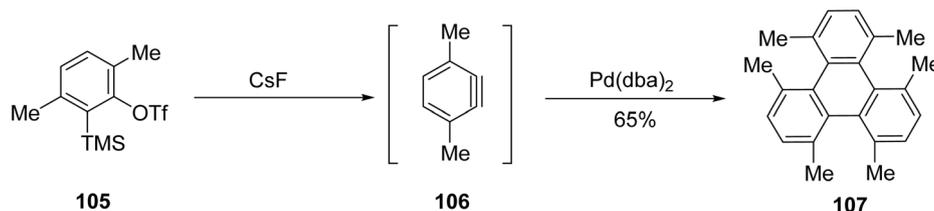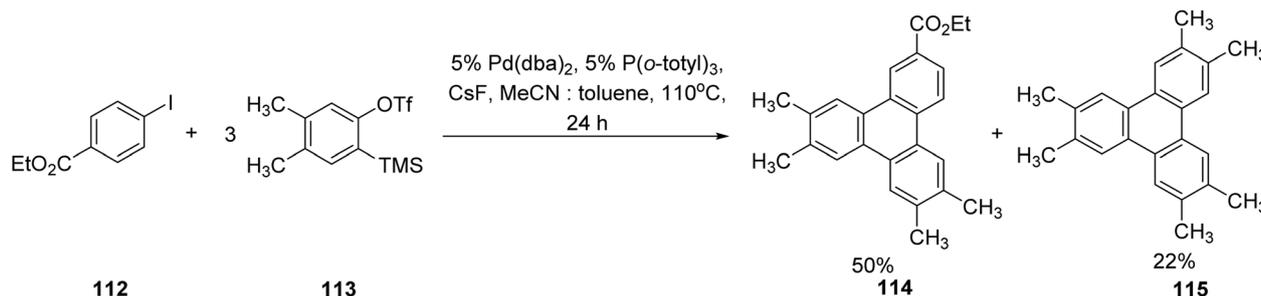

Scheme 29 Synthesis of 1,4,5,8,9,12-hexamethyltriphenylene **107**. Reproduced from ref. 94 with permission from American Chemical Society, copyright 2007.
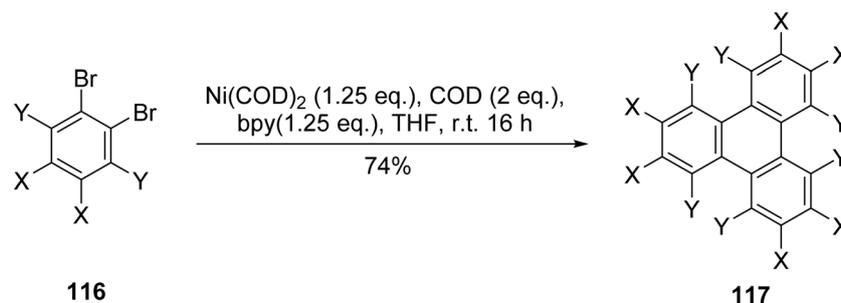
Scheme 30 Cyclotrimerization of aryne with benzyne. Reproduced from ref. 86 with permission from American Chemical Society, copyright 2008.

Scheme 31 Triphenylene synthesis by Pd-catalyzed cyclotrimerization. Reproduced from ref. 70 with permission from American Chemical Society, copyright 2005.

| Sr#	Substrate	Product	Yield %
1	X = H, Y = H	X = Y = H	59
2	X = CH$_3$, Y = H	X = CH$_3$, Y = H	58
3	X = CO$_2$CH$_3$, Y = H	X = CO$_2$CH$_3$, Y = H	74
4	X = Y = F	X = Y = F	20

Scheme 32 Cyclotrimerization of *o*-dibromobenzene by using Yamamoto coupling. Reproduced from ref. 95 with permission from Royal Society of Chemistry, under a Creative Commons Attribution-NonCommercial 3.0 Unported Licence, copyright 2021.

3. Applications for triphenylene and its derivatives

Triphenylene and its derivatives exhibit remarkable versatility, finding applications across various scientific and technological fields. In liquid crystal technology, their ability to form stable columnar mesophases through strong π–π interactions makes them valuable for semi conducting and light emitting properties and molecular self-assembly systems. As catalysts and polymers, triphenylene derivatives are used to create materials with enhanced mechanical and thermal properties, often serving as building blocks for high-performance polymers and catalytic systems in organic synthesis. In the field of chemosensing, triphenylene-derived materials are used as selective sensors capable of detecting ions, molecules, or environmental changes by taking full advantage of their adjustable photophysical characteristics and their strong bonding with the target analytes. Besides that, they are also used in energy storage applications, especially organic batteries and supercapacitors, due to their extended π-conjugation, which is responsible for the improved charge storage and transport abilities. Additionally, triphenylene derivatives are likely to be an attractive area of research in pharmaceuticals and nanotechnology, as their functionalized forms are particularly considered for drug delivery, bioimaging, and synthesis of nanoscaled materials for biomedical applications. Their unique
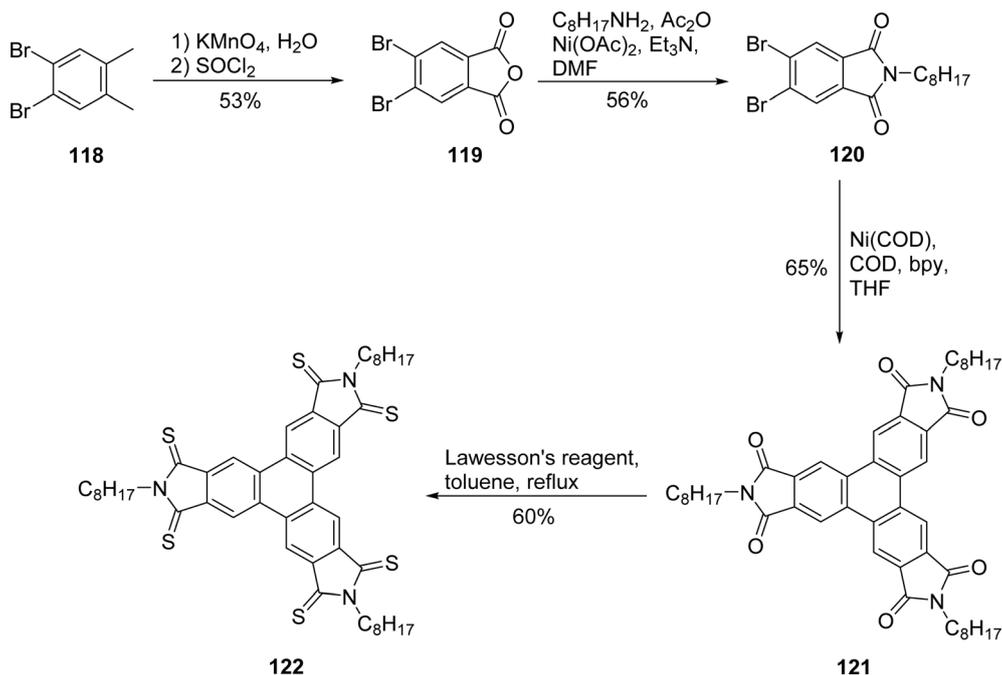
Scheme 33 Synthesis of electron deficient triphenylene trisimide and its thionated analog. Reproduced from ref. 95 with permission from Royal Society of Chemistry, under a Creative Commons Attribution-NonCommercial 3.0 Unported Licence, copyright 2021.

structural and electronic properties position triphenylene as a cornerstone for developing innovative materials in both established and emerging fields (Fig. 8).

3.1. Triphenylene derivatives as liquid crystals

Triphenylenes are among the most common compounds used in liquid crystals applications. The triphenylenes possessing flexible peripheral chains can give rise to columnar liquid crystals, which consist of vertically arranged molecules (Fig. 9). Columnar liquid crystalline materials formed by triphenylenes have been thoroughly reviewed in different literature.[8,14,36,104] In

this section we aim to focus on structural and functional features of triphenylene relevant to their emerging applications.

In optoelectronic and energy storage systems, columnar liquid crystals ordered molecule stacks can take on hexagonal, rectangular, or oblique configurations, enabling effective charge transfer. Tailoring the structure of triphenylenes allows control over their mesomorphic properties. Specifically, modification of side-chains, changing the linker between the side chains and the core, and incorporation of substituents on the core can all be used to control liquid crystalline properties. In addition, the incorporation of triphenylene units into dimeric and trimeric structures can be used to control properties.[8]
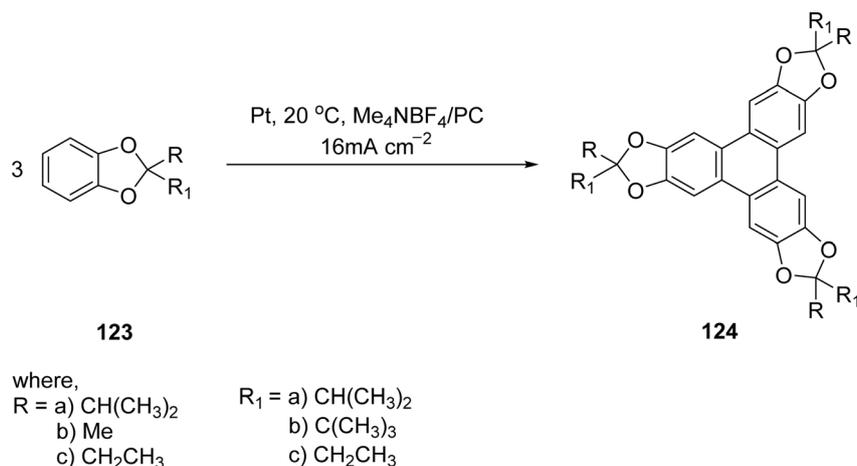
Scheme 34 Anodic oxidation of catechol ketals to 2,3,6,7,10,11-hexahydroxytriphenylene Reproduced from ref. 99 with permission from Beilstein Institute for the Advancement of Chemical Sciences, a German non-profit foundation, copyright 2012.
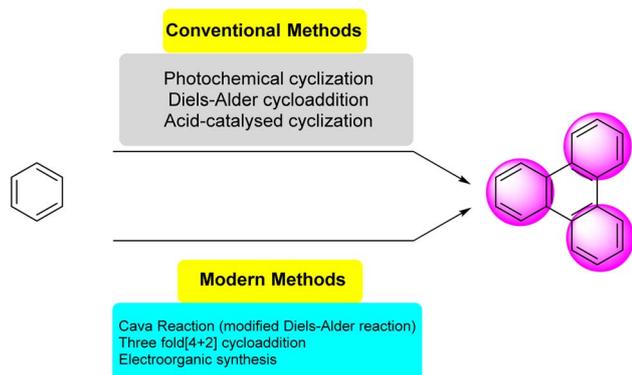
**Fig. 7** Addition of peripheral rings methods to form triphenylene.

The design principles for discotic liquid crystals with varied molecular tails have been comprehensively reviewed.[36] In these systems, modifying the side chains attached to the triphenylene core enables control over mesophase behavior.[105] Zhao *et al.* undertook a study to investigate the effectiveness of using fluorinated chains on the self-assembling behaviour of triphenylene discotic liquid crystals to expand the knowledge concerning their mesomorphic behaviour and thermal stability (Fig. 10).[106] Their studies showed that triphenylenes bearing fluorinated ester side chains **136, 137, 138** exhibited columnar hexagonal mesophases, and that the incorporation of fluorinated side chains increased the clearing points as compared to their non-fluorinated analogs.[107]

Beyond side chains, altering the core has proven impactful; for instance, triphenylene hexacarboxylic ester derivatives with electron-withdrawing ester groups influence the thermal stability, clearing temperatures, and overall mesophase behavior of discotic liquid crystals.[108,109] In a related study, for example, Varshney synthesized compound **140A** by nitration of hexaalkoxytriphenylene **139A** and characterized its liquid crystalline properties. Most significantly, they possessed a wide thermal range in the hexagonal columnar liquid crystal phase. He also succeeded in showcasing structural isomerism by controlling the functionalization of specific sites on the triphenylene core to get different isomers. This work demonstrates that strategic core substitution both in terms of

functional group identity and positional isomerism is a powerful tool for fine-tuning the thermal stability, mesophase range, and functional versatility of triphenylene-based discotic liquid crystals (Fig. 11).[110]

Another approach to controlling the mesomorphic properties of triphenylenes is to link them together *via* groups capable of hydrogen bonding. For example, a novel liquid crystalline 1,3,5-benzenetrisamide bearing three triphenylene units has been synthesized, where intermolecular hydrogen bond-stabilizes columnar discotic liquid phase.[111] This highly ordered compound exhibits a plastic columnar discotic hexagonal phase (ColhP), characterized by exceptional charge carrier mobility for triphenylene based liquid crystal (Fig. 12). The structural design promotes π–π stacking of triphenylene moieties, resulting in robust charge transport pathways. Further optimization of the molecular orientation within the π-stacked columns could enhance charge mobility, making this material highly promising for organic electronic applications.[111]

Early work by Sergeyev and co-workers[8] demonstrated that benzene trisamide derivatives with peripheral triphenylene units could form unusual columnar mesophases, attributed to strong π–π stacking and hydrogen bonding within the trisamide linkers. Building on the concept of covalently linking triphenylene discotic units to a central core, El Mansoury and coworkers reported the synthesis of a series of novel star-shaped oligomers comprising triphenylene discogen units tied to a central benzene core.[112] They showed that although a higher branching within the oligomers could generate liquid crystal properties within the system, longer chains were highly essential for the development of the desired columnar phase **141** (Fig. 13).[112] More recently, Yang and coworkers focused on the development of novel discotic liquid crystal oligomers based on 1,3,5-triazine, featuring triphenylene dimers and trimers.[113] The newly synthesized compound **142** (Fig. 14) exhibits broad mesophase ranges, combining the self-assembling capabilities of triphenylene with the structural versatility of the 1,3,5-triazine core. The presence of triphenylene units in both dimeric and trimeric forms improve the stability and functionality of the mesophases, thus making these materials quite advantageous for high-end applications in liquid crystal displays (LCDs) and optoelectronic devices. Through the
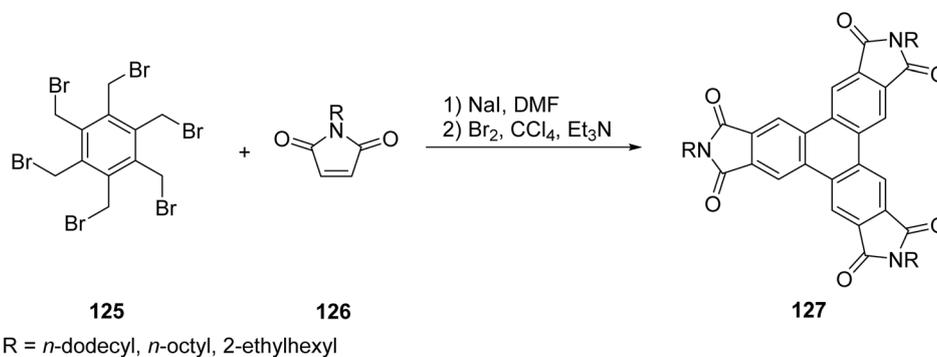
Scheme 35 Synthesis of triphenylene derivatives having carboximides. Reproduced from ref. 100 with permission from American Chemical Society, copyright 2009.
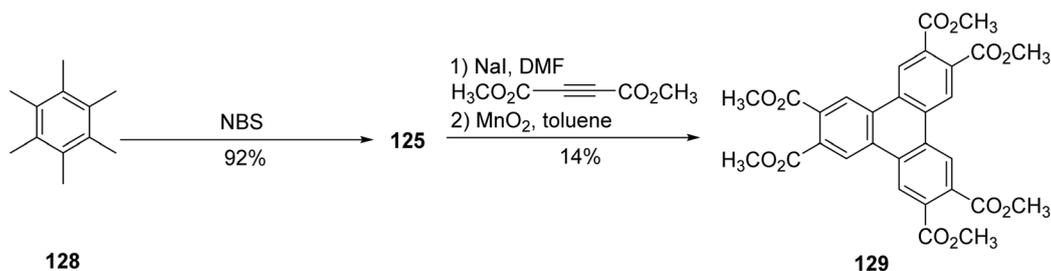
Scheme 36 Preparation of triphenylene hexaester **129**. Reproduced from ref. 101 with permission from John Wiley & Sons, copyright 2012.

analysis of their thermal and optical properties, the research brings out the noteworthy capability of these oligomers for the forthcoming liquid crystalline technologies.

Modifying molecular structures through linkage groups such as in star-shaped and oligomeric triphenylene systems provides additional means to modulate mesophase type and stability.[115] The diversity of the various synthetic strategies shows clearly that the molecular design can make the triphenylene-based discotic liquid crystals suitable for the optoelectronic and energy applications. Zhao and his co-workers started their novel work using the copper-catalyzed coupling cycloaddition reaction to create four different star-shaped oligomer structures.[116] The oligomers were TP-discotic mesogens that played the key role in forming the right order of liquid crystal phases (Fig. 15). The oligomers have three lateral triphenylene units that are connected by methylene spacers to a central 1,3,5-tris(triazolyl) benzene core **143**, where the length of the spacer is a critical factor in the mesophase formation. They further indicated that one non-mesomorphic oligomer could be used to form hydrogen-bonded supramolecular complexes with simple acids in the ratios of 1 : 2 or 1 : 3 that led to the emergence of the columnar mesophases. Such an extension greatly enhanced their research, allowing them to obtain even deeper knowledge about the structural diversity and functional versatility of the materials involved in their study.[116]

Bi *et al.* synthesized and investigated several triphenylene esters with two ester substituents to improve the charge carrier mobility and structural ordering of discotic liquid crystals.[117] These modifications promoted highly ordered columnar superlattice nanostructures through thermotropic self-assembly, which enhanced their electrical properties. Among these the 3,6-substituted triphenylene ester T5E36 **144** (Fig. 16) created a unique helical hexagonal columnar superlattice structure composed of 91 right-handed helices. With bipolar charge carrier mobility of about 10^{-1} cm^2 V^{-1} s^{-1}, the helical superlattice nanostructure enhanced electrical characteristics and increased its appeal in organic electronics.

3.1.1. Oligomeric and fused triphenylene-based rigid architectures. Beyond monomeric discotic systems, significant progress has been made in the development of oligomeric, fused, and rigid molecular architectures incorporating triphenylene units, which offer enhanced π-extension, improved
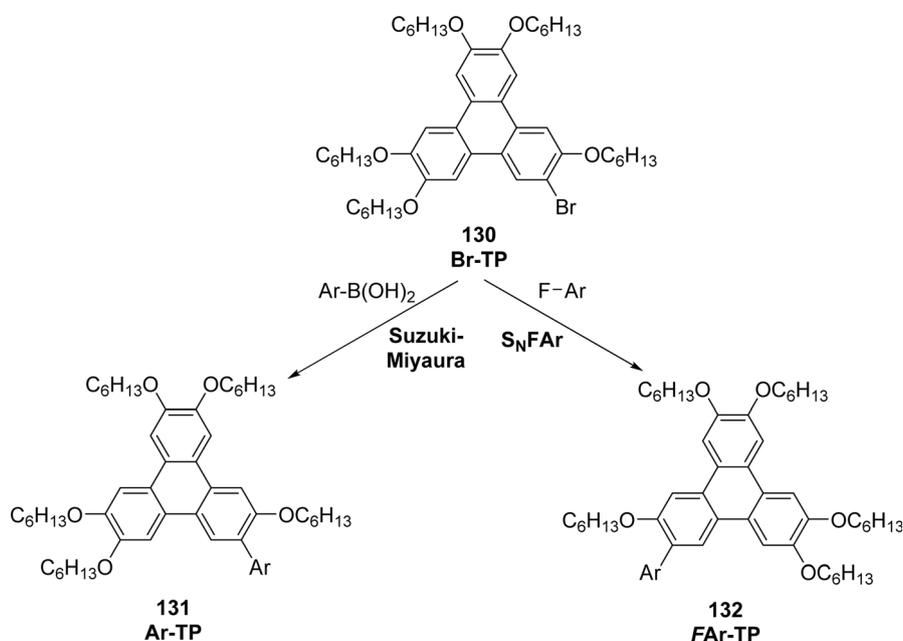
Scheme 37 Synthesis of aryl- and fluoroaryl-functionalized triphenylenes. Reproduced from ref. 102 with permission from Elsevier under the terms of the Creative Commons CC-BY license, copyright 2024.

R = C_3H_7, C_4H_9, C_5H_11, C_6H_13, C_8H_17, C_10H_21, C_12H_25
R' = C_4H_9, C_5H_11, C_6H_13
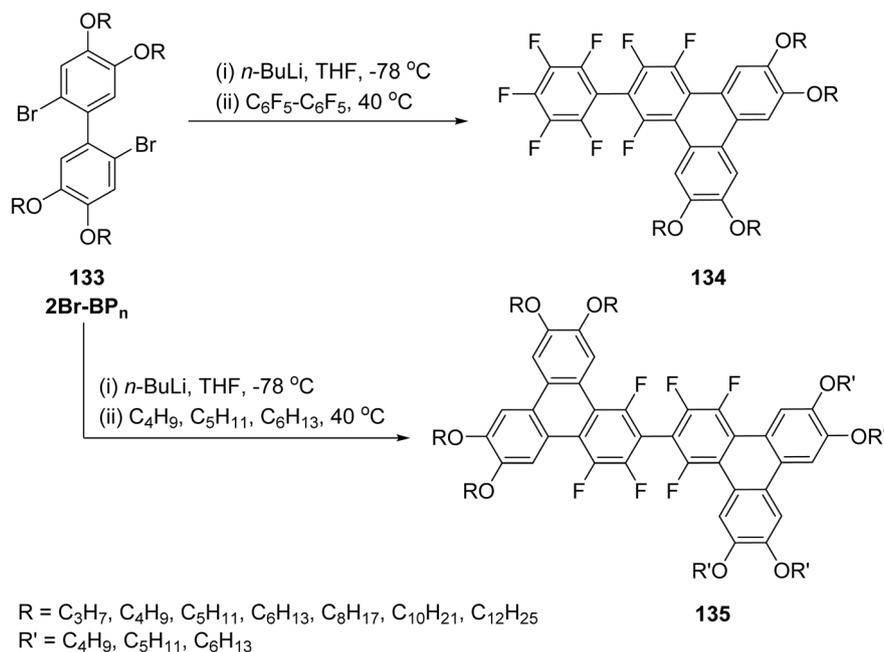
Scheme 38 Synthesis of fluorinated triphenylene. Reproduced from ref. 103 with permission from Beilstein Institute for the Advancement of Chemical Sciences, a German non-profit foundation, copyright 2024.

charge transport, and finely tunable self-assembly behavior. These structurally complex systems represent an important evolution in triphenylene chemistry and have attracted increasing attention over the past decade.

Early studies demonstrated that covalently linked triphenylene oligomers and fused polycyclic frameworks could be accessed through controlled oxidative cyclization, annulative coupling strategies, and stepwise aryl–aryl bond formation,

leading to rigid, shape-persistent architectures with extended conjugation. Triphenylene dimers represent a structurally distinctive class of π-conjugated systems, and when two triphenylene units are interconnected at the 3,6-positions via dipyrromethene linkers, they give rise to a novel family of macrocyclic architectures. These assemblies can be regarded as rigid, porphyrin-like expanded macrocycles in which structural constraints enforce near coplanarity despite the presence of
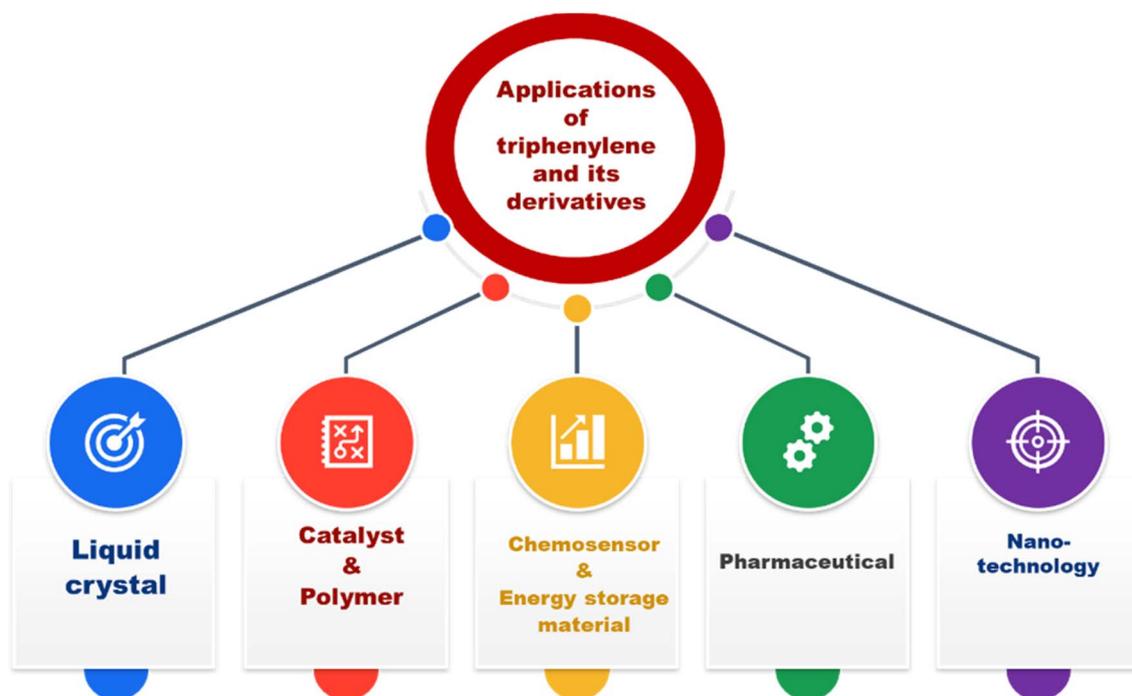

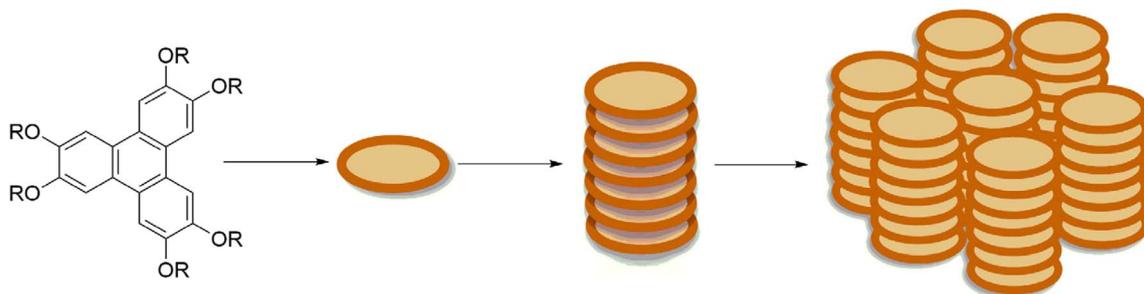**Fig. 8** Applications of triphenylene and its derivatives.

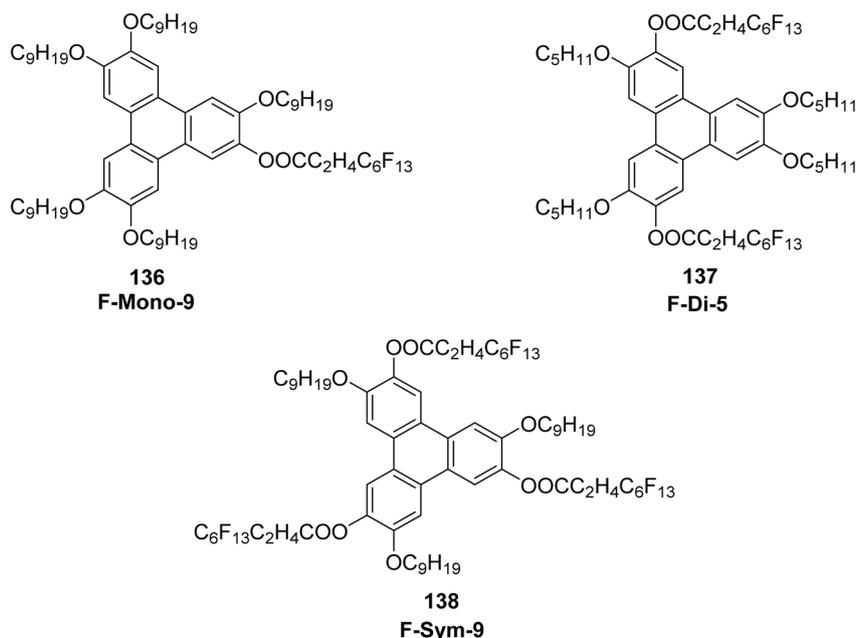**Fig. 9** Self-assembly of TP as DLCs into columnar phase.

Fig. 10 Triphenylene discotic liquid crystals with fluorinated ester chains studied. Reproduced from ref. 107 with permission from Royal Society of Chemistry, copyright 2011.

a formally antiaromatic π-electron framework.[118] Notably, the macrocyclization process results in an unexpected stabilization of the dipyrromethene chromophoric units, highlighting the beneficial electronic effects induced by rigidification and extended conjugation within the macrocyclic scaffold.[119] Later on, quinoxalino[2′,3′:9,10]phenanthro[4,5-*abc*]phenazine (QPP) derivatives **145** are of interest as electron acceptors, fluorescent

materials, and self-organizing organic semiconductors. Condensation of tetraketopyrene with electron-rich diamino terphenylene or triphenylene units yields donor–acceptor QPP systems that exhibit broad columnar mesophases, strong fluorescence across solution and solid states, and effective electron-accepting behavior. The study also reports the first synthesis of diamino-tetraalkoxytriphenylene, providing a useful new
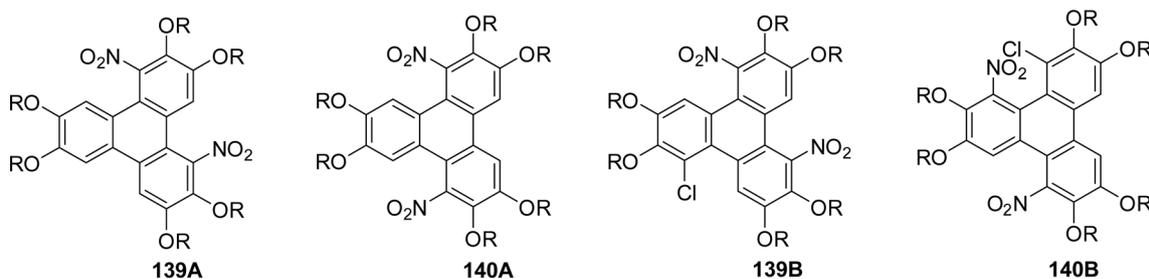

Fig. 11 Dinitro substituted hexa(alkoxy)triphenylene and monochlorohexa(alkoxy) triphenylene. Reproduced from ref. 110 with permission from Taylor & Francis, copyright 2024.
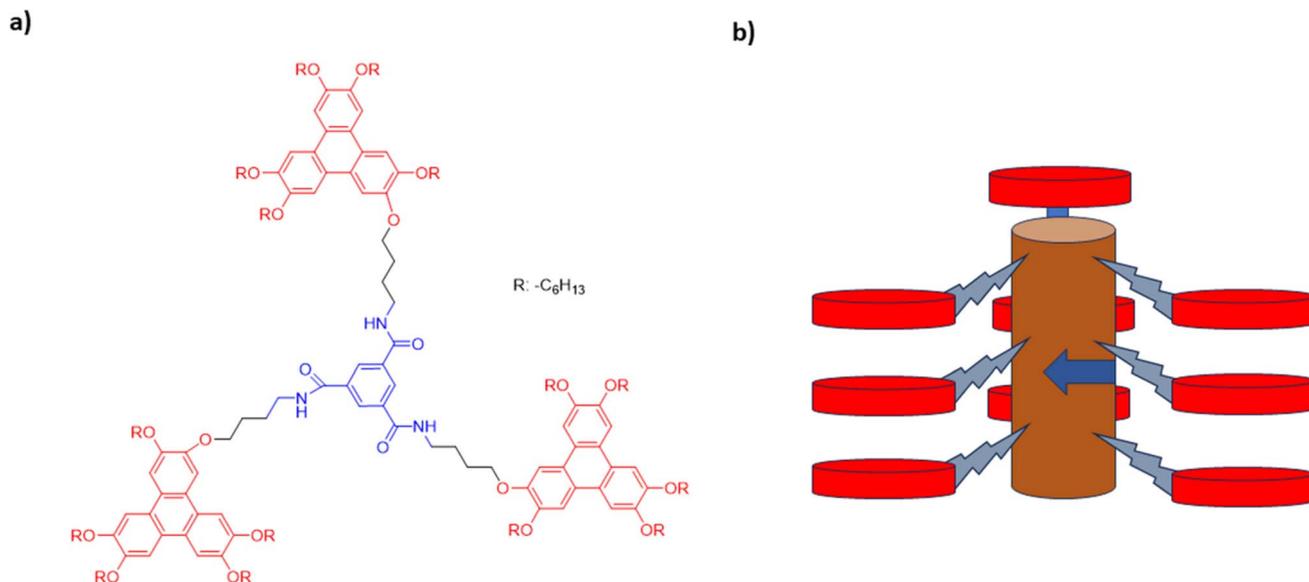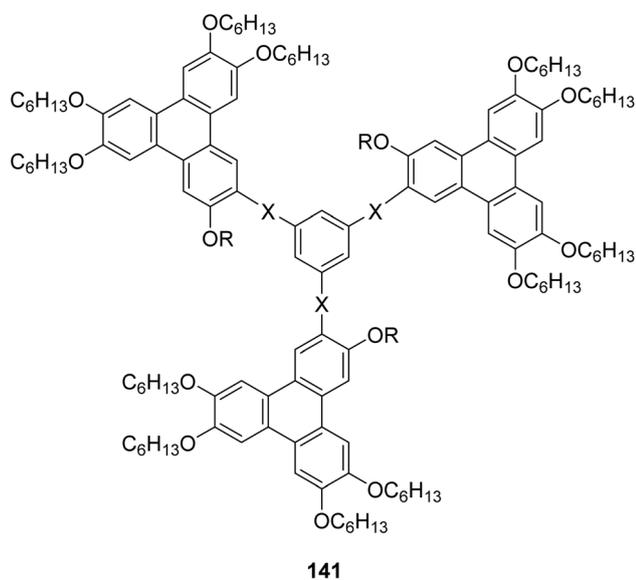
a)

b)

Fig. 12 (a) Structure of C_3-symmetrical trisamide derivative 1 (b) image showing the central trisamide hydrogen-bond stabilized column (blue) surrounded by three triphenylene π-stacked coilumns (red). The hydrogen bond helical network is indicated by the blue arrow. Reproduced from ref. 111 with permission from American Chemical Society, copyright 2006.

141

141A: R = -C_6H_13 X = -CH_2O
141B: R = -CH_3 X = -O(CH_2)_4O
141C: R = -C_6H_13 X = -CH_2O(CH_2)_6O

Fig. 13 Model 'star-shaped' oligomers. Reproduced from ref. 112 with permission from Taylor & Francis, copyright 2012.

building block for functional material design (Fig. 17).[120] These pioneering contributions established synthetic blueprints for assembling higher-order triphenylene-based systems while maintaining structural precision.

Subsequent efforts focused on electronic communication and photophysical modulation within fused or oligomeric triphenylene arrays. Investigations revealed that increasing molecular rigidity and conjugation length significantly influences exciton delocalization, fluorescence behavior, and charge carrier mobility.[121] The incorporation of peripheral δ-methyl-branched alkyl chains together with aromatic moieties, including o-terphenyl or triphenylene units, onto a symmetry-lowered crown-ether core **146** (Fig. 18) results in the formation of hexagonal columnar mesophases that are stable at room temperature, with mesophase temperature ranges extending up to 147 K.[122] These findings underscored the importance of controlled fusion patterns and molecular topology in dictating functional properties.

More recent reports expanded this concept toward functional materials and device-relevant applications, including organic electronics and emissive systems. Several studies demonstrated that rigid triphenylene-containing oligomers exhibit enhanced thermal stability, improved mesophase organization, and superior optoelectronic performance compared to their monomeric analogues. Two new large N-heteroarene discotic systems based on triphenylene-type architectures were prepared using a modular cross-coupling/annulation strategy. Carbazole- and fluorene-fused ditriphenylene derivatives were synthesized via Suzuki–Miyaura coupling of suitable diboronic esters with alkylated 2-bromobiphenyl precursors, followed by FeCl_3-mediated Scholl cyclization **147** (Fig. 19). Related fluorenone-fused ditriphenylenes were accessed through an inverted coupling sequence. Polarized optical microscopy revealed that several of these triphenylene-derived "butterfly" structures (carbazole (CTP), fluorenone (FTP) and fluorene (LTP)) exhibit mesomorphic behavior, self-assembling into hexagonal columnar phases characterized by fan-shaped textures, consistent with their rigid, π-extended discotic cores.[123]

The work describes the synthesis of rigid π-bridged triphenylene dimers and highlights their liquid-crystalline
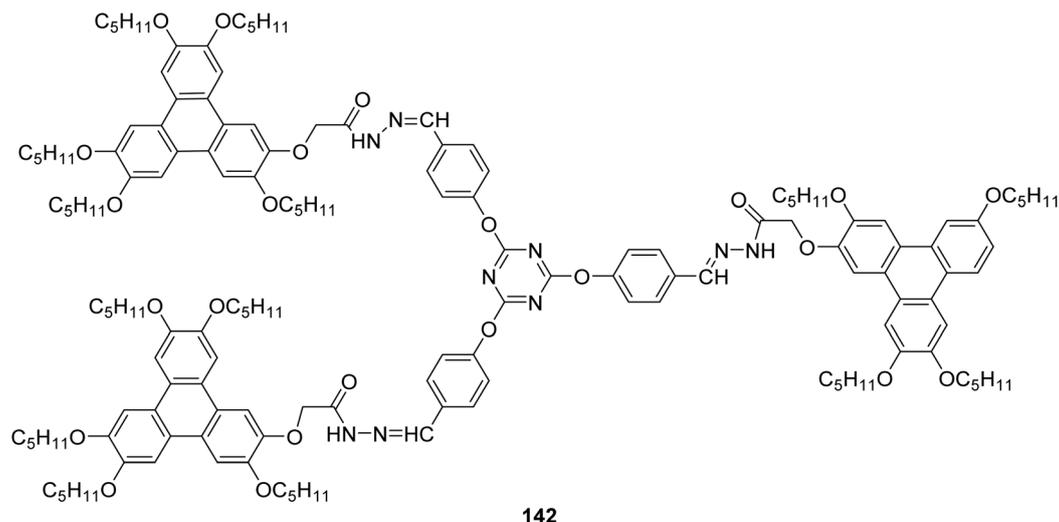
Fig. 14 Chemical structure of 1,3,5-triazine-based triphenylene trimer. Reproduced from ref. 114 with permission from Taylor & Francis, copyright 2012.

behavior. Covalent linking of two triphenylene units produces enlarged, rigid aromatic cores that promote strong π–π interactions and efficient self-assembly. Several dimers exhibit stable hexagonal columnar mesophases over wide temperature ranges, showing enhanced mesophase stability compared with monomeric triphenylenes. This study demonstrates that π-bridging is an effective approach to modulate the self-organization and optical properties of triphenylene-based discotic liquid crystals.[118] These attributes are particularly

advantageous for applications requiring long-range molecular order and stability.

Deng *et al.*, reported the design and synthesis of butterfly-shaped ditriphenylenothiophene derivatives, exploring how variations in the polyarene core topology influence their liquid crystalline behavior.[124] The compounds self-assemble into columnar mesophases, with the core geometry strongly affecting the organization and stability of the mesophase. Optical studies reveal that the fluorescence properties are

Fig. 15 Star-shaped triphenylene discotic oligomers. Reproduced from ref. 116 with permission from Royal Society of Chemistry, copyright 2015.

144

Fig. 16 Chemical structure of the T5E36. Reproduced from ref. 117 with permission from Royal Society of Chemistry, copyright 2019.
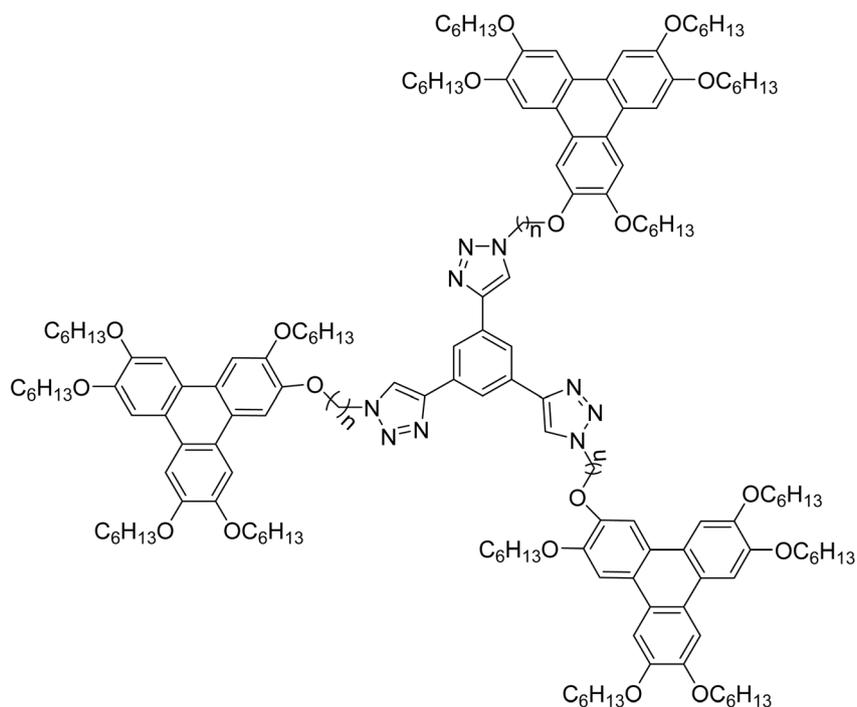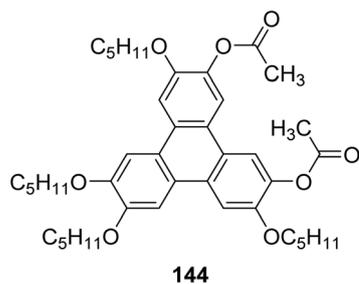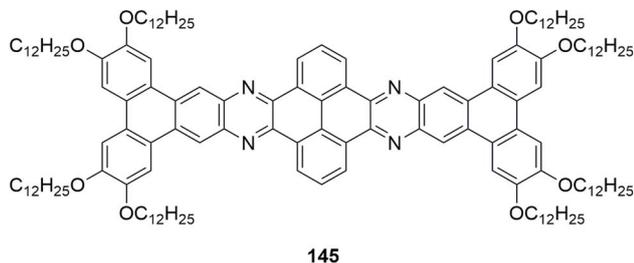
145

Fig. 17 Chemical structure of QPP-triphenylene derivative. Reproduced from ref. 120 with permission from American Chemical Society, copyright 2013.

146

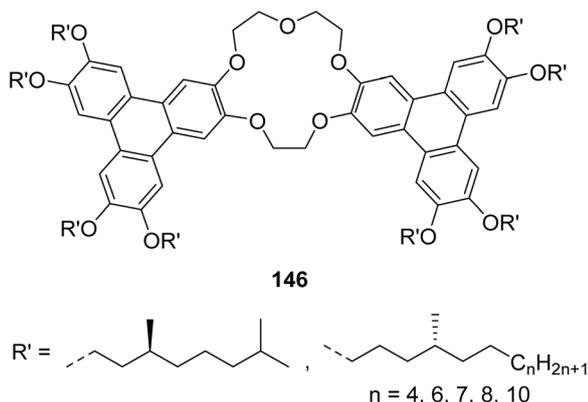$$R' = \quad , \quad C_nH_{2n+1}$$

n = 4, 6, 7, 8, 10

Fig. 18 Chemical structure of [15]crown-5 derivative. Reproduced from ref. 122 with permission from John Wiley & Sons, copyright 2016.

modulated by the molecular arrangement, while photoconductivity measurements demonstrate enhanced charge transport along the columnar stacks. Overall, this work highlights the critical role of polyarene core topology in tuning the self-assembly, optical, and electronic properties of triphenylene-based liquid crystals, offering insights for the design of functional discotic materials.[124]

Advanced synthetic methodologies have further enabled access to diverse fused triphenylene motifs, including ladder-type structures and extended polycyclic aromatic hydrocarbons **148**, broadening the structural landscape of triphenylene-based materials in liquid crystals. This work reports the synthesis of triphenylene dimers connected *via* linear and bent

147
CTP, FTP, LTP

X = NC$_8$H$_{17}$, CO, CMe$_2$, C(C$_8$H$_{17}$)$_2$
R = C$_n$H$_{2n+1}$
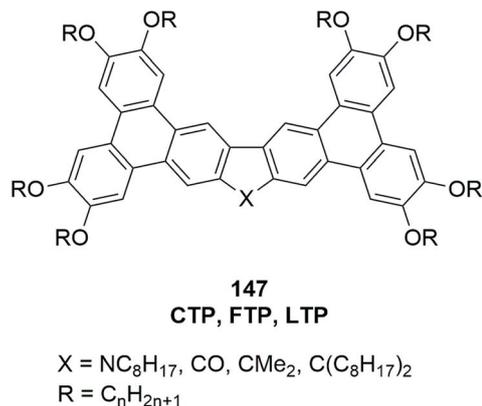
Fig. 19 Chemical structure of CTP, FTP and LTP butterflies and precursors. Reproduced from ref. 123 with permission from John Wiley & Sons, copyright 2021.

alkyne–aryl–alkyne linkers (Fig. 20) and investigates their mesomorphic behavior.[125] The rigid π-conjugated bridges promote strong π–π stacking, facilitating the formation of well-ordered columnar liquid-crystalline phases. The study highlights how linker geometry influences the stability, temperature range, and alignment of the mesophases. These structurally tunable triphenylene dimers demonstrate potential for applications in discotic liquid crystal devices, including organic electronics and optoelectronic materials, where controlled self-assembly and charge transport are critical.[126] Such systems often display unique solid-state packing and enhanced intermolecular interactions, contributing to improved charge transport characteristics.[125]

Donnio *et al.* (2023) presented the development of star-shaped triphenylene–triazine architectures **149** as a new class of multi-stimuli-responsive discotic liquid crystals (Fig. 21).[127] By integrating triphenylene discotic units with a triazine core, the resulting materials exhibit well-defined columnar liquid-crystalline phases driven by strong π–π stacking and peripheral chain organization. These systems respond sensitively to external stimuli such as temperature, light, and chemical environment, enabling reversible modulation of their mesomorphic and optical properties. Owing to their ordered columnar structures and tunable responsiveness, triphenylene–triazine discotic liquid crystals show significant potential for
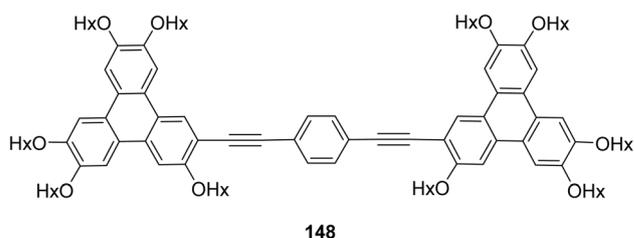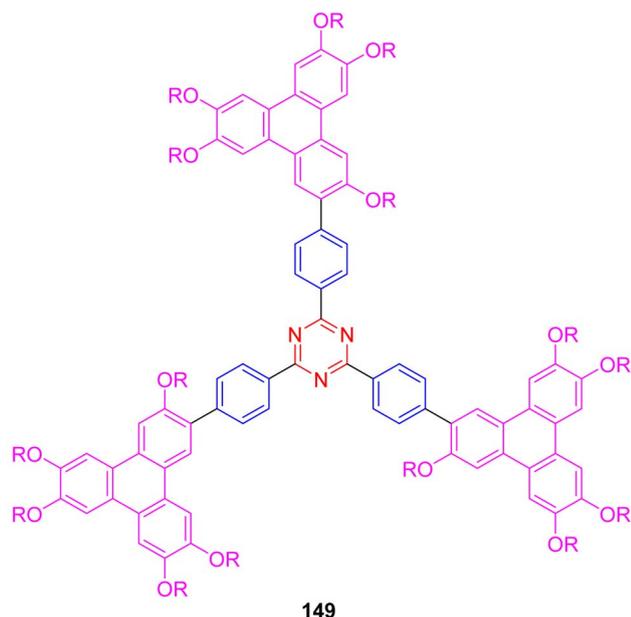
148

Fig. 20 Chemical structure of alkyne–arylalkyne bridged triphenylene dimer. Reproduced from ref. 126 with permission from John Wiley & Sons, copyright 2022.

where,
R = -C₆H₁₃, -C₈H₁₇, -C₁₂H₂₅

where,
R = $-C_6H_{13}$, $-C_8H_{17}$, $-C_{12}H_{25}$

Fig. 21 Molecular structure of star-shaped triphenylene-phenyl-triazine derivative. Reproduced from ref. 127 with permission from the Chinese Chemical Society (CCS) and the Shanghai Institute of Organic Chemistry (SIOC), copyright 2023.

applications in organic electronics, optoelectronic devices, and smart functional materials.[127]

Very recent contributions highlight the growing relevance of these rigid triphenylene architectures in next-generation functional materials, including luminescent systems and emerging device platforms. For example, tetraphenylethylene (TPE) and triphenylene (TP) units were combined within crossed-shaped tetrads (TPE-TP4; **150** and TPE-ThTP4; **151**) *via* Suzuki–

Miyaura coupling to develop multifunctional mesomorphic materials.[128] TPE provides strong aggregation-induced emission (AIE), while TP promotes columnar self-assembly. TPE-TP4 (Fig. 22) exhibits crystalline behavior with reversible melting, whereas TPE-ThTP4 forms a rectangular multicolumnar (Col_{rec}) phase over a broad temperature range (∼300 °C). Both compounds self-assemble into fibrous gels in various solvents and display strong fluorescence in solution and thin films (460–550 nm) with solvent-dependent quantum yields up to 84.5%. These findings highlight the potential of combining discotic mesogens with AIE-active units for advanced liquid crystal-based optoelectronic applications.[128]

A triskelion-shaped mesogen was constructed by linking a central hexabenzocoronene (HBC) core to three radial triphenylene (TP) units **152** (Fig. 23).[129] The resulting π-extended oligomer exhibits a broad temperature columnar mesophase with self-sorted HBC and TP stacks arranged in a rectangular 2D lattice. Photophysical studies show combined absorption features from both HBC and TP, with emission primarily from HBC. The compound also displays ambipolar charge transport with a dominant electron mobility, highlighting its potential for liquid crystal-based electronic applications.[129] These studies collectively demonstrate that oligomeric and fused triphenylene systems represent a fertile area for future exploration, particularly at the interface of molecular design, self-assembly, and materials performance.

Taken together, these works emphasize that rigid and π-extended triphenylene-containing systems constitute a crucial and rapidly advancing subfield, complementing classical discotic liquid crystals and opening new avenues for high-performance organic materials.

3.1.2. Multi- and metal-related functionalization of triphenylene derivatives. Recent advances in triphenylene chemistry have extended beyond classical discotic liquid crystals to
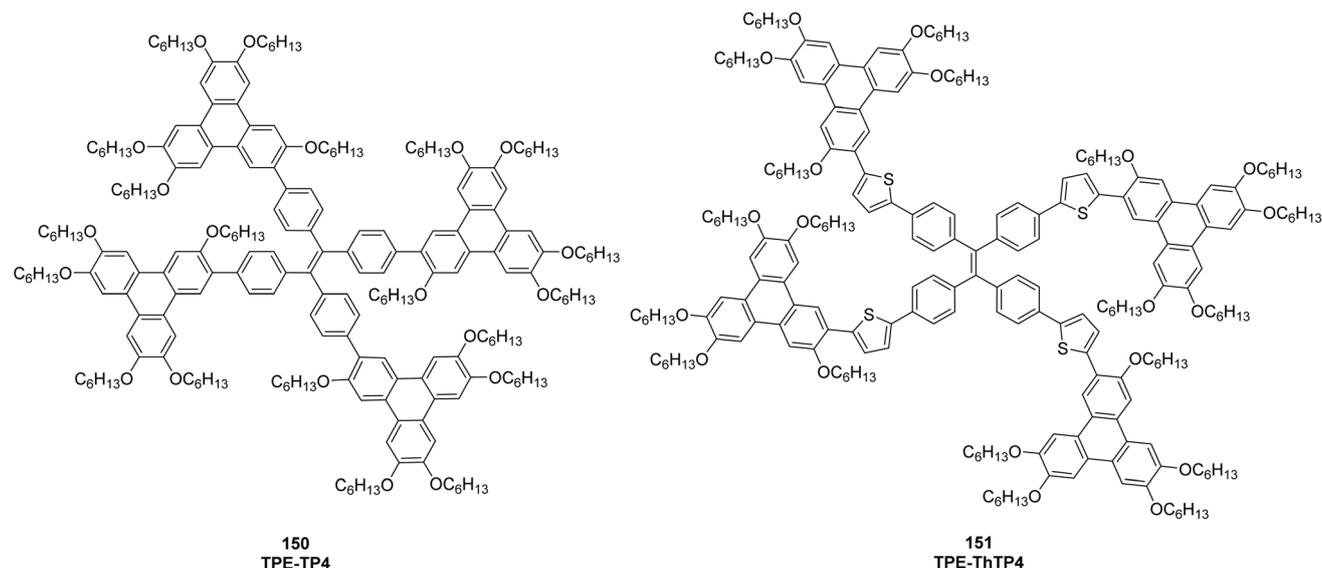

Fig. 22 Star-like tetraphenylethylene-triphenylene tetrads **150** (TPE-TP4) and **151** (TPE-ThTP4). Reproduced from ref. 128 with permission from Elsevier, copyright 2025.
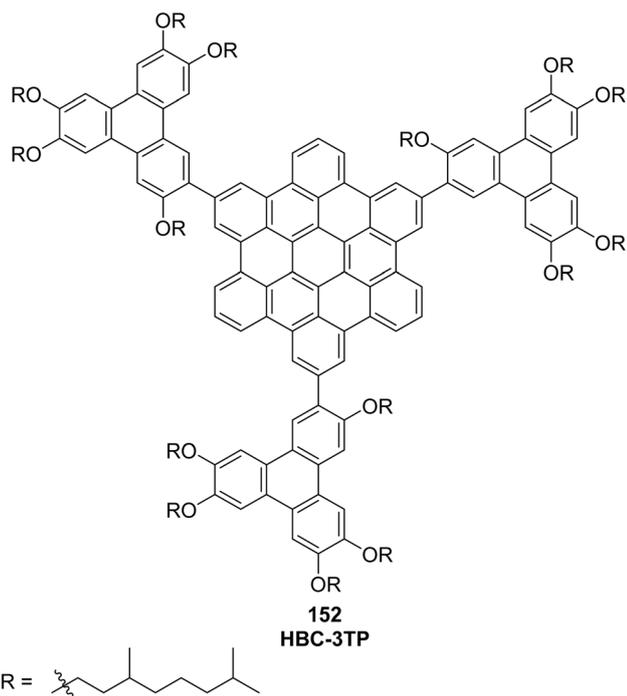
© 2026 The Author(s). Published by the Royal Society of Chemistry

152
HBC-3TP

R =

encompass multifunctional and metal-functionalized systems that offer enhanced structural complexity and broadened application potential.

Direct functionalization of the central aromatic core remains synthetically challenging due to steric and electronic constraints; however, new amidoalkylation protocols have enabled efficient C–H alkylation at internal triphenylene positions, producing C_3-symmetric tris-alkylated derivatives in good yields and introducing versatile sites for further derivatization and tuning of electronic properties.[130]

C_3-Symmetric triphenylene derivatives functionalized with amide groups at the 1-, 5-, and 9-positions **153** were designed and synthesized as modular building blocks for self-assembly (Fig. 24). The molecules formed supramolecular gels through a combination of hydrogen bonding, π–π stacking, and van der Waals interactions. Furthermore, by varying the length of the peripheral alkyl chains, these assemblies exhibited liquid crystalline mesophases. This study highlights a representative example of functional C_3-symmetric triphenylene-based supramolecular materials.[131]

Dendronized triphenylene derivatives **154** were synthesized and shown to undergo hierarchical self-assembly into well-defined supramolecular architectures, including helical pyramidal columns and chiral spherical aggregates (Fig. 25).[132] The formation of these structures is driven by a combination of π–π stacking, hydrogen bonding, and steric effects of the peripheral dendrons. These assemblies exhibit liquid crystalline behavior, with the ability to form columnar mesophases and chiral superstructures. This study demonstrates how

functionalization of the triphenylene core with dendritic units enables precise control over molecular organization, offering potential applications in chiral optoelectronic materials and advanced liquid crystalline systems.[132]

Mesogenic Rh(L4) complexes were investigated for their liquid crystalline behavior, revealing the formation of columnar mesophases in which RhI···RhI interactions and triphenylene-discotic cores segregate into distinct columns.[133] The presence of the counterion $A^- = [Au(CN)_2]^-$ influences the packing and enhances charge transport, particularly hole mobility, within the mesophase. This study highlights how metal–metal interactions and discotic triphenylene units can be strategically combined to design liquid crystalline materials with tunable electronic properties.[133]

Coordination of metal ions to triphenylene-based Schiff base derivatives **155** significantly enhances hole mobility in their multicolumnar liquid crystalline mesophases (Fig. 26). The study demonstrates that metal–ligand interactions promote more ordered columnar stacking, improving charge transport while maintaining the mesomorphic behavior of the triphenylene cores. These findings underscore the potential of metal-functionalized triphenylene mesogens for high-performance organic electronic applications.[134]

Triphenylene–bis(dithiolene)nickel complexes **156** form columnar liquid crystalline mesophases that exhibit soft photothermal properties (Fig. 27). The organized columnar arrangement of the triphenylene cores, combined with the nickel-dithiolene units, enables efficient light absorption and conversion to heat, highlighting their potential for photothermal applications in soft materials and optoelectronic devices.[135]

Imidazolium-annulated triphenylene derivative **157** exhibits discotic columnar mesophases driven by the positive core charge of the imidazolium units (Fig. 28). The electrostatic interactions, combined with π–π stacking of the triphenylene cores, promote organized self-assembly into columnar structures, demonstrating the role of charged cores in modulating mesomorphic behavior and enabling potential applications in ionic liquid crystalline materials.[136]
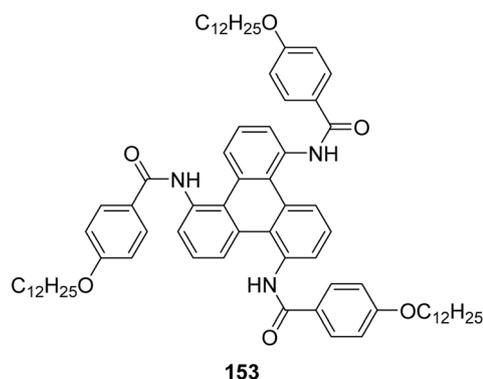

153

Fig. 24 Chemical structure of C_3-symmetric triphenylene derivative functionalized with amide groups at the 1-, 5-, and 9-positions. Reproduced from ref. 131 with permission from Royal Society of Chemistry, copyright 2017.
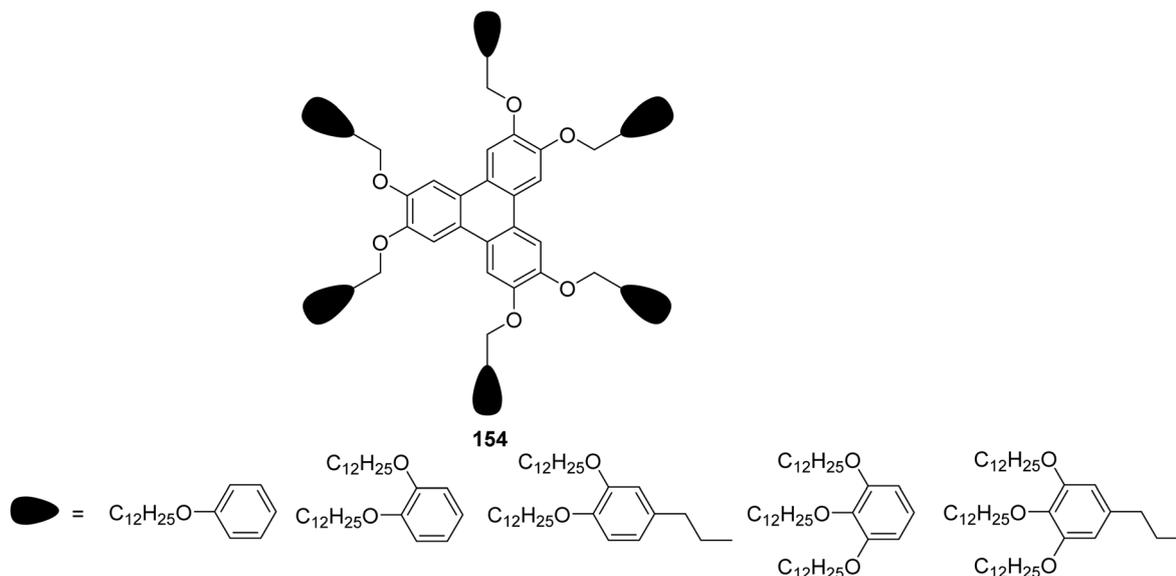
Fig. 25 Dendronized triphenylene derivatives **154**. Reproduced from ref. 132 with permission from American Chemical Society, copyright 2009.

Collectively, these developments demonstrate that multi-functionalization strategies and metal incorporation expand the design space of triphenylene-based compounds well beyond simple discotic mesogens, enabling tailored self-assembly, enhanced electronic functionality, and new applications in organic electronics, sensing, and hybrid materials.

3.2. Triphenylene derivatives as catalysts

Triphenylene-based materials have emerged as catalysts due to their rigid, planar and π-conjugated structures which allow for strong π–π stacking interactions and charge transfer. These properties make them extremely suitable for photo-catalysis and electro-catalysis where light absorption and electron mobility are important. Their enlarged π-systems give rise to their catalytic potency by making the redox cycle easier, stabilizing the intermediate steps, and providing either electrons or

accepting them. Besides, the molecular structures can be tailored to the characteristics required through functionalization which in turn leads to various applications in oxygen reduction, hydrogen generation, pollutant degradation, and other organic transformations. Their role in eco-friendly catalytic systems is further backed up by their durability, versatility and thermal stability.

Triphenylene units, having an identity of their own, can endow strong π-conjugated systems for the accurate placement of catalytically active groups and tuning the electronic properties. For example, the rigid triphenylene structure plays a crucial role in controlling the geometry of a triphenylene-tris-NHC ligand synthesized and coordinated to Ir and Au centres,[137] thus resulting in catalytic (yield/turnover) activity that is better than simple mono-metallic analogs. One potential direction for developing the next generation of catalysts could be the use of triphenylene in two-dimensional polymers. To illustrate, Zhao
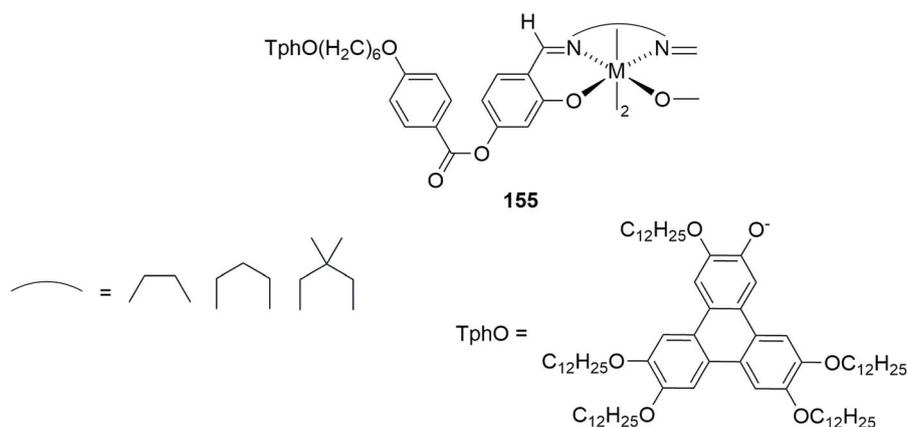

Fig. 26 Chemical structure of triphenylene-based Schiff base metal complexes. Reproduced from ref. 134 with permission from American Chemical Society, copyright 2020.
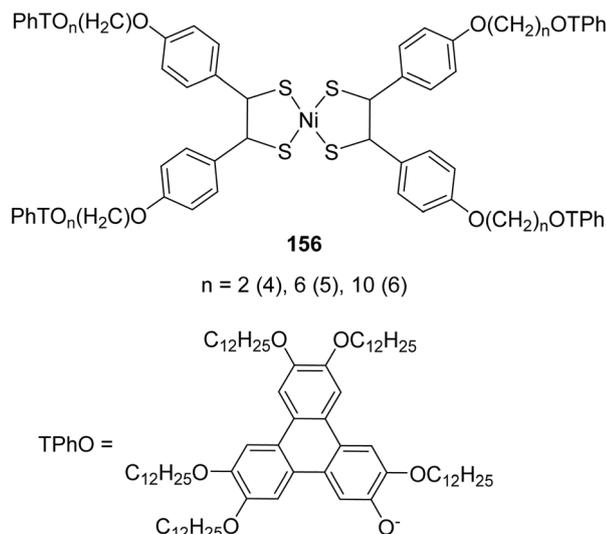
156

n = 2 (4), 6 (5), 10 (6)

TPhO =

Fig. 27 Chemical structure of triphenylene-bis(dithiolene)nickel complexes. Reproduced from ref. 135 with permission from Royal Society of Chemistry, copyright 2024.

157

Fig. 28 Chemical structure of imidazolium-annulated triphenylene derivative. Reproduced from ref. 136 with permission from Royal Society of Chemistry, copyright 2024.

and co-workers have provided evidence that nitrogen-doped triphenylene-graphene monolayers are highly active as catalysts.[138] These monolayers are capable of driving the reactions of water splitting, particularly the reactions of hydrogen and oxygen evolution, that under normal circumstances would require significant energy input, with almost no energy needed at all. Their catalytic efficiency is significantly improved in both acid and base environments, akin to the activity of ion exchange resins. Most importantly, the incorporation of nitrogen into the monolayers greatly facilitates these reactions and gives rise to catalytic activities similar to those of noble metals. Thus, this study significantly points out the attractiveness of the nitrogen-doped triphenylene-graphene monolayers as cheap non-precious metal catalysts, which leads to a practical and efficient supplying strategy of photocatalytic systems for water splitting and clean hydrogen fuel production near those metals.[138]

Only a handful of two-dimensional carbon-based substances are able to remove water entirely *via* photocatalysis although their carrier mobility is high and they have porous structures. According to a recent computational study, the triphenylene-acetylenic framework (compound **158** [GDY] & **159** [TDY]) possessing an electrical band structure favorable for water splitting was one of the promising eco-friendly, low-cost photocatalysts.[139,140] The focus of this paper was on triphenyldiyne, a structure similar to graphene, where the replacement of a benzene ring with a triphenyl group increases the localization of the electronic states. The monolayer of TDY displays an impressive absorption coefficient over the range of visible light and has a direct bandgap of 2.70 eV. Its excellent carrier mobility opens up channels for rapid charge transfer making it possible to have very good redox capabilities to assist hydrogen evolution reactions (HER). In addition, the nickel doping lowers the overpotential needed for the oxygen evolution reaction
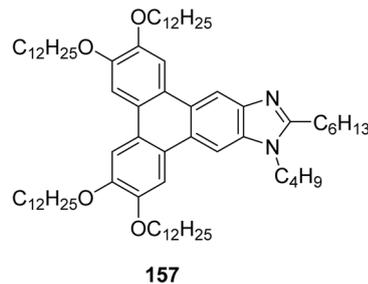
(OER), thus raising the efficiency of the water-splitting process (Fig. 29).[139]

It is important to mention that although these characteristics were predicted by computation, there has been an experimental breakthrough in the production of triphenylene-cored graphdiyne analogues by Matsuoka and colleagues.[141] A modified liquid/liquid interfacial polymerization technique was used to produce TP-GDY with hexaethynyltriphenylene monomer. The TP-GDY film produced had a free-standing structure, was smooth in texture, produced in large domains (>1 mm), and was analyzed through a range of microscopic, spectroscopic, and analytical methods.

The development of small-molecule catalysts made from triphenylene has shown that the aromatic core is a material with more applications.[20] Peris and co-workers have turned triphenylene-based tris(NHC) ligands **162** into scaffolds for homogeneous catalysis after extensive exploration, making use of their rigid, planar, and π–rich aromatic core to boost the catalyst–substrate interactions *via* π–π stacking.[20] In one of their studies, they developed a promising new type of Au^{I} catalyst for organic reactions. This catalyst features a rigid, flat molecule with a triphenylene core at its center, "decorated" with three groups containing nitrogen and a heavy metal (palladium or gold). The peculiarity of this success is found in the geometry of the catalyst which has a 3D structure. The structure of tetra-substituted triphenylene core enable aromatic molecules-often
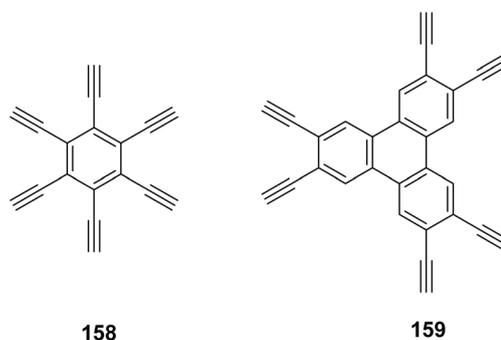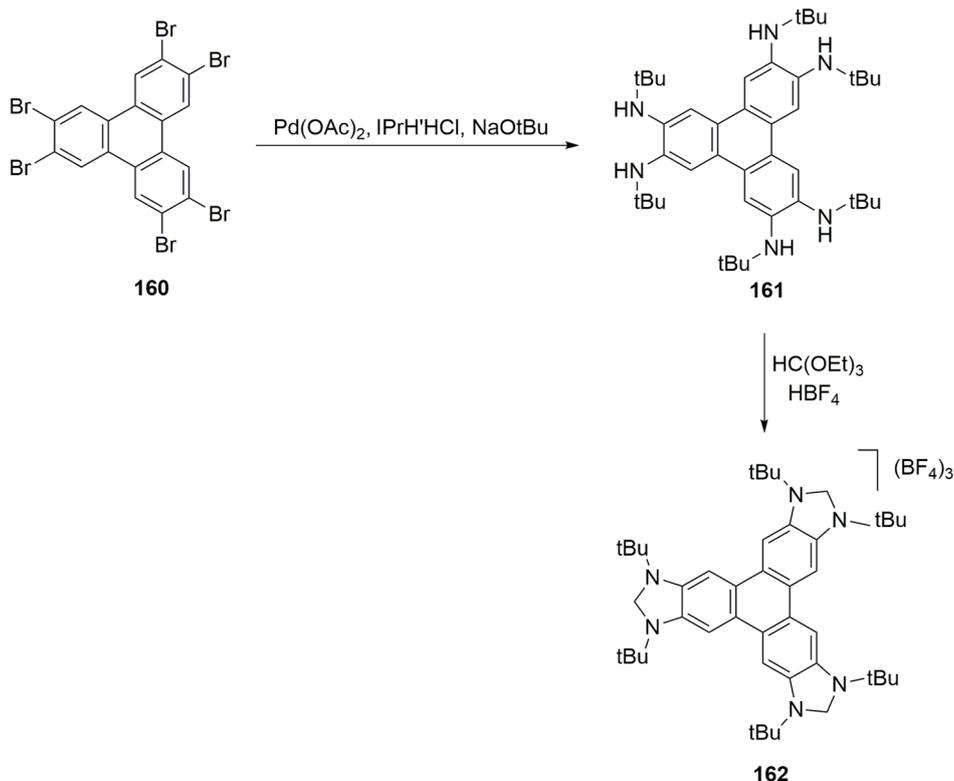

158   **159**

Fig. 29 Chemical structure of graphdiyne (GDY) and triphenyldiyne (TDY). Reproduced from ref. 139 with permission from Royal Society of Chemistry, copyright 2020.

Scheme 39   Synthesis of D_{3h}- symmetric trisazolium salt. Reproduced from ref. 20 with permission from Royal Society of Chemistry, copyright 2013.

a common component in the organic reactions to interact with the catalyst more effectively. This opens avenues for improved design of homogeneous catalysts, which are used in a majority of the processes in industries (Scheme 39).[20]

Building on same concept, a series of triphenylenes with *N*-heterocyclic carbene groups (**163**, **164**) were reported as potential transition metal ligands for catalysis.[142] These triphenylene based tris-NHC ligand exhibits unique topological features, enabling the coordination of three metal fragments within a pseudo-D_{3h} symmetric environment, characteristic not observed in other tris-NHC ligands reported so far. The rigid triphenylene core facilitates supramolecular interactions between the ligand and aromatic substrates, resulting in catalysts (Palladium (Pd) and Gold (Au) complexes) that outperform their monometallic counterparts lacking a polycyclic aromatic framework (Fig. 30).

Using the substrates containing aryl groups, three test reactions: Compound **163** was produced by hydroaminating phenylacetylene. Compound **164**, a precursor to the tris(NHC) triphenylene complexes of Au(ɪ)Cl and Pd(ɪɪ), was produced by a Suzuki–Miyaura coupling and a Csp³–Csp² (aryl) coupling. In fact, catalysts were marginally more efficient than their monometallic (benzimidazol-2-ylidene ligand) and unconjugated trismetallic (triptycene ligand) counterparts, as seen by the 7–20% increase in yields of catalyzed processes over uncatalyzed ones.[143]

Two triphenylene-based tris(*N*-heterocyclic carbene)-gold–acetylide main-chain organometallic microporous polymers were obtained and characterized.[144] They have spherical shapes and showed high activity in catalytic reduction of nitroarenes with NaBH₄ and Strecker reaction for aα-aminonitriles synthesis. The activity may be due to Au nanoparticle formation. Gonell and coworkers reported the preparation of a planar triphenylene derived tris-NHC which can be utilized to prepare a range of Pd and Au ancillaries with better catalytic performance.[145] Due to the symmetry of the ligand and the presence of
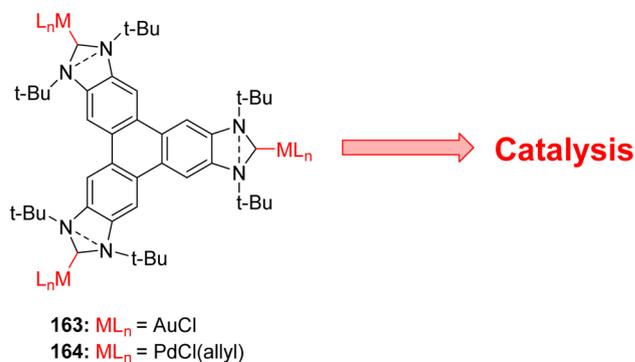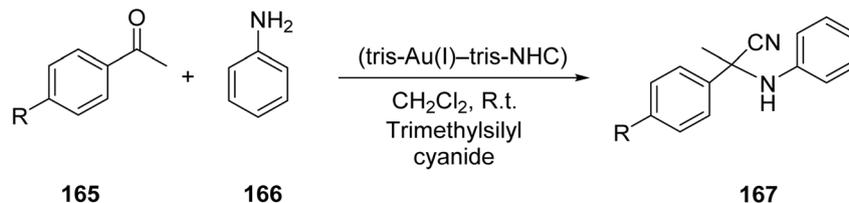
Fig. 30   Tris(*N*-heterocyclic carbene) ligands based on triphenylene for Pd(ɪɪ) (**163**) and gold(ɪ) (**164**) that shown catalytic advantages in benchmark processes. Reproduced from ref. 143 with permission from Royal Society of Chemistry, copyright 2013.

© 2026 The Author(s). Published by the Royal Society of Chemistry

Scheme 40 Three-component Strecker reaction of ketones using triphenylene catalyst. Reproduced from ref. 145 with permission from John Wiley & Sons, copyright 2014.

where,
R = Me, OMe, Br
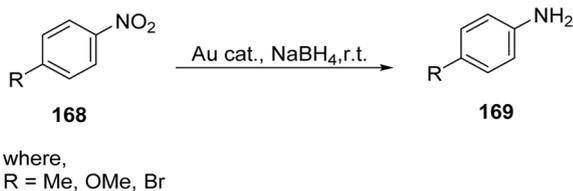
Scheme 41 Reduction of nitroarenes to anilines. Reproduced from ref. 145 with permission from John Wiley & Sons, copyright 2014.

three *p*-species in this tris-NHC complex, they expected similar molecular connection that would lead to the formation of interesting extended structure that can exhibit some exotic physical and chemical properties. Moreover, for the synthesis of triphenylene-based tris-NHC **167**, which is favorable compared to the ligands used in the that three carbenes share an extended *p*-delocalized polyaromatic system. Presumably, it is capable of being used as a component molecular building block to synthesize electronically active materials (Scheme 40).[145]

Moreover, although 1D organometallic polymer derived from NHC and comprising a π-extended system has been reported, the corresponding π-extended 2D or 3D materials have yet been described. Recently, triphenylene-based tris-NHC–gold–acetylide metallopolymeric materials were synthesized *via* a straightforward mixing approach. These compounds demonstrated catalytic utility in the three-component Strecker reaction to afford α-aminonitriles, as well as in the reduction of nitroarenes to anilines (Scheme 41).[145]

3.3.   Triphenylene derivatives as light emitting materials

Triphenylene is a π-conjugated, planar molecule that exhibits superior photostability and thermal stability. Triphenylenes have attracted attention as light-emitting materials due to their stiff planar structure, high temperature stability, and efficient fluorescence. It functions as a core for light-emitting components in OLEDs, particularly those that generate blue or blue-green light. One of the challenges of incorporating triphenylenes into light-emitting devices is that they tend to aggregate in the solid state, which causes fluorescence quenching. Therefore, one of the important design considerations for light-emitting triphenylenes is preventing aggregation.[146]

For example, Saleh and coworkers studied the synthesis of new blue-emitting triphenylene-based polymers used in polymer light-emitting diodes (PLEDs).[18] Various soluble triphenylene derivatives were polymerized using Suzuki–Miyaura and Yamamoto reactions to give polymer **170** and compound **171**, which are blue emitters (Fig. 31). Thus, obtained polymers revealed a feature that polymers were emitting blue light. It is important to note that in solutions and thin film applications, the light-emitting properties remained constant. Nevertheless, the researchers noticed that the deposition of thin films altered some of its previously observed properties of light absorption and emission than those of the solutions. This indicates that TP-based polymers could be potential candidates for blue-PLEDs by remotely monitored light-emitting properties and behavior of the polymers inside thin film devices.[18]

Based on these studies, Saleh and colleagues extended their research to structurally modify the polymers by changing side chains in order to enhance OLED device performance.[147] Three
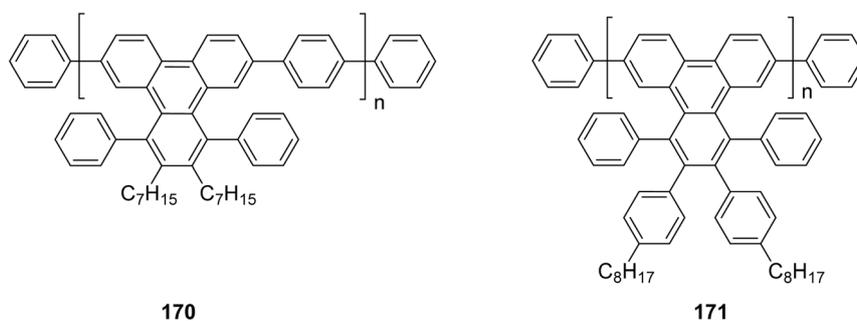

Fig. 31 Polymers **170** synthesized *via* Suzuki–Miyaura coupling reaction. Polymers **171** synthesized *via* Yamamoto Coupling reaction. Reproduced from ref. 18 with permission from American Chemical Society, copyright 2010.
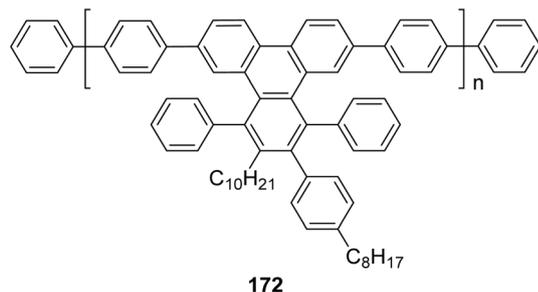
Fig. 32 Structure of poly(2-heptyl-3-(4-octylphenyl)-1,4-diphenyl-6,11-triphenylenyl-1,4-benzene). Reproduced from ref. 147 with permission from John Wiley & Sons, copyright 2009.

different conjugated triphenylene polymers were investigated by them for their potential use in OLEDs. Each polymer had a core structure of triphenylene units but side chains differed in that phenyl and alkyl groups are attached. The research effort was aimed at optimization device performance, specifically reducing the voltage required to turn on the OLED (onset voltage) and boosting its efficacy converting electricity into light (luminance efficiency). Poly(2-heptyl-3-(4-octylphenyl)-1,4-diphenyl-6,11-triphenylenyl-1,4-benzene) **172** showed the most promising properties, with both lower onset voltage and higher luminance efficiency (0.73 cd A^{-1}), indicating that it is crucial to carefully select components within an OLED in order to achieve

optimum performance (Fig. 32). This means that altering side chain structure of triphenylene polymers may be an effective approach to designing efficient OLEDs.[147]

Two novel iridium complexes, YF3 (**173**) and YF4 (**174**), with a triphenylene unit have been developed by Wang and coworkers for potential use in OLEDs (Fig. 33).[148] Here, the triphenylene units do not participate in the emission, rather they facilitate charge transport and improve device performance. When solid or dissolved, both YF3 and YF4 show strong blue-green emission. Interestingly, the film of YF4 complex annealed at 600 °C gave the best performance. It was through this annealing process that an extremely high hole mobility value of 0.001 cm^2 V^{-1} s^{-1} necessary for efficient OLED operation was achieved. This highlights the effectiveness of ancillary ligand modification in enhancing electroluminescent device efficiency. It also indicates that integrating TP units into iridium complexes can lead to excellent OLEDs.

Pal and coworkers have synthesized a new series of DLCs based on triphenylene and pentaalkynylbenzene units (**175**, Fig. 34).[149] Long alkoxy chains promote the transfer of charge and solubility, while the central triphenylene unit increases the efficiency of photoluminescence. OLED devices thus have efficient blue emission and pure colour.[149] These non-symmetric molecules emit blue light in solution and align well in specific ordered structures. The researchers used two of the DLCs as emitters in doped OLED devices. The device made with
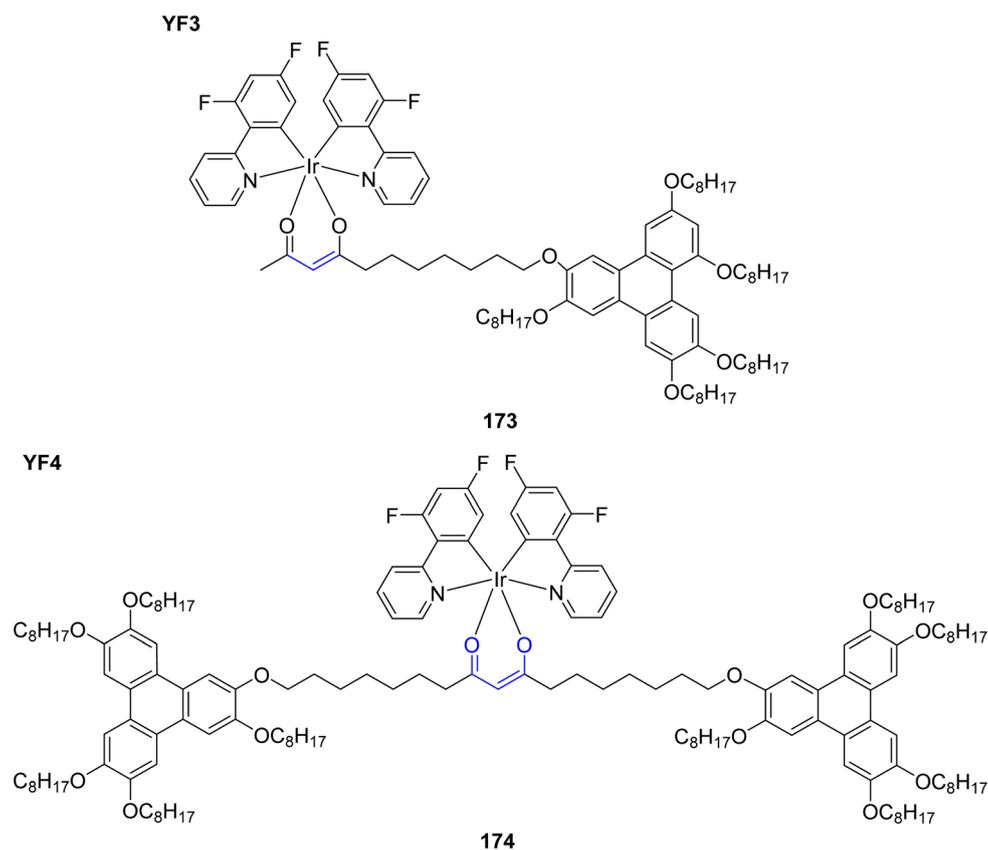
Fig. 33 Chemical structure of YF3 & YF4. Reproduced from ref. 148 with permission from Royal Society of Chemistry, copyright 2017.
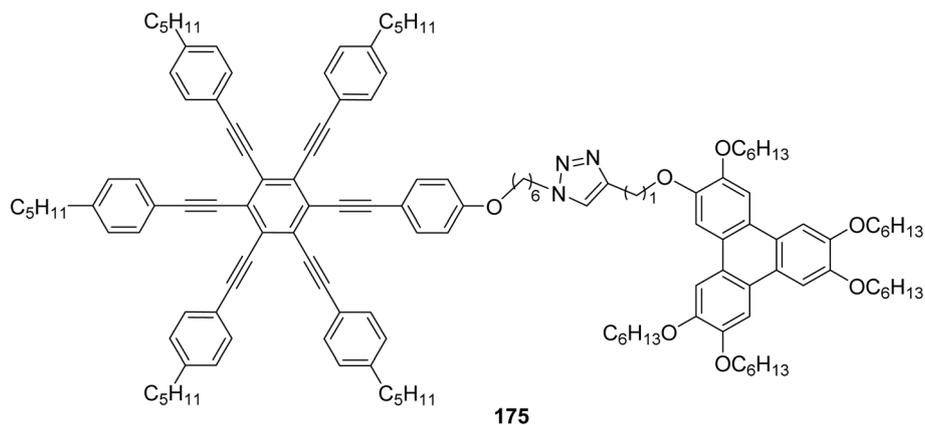
Fig. 34 Chemical structure of target compounds **175**. Reproduced from ref. 149 with permission from Royal Society of Chemistry, copyright 2019.
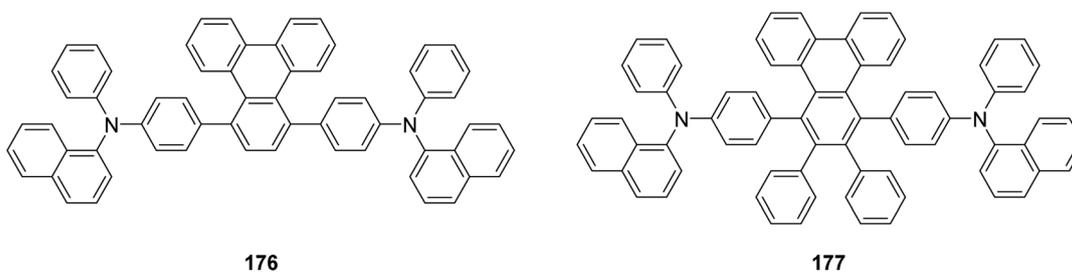
Fig. 35 Chemical structures of substituted triphenylene derivatives with diarylamino groups. Reproduced from ref. 150 with permission from Elsevier, copyright 2011.
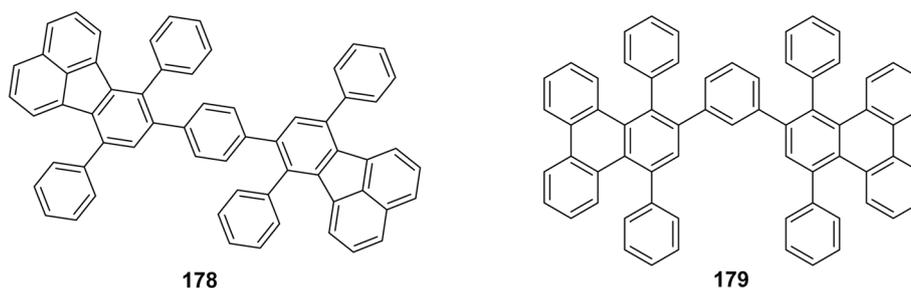
Fig. 36 Chemical structures of 1,4-bis(7,10 diphenylfluoranthen-9-yl)benzene and 1-(1,4-diphenyltriphenylen-2-yl)-3-(1,4-diphenyltriphenylen-3-yl) benzene. Reproduced from ref. 152 with permission from Elsevier, copyright 2015.

175 (Fig. 34) exhibited the best performance, achieving good efficiency and color purity.[149]

In addition to light emitting materials, the semiconducting properties of triphenylene derivatives means they can also be explored as charge transport materials. Park and coworkers synthesized two new hole transport materials for OLEDs, substituted triphenylene derivatives with diarylamino groups **176** and **177** (Fig. 35) known for their thermal stability.[150] These materials were compared to a commonly used material, *N,N′*-di(naphthalene-1-yl)-*N,N′* diphenyl benzidine (NPB). The study found that both **176** and **177** performed well as hole transport layers in OLEDs due to their thermal stability. This makes them suitable for applications requiring high thermal stability and low power consumption.[150]

In a subsequent study, the same group synthesized novel blue emitters. These emitters are built from triphenylene and diphenyl fluoranthene derivatives (Fig. 36).[151] To evaluate the electroluminescence efficacy of the new emitters, these were embedded into multistack OLEDs. Using these emitters, publicize devices shown enhanced luminous, power, and external quantum efficiencies. Compound **178** showed higher luminous efficiency of 2.34 cd A^{-1}, and CIE (0.17, 0.23). In contrast, Compound **179** exhibited deeper blue emission with CIE (0.16, 0.11). Thus, compound **178** offers better performance, while compound **179** achieves pure blue color. The function of triphenyl fluoranthene derivatives and triphenylene for blue emitters in OLED suggests that they have potential for applications.[152]
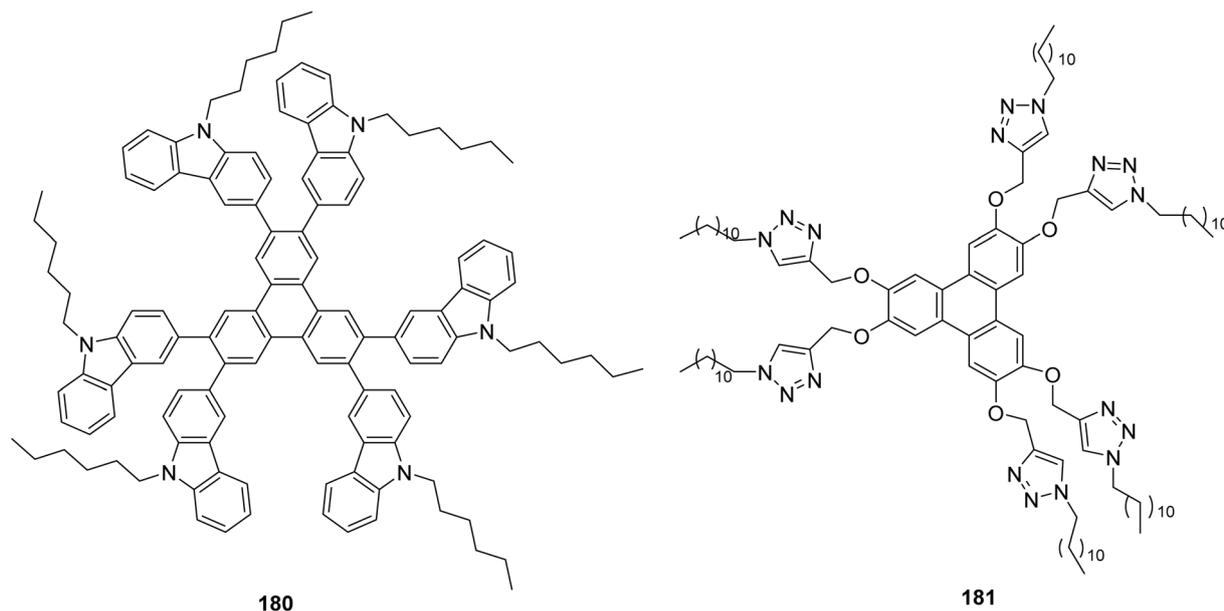
Fig. 37 Chemical structure of carbazole substituted triphenylene and triazole modified triphenylene. Reproduced from ref. 153 with permission from Royal Society of Chemistry, copyright 2013.

3.4. Triphenylene derivatives as sensors

Triphenylenes are increasingly popular in sensor design because of their outstanding photostability, adjustable electrical characteristics, and stiff, π-conjugated architectures. Stable signal production and effective interaction with analytes are made possible by these features. Sensors may be designed for selective detection by adding functional groups to the triphenylene core, which makes them useful for chemical, biological, and environmental sensing applications.[153,154]

Triphenylene derivatives **180** and **181** (Fig. 37) interact with electron-deficient nitroaromatics by means of their electron-rich π-systems, resulting in highly sensitive sensors for nitroaromatic compounds. The use of them in detecting traces of nitroaromatic explosives depends on the quenching of

fluorescence that results from this interaction.[153] Fluorescence titrations were performed using these compounds (5 μM) in a THF : H_2O (9.5 : 0.5) combination with several nitroaromatic derivatives. Because of its extended conjugation, derivative **180**, which contains carbazole moieties, has a strong emission intensity. Conversely, derivative **181**, which contains triazole moieties, may form supramolecular aggregates both in solution and in bulk. Because of its ordered structure, derivative **181** shows a more sensitive reaction to nitroaromatic derivatives than derivative **180**, even though derivative **181** has a higher emission intensity. Photoinduced electron transfer (PET) is used for detection, which quenches the fluorescence. Because of its ordered arrangement and aggregation behaviors, **181** offers greater sensitivity than **180**, which displays strong emission due to reached conjugation. The study highlights how

Fig. 38 Chemical structures of super triphenylenes. Reproduced from ref. 155 with permission from Elsevier, copyright 2012.

Fig. 39 Structure of triazole modified triphenylene. Reproduced from ref. 156 with permission from Royal Society of Chemistry, copyright 2012.
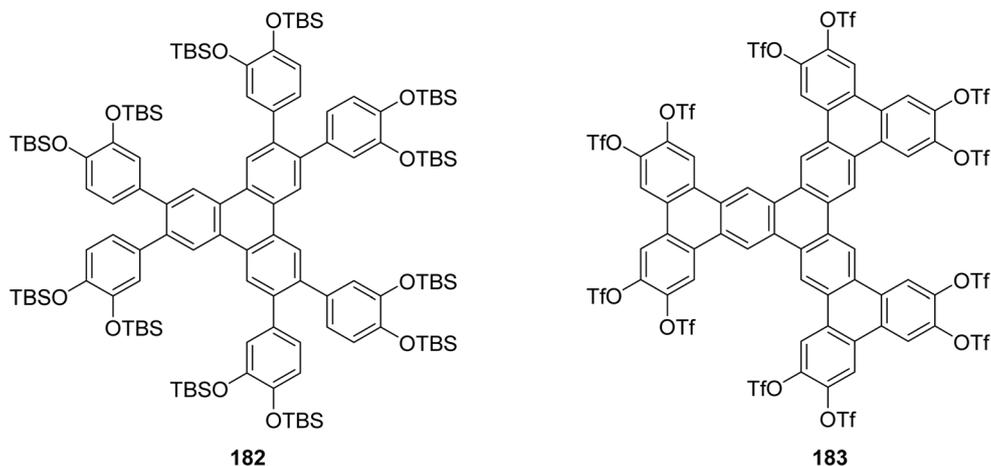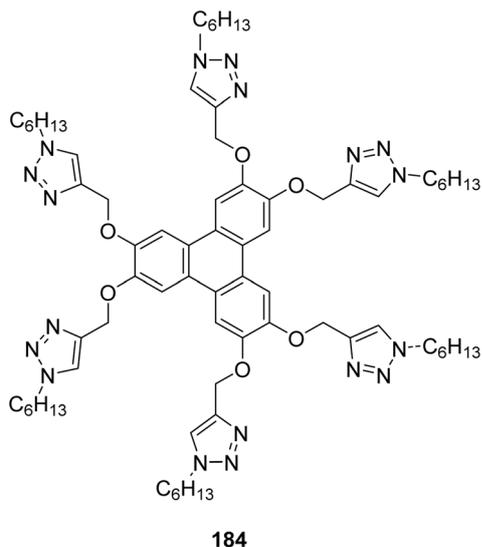
molecular organization enhances nitroaromatic selective detection. The current work thus highlights the significance of well-organized systems for the sensitive identification of nitroaromatics.[153]

The Lewis acid coordination or hydrogen bonding is the basis for the majority of the known fluoride ion receptors. The lack of sensitivity toward fluoride ions at low concentrations severely limits their effectiveness as highly selective systems. Conversely, reaction-based receptors, such as chemo dosimeters, have elevated selectivity and sensitivity.[155] Triphenylene derivative **182** (Fig. 38) with twelve OTBS groups has been produced in good yield.[155] As tetrabutylammonium fluoride is used to deprotect OTBS groups, it experiences an unparalleled irreversible cyclization to super triphenylene **183** by the addition of triflic anhydride (Fig. 38), which enables it to function as

a highly selective chemosensor for F-ions. This transformation leads to a marked enhancement in fluorescence, due to the formation of a rigid, planar π-conjugated system upon cyclization, which restores the emissive properties of the molecule. Additionally, it has been shown how useful TLC strips coated with derivative **182** are for quickly detecting fluoride ions in aqueous conditions.

Competitive experiments were conducted in the presence of F^- at 12 M mixed with Cl^-, Br^-, I^-, OAc^-, HSO_4^-, NO_3, H_2PO_4, and CN^- at 200 M to test the practical applicability of compound **182** as a F^- selective sensor. No obvious change in fluorescence behavior was seen either is the presence or absence of the other anions besides F^-. A TLC strip was prepared by immersing it in the **182** solution in THF in order to test its practical usefulness for fluoride detection in water. The strip was first air-dried and then dipped into a potassium fluoride solution where a color change was instantly seen which was an indication of the presence of fluoride ions.[155]

Given the ability of triazole groups to act as multi-dentate ligands for metal coordination, the inclusion of six triazole moieties in compound **184** prompted an investigation into its binding interactions with various metal ions (Fig. 39). This study aimed to explore the compound's coordination behavior, which could provide insights into its potential applications in metal-ion sensing, catalysis, and other coordination-driven processes. They added aliquots of various metal ions to DMSO and conducted UV-Vis and fluorescence studies to assess compound the binding capacity of compound **184** toward metal ions.[156]

Since anions play a significant role in a variety of clinical, biological, and environmental systems, there is considerable interest in the development of chemo sensors for anion detection. UV-Vis and fluorescence spectroscopy have been used to examine the binding behavior of an in situ-prepared TP-based copper ensemble toward different anions. Among the many anions studied, the **184** ensemble reacts to CN^- ions and is sensitive to cyanide ions, even when blood serum milieu and
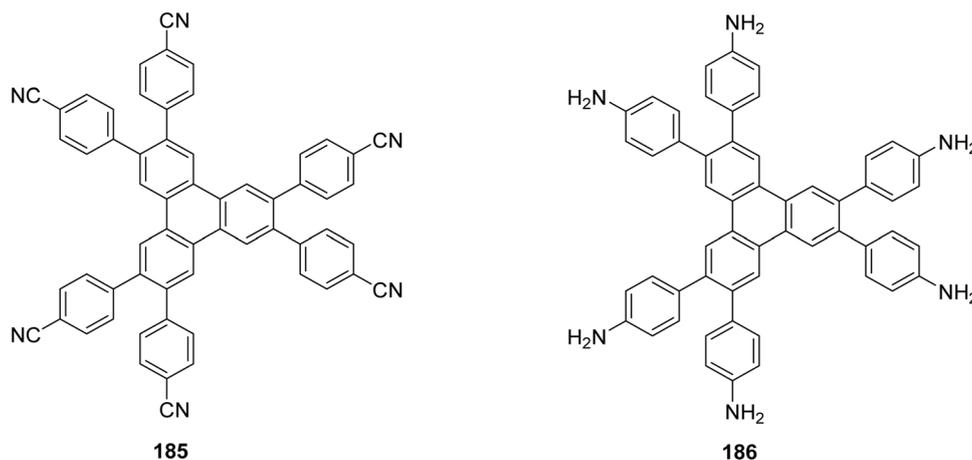
Fig. 40 Chemical structure of triphenylene derivatives. Reproduced from ref. 158 with permission from Royal Society of Chemistry, copyright 2015.

bovine serum albumin are present. Additionally, they used TLC strips coated in compound 132HF solution for the solid-state detection of copper and cyanide ions as a practical use of **184**.[156]

An alternative approach to using triphenylenes as a sensor takes advantage of their tendency to self-assemble and aggregate in solution. For example, compounds **185** and **186** (Fig. 40) exhibit aggregation enhanced emission in aqueous media.[157] In the presence of picric acid, this luminescence is quenched by energy transfer from the aggregates to picric acid. It is noteworthy that this system showed excellent sensitive to picric acid able to identify even minute amounts of explosive picric acid in aqueous media at nanomolar concentrations. Additionally, the derivative **185** solution-coated test strips have an up to 22.9×10^{-15} g cm^{-2} detection limit for picric acid, making it an affordable, portable, and user-friendly approach for on-site trace detection.[158]

3.5. Triphenylene derivatives as COFs

Covalent organic frameworks (COFs) are a unique class of highly porous, crystalline materials composed entirely of light elements such as hydrogen, boron, carbon, nitrogen, and oxygen, all interconnected through strong covalent bonds.[159] Due to its delocalized π-system, rigid planar structure, excellent stability, and tunable architecture, triphenylene is a valuable building block in the construction of both COFs and Metal–Organic Frameworks (MOFs).[154,160] These characteristics of the triphenylene-based materials help in the formation of supramolecular interlayer stacking within the MOFs and COFs that eventually lead to an increase in their thermal and chemical stability as well as electrical conduction. Moreover, the resulting materials exhibit uniform nanoporous channels, contributing to high surface area and porosity, properties that are highly
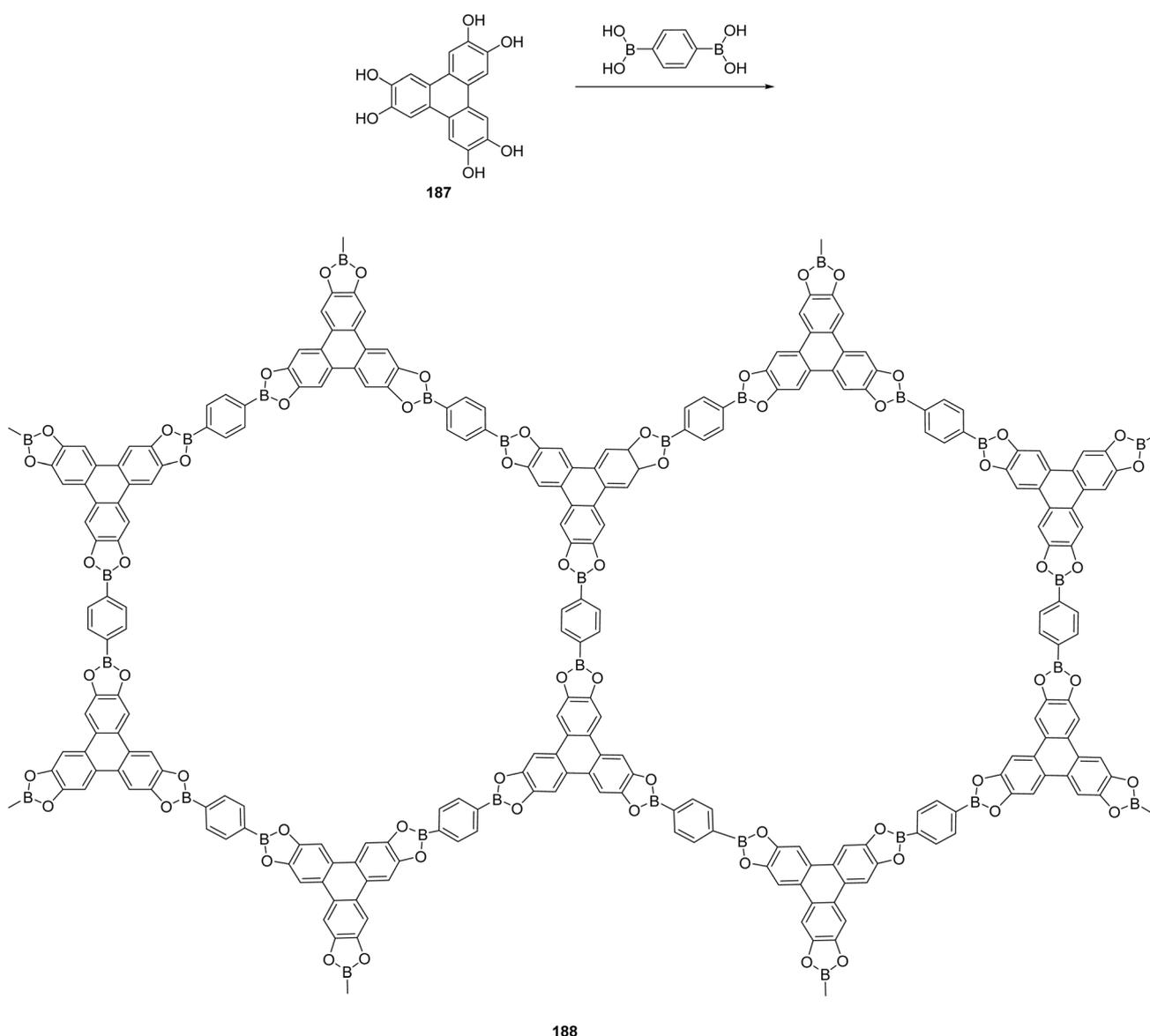
Fig. 41 First COFs constructed through the condensation reaction of hexahydroxytriphenylene with benzene-1,4-diboronic acid. Reproduced from ref. 161 with permission from American Association for the Advancement of Science, copyright 2005.

desirable for gas storage, molecular sieving, and ion exchange applications.[160]

The first COFs were reported by Côté, Yaghi, and coworkers in 2005, where they produced microcrystalline networks by condensation of boronic acids with diols to form boronate ester linkages.[161] Specifically, COF **188** was constructed through the condensation reaction of hexahydroxytriphenylene **187** with benzene-1,4-diboronic acid (Fig. 41). These frameworks represented the first examples of porous, crystalline organic materials assembled entirely through covalent bonds, exhibiting both high surface area and long-range order.[161]

Bein and co-workers later studied thieno[2,3-b]thiophene-based COFs, where the incorporation of sulfur atoms into the central ring system contributed to both high surface area and improved crystallinity.[162] These improved properties make the COFs more effective for photocatalysis. Interestingly, the study also revealed that non-planar aromatic systems can "lock" COF layers together. This finding suggests that this locking mechanism might be applicable to other structural cores as well.[163] Jiang investigated luminescence and semiconducting behavior of a new class of materials called Triphenylene-Pyrene COFs, which are COFs with extended π-conjugated systems, formed by combining hexahydroxytriphenylene **187** and pyrene-2,7-diboronic acid **189**, resulting in a unique belt-like hexagonal structure. This structure is particularly interesting because it efficiently captures light over a broad range of wavelengths. As a result, these COFs can transfer this energy throughout the material, leading to blue luminescence.[164] The change in fluorescence intensities at 474 and 402 nm indicates electronic coupling, favoring energy transfer in the extended TP-COF structure. The material's stability was demonstrated through continuous on-off switching without important weakening of the electric current. The self-condensation of **189** also resulted in PPy-COF with a pore diameter of 1.73 nm and a surface area of ($923 \text{ m}^2 \text{ g}^{-1}$) (Fig. 42).[165] PPy-COF displayed photoconducting behavior as well as p-type semiconducting behavior with electrical conductivity of the same order as that of triphenylene-pyrene COF.

Chen and colleagues successfully synthesized uniform hollow spherical 2D COFs using 2,3,6,7,10,11-hexakis(4-aminophenyl)triphenylene as a building block (HAPTP).[166] The resulting COF **192** is distinguished by its high crystallinity, uniform structure, and a remarkable pore volume reaching 1.947 $\text{cm}^3 \text{ g}^{-1}$, positioning them as ideal nanocarriers for controlled drug delivery. HAPTP was synthesized by using a Suzuki cross-coupling reaction between 2,3,6,7,10,11-hexabromotriphenylene and boronic ester achieving quantitative yield. Morphology exposure by SEM and TEM revealed hollow spherical morphology resulting in high ibuprofen, a non-steroidal anti-inflammatory drug, loading capacity and sustained release as shown in Fig. 43.

Considering the low dispersibility and solubility of COFs, Chen and colleagues prepared a water-soluble nanocomposite COF@IR783 by assembling cyanin IR783 with a triphenylene COF.[167] The COF itself was synthesized through a co–condensation reaction between 2,3,6,7,10,11-hexahydroxytriphenylene (HHTP) pointed at vertices and 5,15-bis(4-boronophenyl) porphyrin (Por) at center, resulting in a porous hexagonal framework.[168] The resultant 2D COF with IR783, exhibited a nanoscale morphology (∼200 nm), aqueous dispersibility, and a negative charge (−36 mV), all of which are beneficial for extending blood circulation time and enhancing the enhanced permeability and retention (EPR) effect (Fig. 44). It was also used as a drug carrier for the prodrug cisaconityl-doxorubicin (CAD). The combination of photothermal therapy (PTT) and chemotherapy led to a significant reduction in the viability of 4T1 cells *in vitro*, with a cell survival rate of 19.8%.

Chen and coworkers presented COF created by stacking 2D covalent organic nanosheets (CONs) into long range ordered π-columnar structures and periodically ordered bicontinuous heterojunction networks.[167–170] The electron and hole lifetimes of CONs can be extended, and effective carrier separation can be achieved because of their molecular hetero structure. In the meantime, type I PDT mechanism allows electrons to decrease O_2 to O_2^-, which was advantageous for ROS formation. In this experiment, liquid ultrasonic exfoliation was used to directly manufacture CONs from bulk triphenylene-porphyrin COFs. Under 635 nm laser irradiation, intravenous injection of the resultant CONs into nude mice resulted in a considerable tumor ablation.[168]

Bein and colleagues developed a triphenylene-based COF by co-condensing thieno[3,2-b]thiophene-2,5-diyldiboronic acid (TTBA) with hexahydroxytriphenylene (HHTP).[162] The resulting COF effectively incorporated [6,6]-phenyl-C61-butyric acid methyl ester (PCBM), as evidenced by BET surface area reduction and photoluminescence quenching. A photovoltaic device using ITO/TT-COF : PCBM/Al achieved a power conversion efficiency of 0.053% with 0.62 V open-circuit voltage. Monte Carlo simulations suggested that increasing pore size could further enhance charge transfer. This COF highlights potential for use in organic photovoltaic applications.

3.6. Triphenylene derivatives as pharmaceuticals

Triphenylene derivatives have gained increasing interest in the pharmaceutical field due to their diverse chemical structures and potential therapeutic properties. Their polycyclic aromatic nature enables them to interact effectively with biological systems, showing promising results in various pharmacological activities such as antimicrobial[171] and anticancer[172] effects. Modifications to the triphenylene core, including
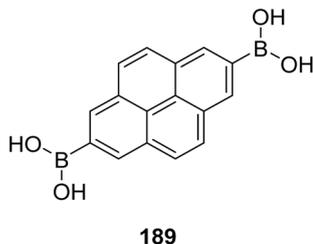

189

Fig. 42 Chemical structure of pyrene-2,7-diboronic. Reproduced from ref. 165 with permission from John Wiley & Sons, copyright 2017.
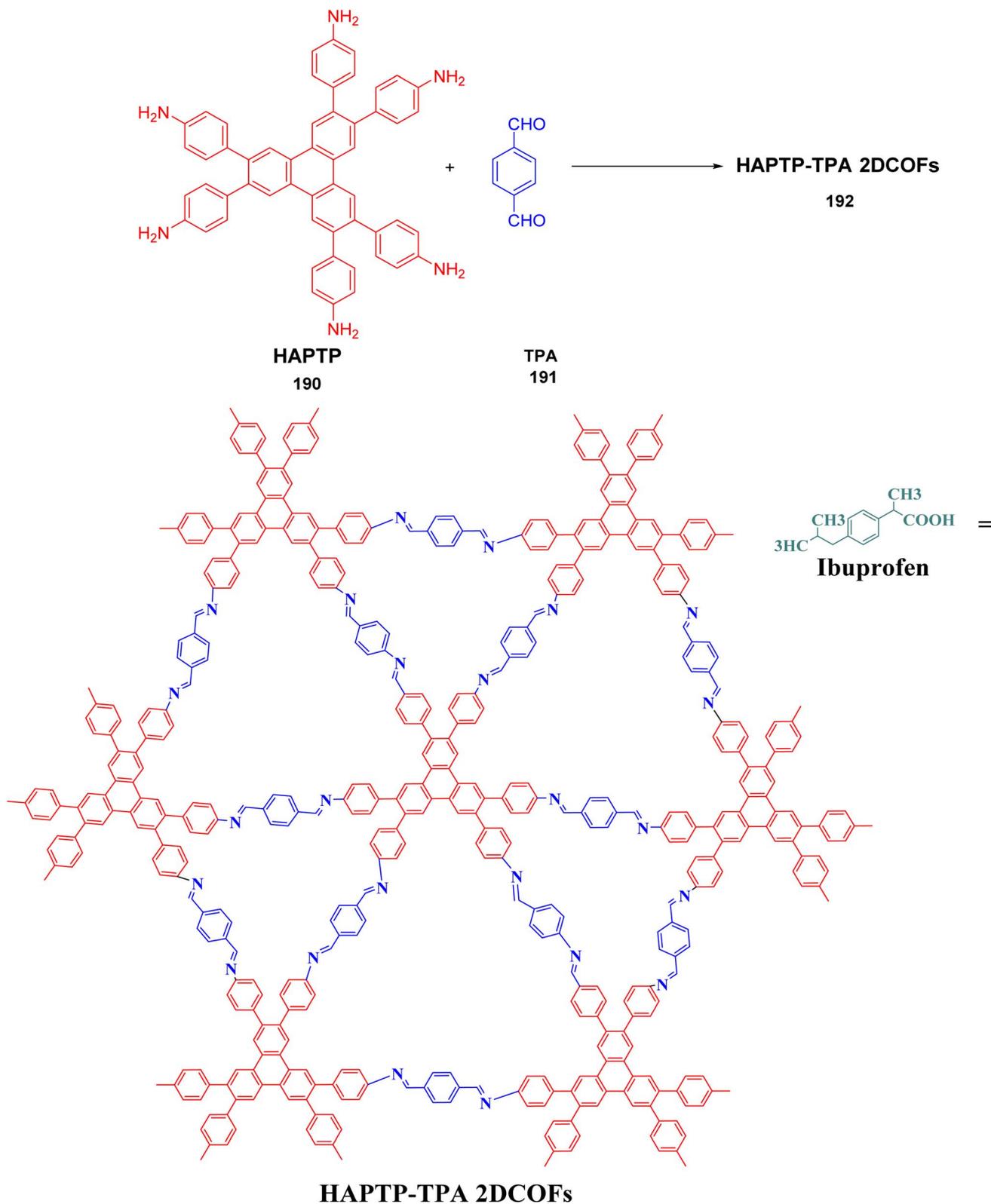
Fig. 43 Schematic illustration of an IBU molecule in a triangular pore of HAPTP-TPA 2DCOFs. Reproduced from ref. 166 with permission from American Chemical Society, copyright 2023.

functionalization and substitution with different functional groups, further enhance their bioactivity and selectivity, making them suitable candidates for drug development and delivery systems.[173] Additionally, the ability of these derivatives to form self-assembled structures adds another layer of versatility for use in advanced pharmaceutical applications.
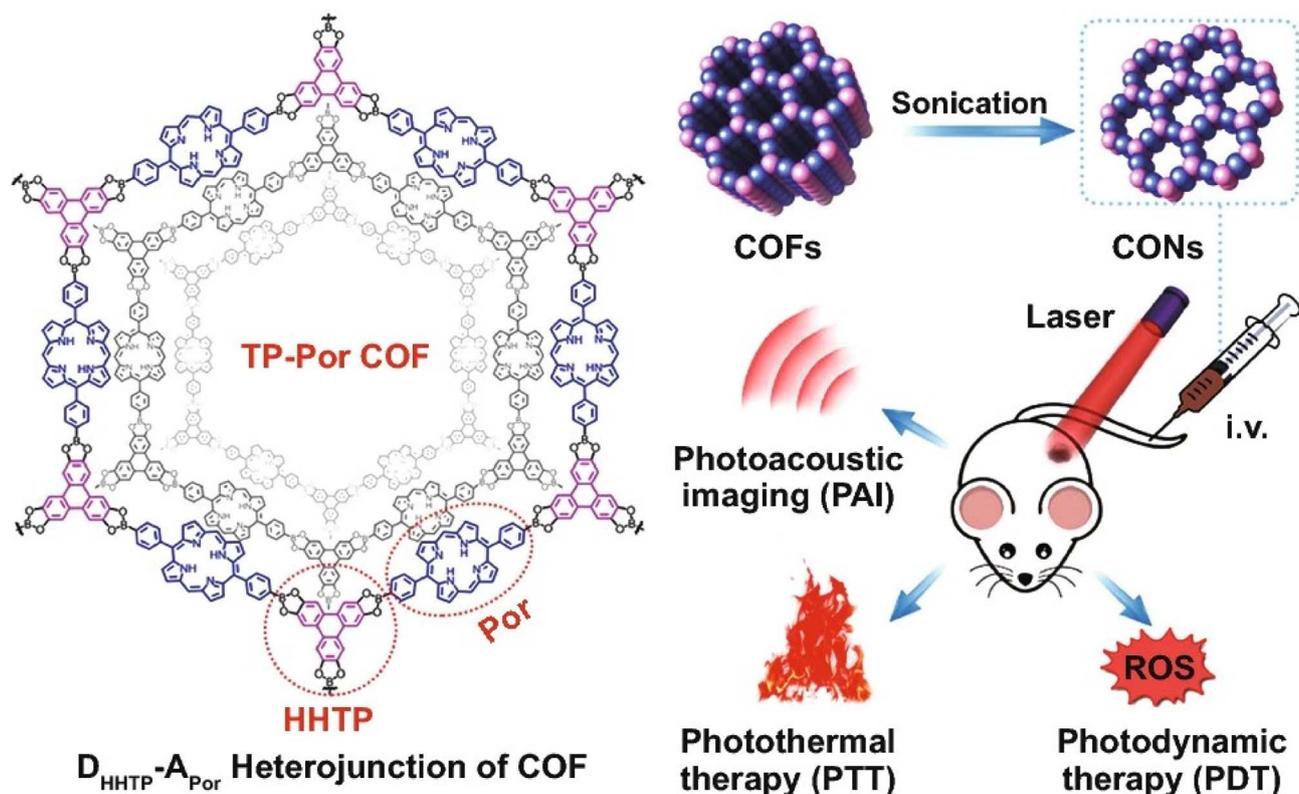
Fig. 44 Schematic illustration of 2D CON fabrication and *in vivo* cancer therapy. Reproduced from ref. 168 with permission from American Chemical Society, under the terms of the CC BY 3.0 license, copyright 2019.

Triphenylene dimethyl succinimide (TDS) is a novel class of organic compounds that have potential for treatment of acquired immune deficiency syndrome (AIDS).[174] Loret and coworkers designed ten derivatives of TDS (**193** in Fig. 45) and verified their efficacy against Tat, which is a viral protein having key role in the HIV virus lifecycle, helping in virus replication and spreading in body.[174] HIV infected cells secrete Tat which transactivate distant infected cells inducing immunodeficiency in non-infected T-cell and causing other issues like Kaposi's sarcoma. TDS molecules bind with Tat protein and inhibits activation of HIV-LTR in HeLa cells at μM concentration. Mickael and coworkers also synthesized a new family of antivirals having TP aromatic ring substituted with one carbon chain bearing the same succinimide group.[175]

Naidek and coworkers synthesized 2,3,6,7,10,11-hexahydroxytriphenylene (HHTP), which exhibits catechol redox-properties, accessible higher oxidation state thus causing cytotoxic effects on 5 human cancer cell lines.[176] They compared the cellular toxicity of HHTP with a standard chemotherapy drug cisplatin, which is widely used in the treatment of several human cancers. They treated human glioma cell lines with HHTP and cisplatin at concentrations ranging from 5 to 25 μmol L^{-1} for 48 hours finding that the *in vitro* cytotoxicity of HHTP was nearly identical to that of cisplatin across all tested drug concentrations. HHTP also exhibits effects comparable to those of other polyphenolic compounds, such as curcumin, apigenin, genistein, epigallocatechin, and epigallocatechin-3-

gallate, which are known to make apoptosis in glioma and lung tumor cells and enhance the anti-neoplastic efficacy of chemotherapeutic drugs.[177]

Hayashida and coworkers prepared a water-soluble cyclophane hexamer (Fig. 46) *via* Williamson ether synthesis of tetraaza[6.1.6.1]paracyclophane bearing a bromoacetamide moiety with hexahydroxytriphenylene as core and as central platform for multivalent receptor.[172,178] It can serve as molecular receptor to bind daunorubicin (DNR) and doxorubicin (DOX), which are anticancer drugs. An aqueous HEPES buffer was used to assess the binding interactions with these drugs, through fluorescence emission measurements. The association constant was found to be significantly high at $1.3 \times 10^5 \ M^{-1}$, in contrast to the lower value of $3.3 \times 10^2 \ M^{-1}$ observed with a single macrocycle, which can be attributed to the multivalent effect.
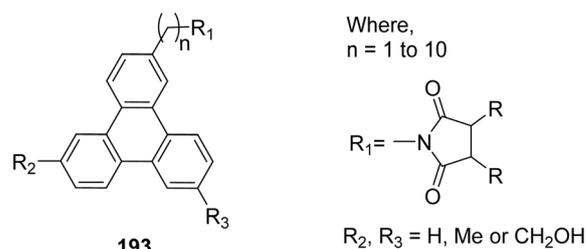
Fig. 45 TDS derivatives synthesized **193**. Reproduced from ref. 174 with permission from De Gruyter, copyright 2001.

194

Hexa-cyclophane Triphenylene
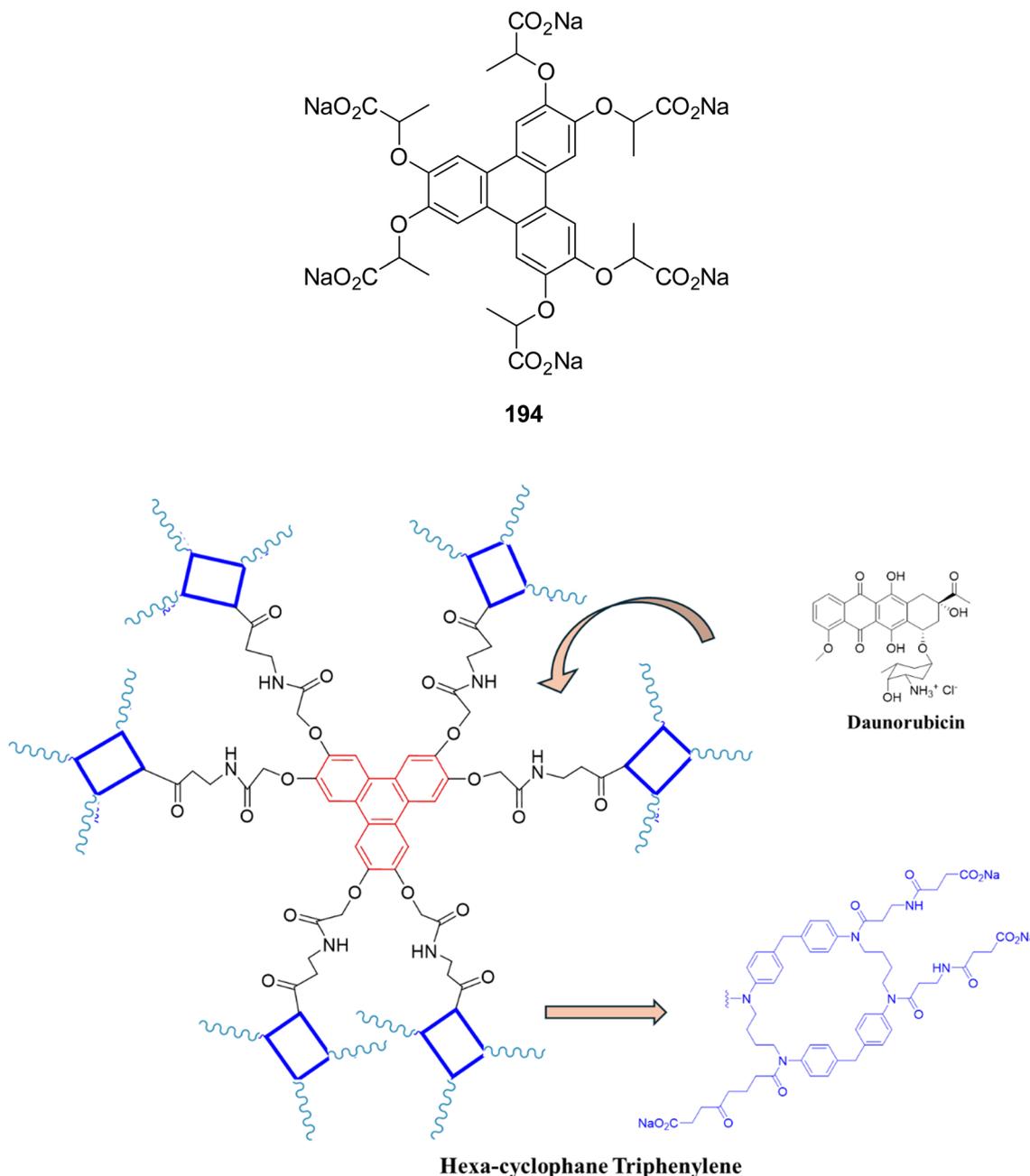
Fig. 46 Water-soluble hexa-cyclophane triphenylene that detect daunorubicin, an anticancer drug. Reproduced from ref. 172 and 178 with permission from American Chemical Society, copyright 2016.

The complex formation is primarily driven by a hydrophobic effect that facilitates the association between the triphenylene core and the amphiphilic guest, along with additional weak interactions.

Bibal created a triphenylene hexacarboxylate **194** that is soluble in water and intended to complex biological ammoniums like dopamine, serotonin, aceylcholine, L-dopa *etc.*[179] Then, this simple receptor provided a hydrophobic centre and negatively charged groups to target substances that are amphiphilic, like neurotransmitters. The monitoring of acetylcholine complexation by infrared spectroscopy indicated that the guest's ammonium group was interacting with the host carboxylate groups (exchange with sodium) while the ester group of the guest was desolvated during complexation. The triphenylene hexacarboxylate was able to recognize D-glucosamine ($K_a = 87$ M^{-1}) and acetylcholine ($K_a = 94$ M^{-1}) with a moderate strength in phosphate buffered water. In phosphate buffered water, catecholamines that had an aromatic group attached to them were complexed with greater binding constants ranging from 200 M^{-1}. Molecular dynamics revealed two types of host–guest interactions in water: π–π interactions and ionic interactions (between CO_2^- and ^+H_3N groups).
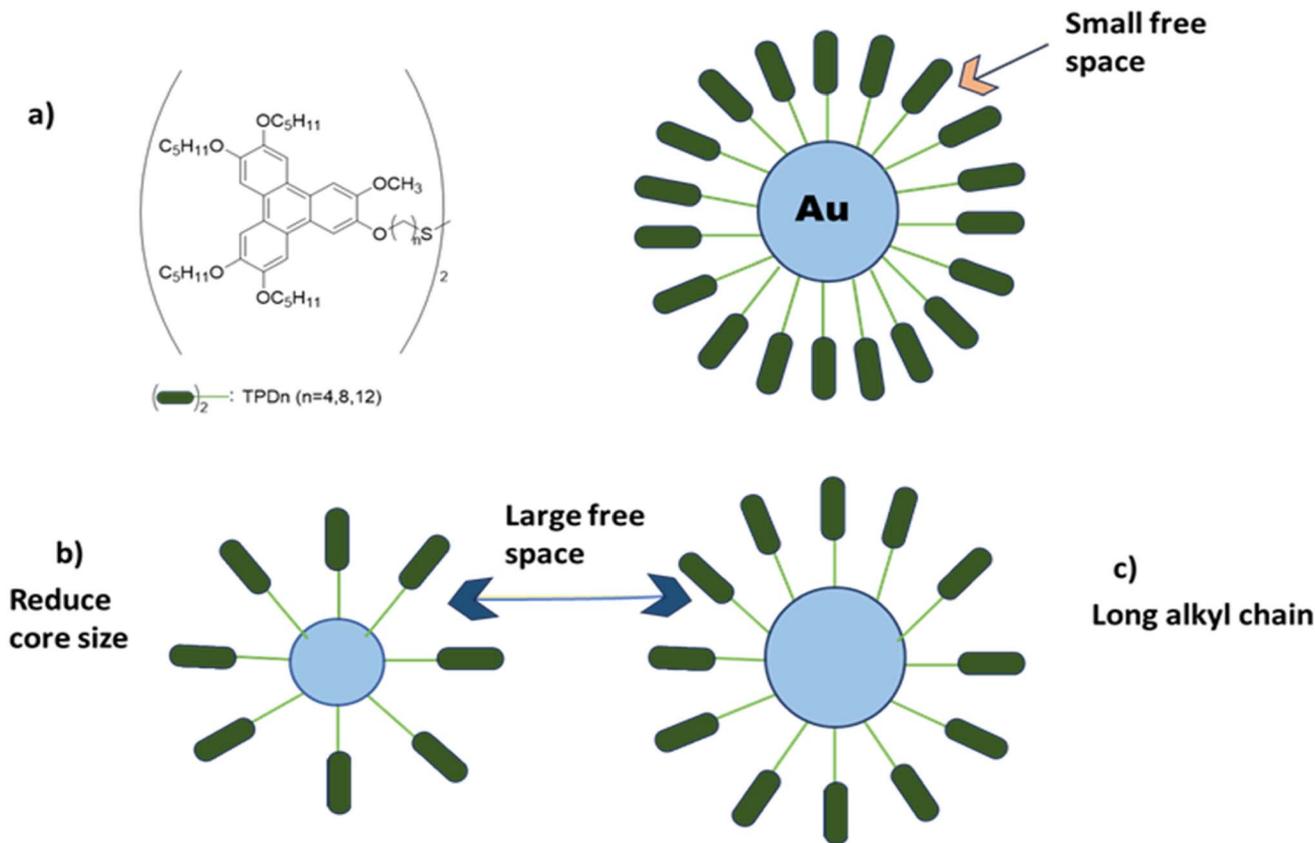
Fig. 47 There are three methods to create a 1D arrangement of NPs: (a) create molecules by combining gold nanoparticles stabilized by TPD*n* and triphenylene ligands (TPD*n*, *n* = 4,8, or 12); increase the amount of free space between the triphenylene moieties: (b) utilize a longer alkyl chain; (c) decrease the size of the core. Reproduced from ref. 181 with permission from Royal Society of Chemistry, copyright 2007.

Remarkably, no contact was found between the host and analogous guests such as L-dopa, D-glucose (lack of an ammonium group), and choline (more hydrophilic than acetylcholine). Thus, in phosphate-buffered water, the triphenylene hexacarboxylate showed a slight selectivity towards biological ammoniums.

3.7. Triphenylene derivatives in nanotechnology

Triphenylene derivatives have found significant applications in nanotechnology due to their rigid, planar structure, strong $\pi-\pi$ stacking interactions which facilitates their integration with nanoparticles to develop functional nanocomposites for chemical sensing, drug delivery and optoelectronic applications.

One of the notable applications involves the use of silver nanoparticles (AgNPs) functionalized with bis-acridinium lucigenine (LG) for surface-enhanced Raman scattering (SERS)-based detection of triphenylene.[180] This allows the ability to locate organic contaminants with more accuracy. The acridinium planes are staggered, creating cavities for hydrophobic triphenylene. The orientation of LG changes with triphenylene concentration, with perpendicular orientation preferred. This technique can detect trace triphenylene concentrations, making it a potential organic pollutants chemical sensor. LG concentration did not significantly affect the Raman signal, but the

limit of detection was approximately 10^{-7} M. When triphenylene interacted with LG, its structural shape remained unchanged, but when the concentration of triphenylene decreased, its orientation changed. This study investigated the interaction between triphenylene and LG in the formation of a LG/triphenylene complex on metal surfaces, using LG-functionalized Ag nanoparticles for triphenylene detection and analyzing SERS spectra to understand triphenylene's interaction with LG.[180]

Kumar and colleagues described triphenylene based discotic liquid crystals have been used to functionalize gold nanoparticles (GNPs), resulting in nanocomposites with enhanced electrical conductivity and stable mesophase behavior[181] (Fig. 47). These were synthesized and uniformly dispersed within a columnar DLC matrix. Thermophysical characterization confirmed the incorporation of the nanoparticles into the matrix without disrupting the intrinsic mesophase organization, aside from minor shifts in transition temperatures. Most notably, doping the columnar matrix with these functionalized nanoparticles led to a remarkable enhancement in electrical conductivity, exceeding six orders of magnitude, under ambient conditions.

Shen and coworkers reported the self-assembly of gold nanoparticles (AuNPs) functionalized with newly synthesized hexaalkoxy-substituted triphenylene-based discotic liquid
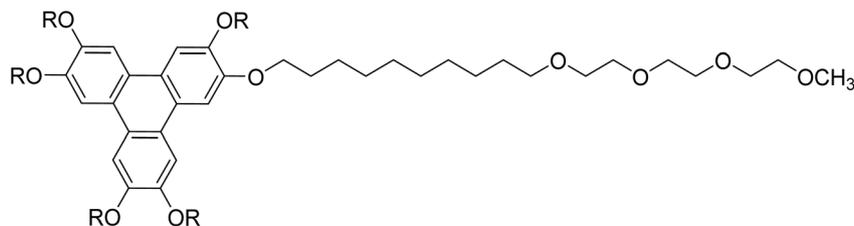
195

Fig. 48 Chemical structure of the TP_{C10TEG}. Reproduced from ref. 184 with permission from American Chemical Society, copyright 2023.

crystal ligands.[182] A stripelike (2D linear) nanoparticle arrangement is attained in a 0.5 μm area due to strong π–π stacking. The degree of π–π interaction between adjacent triphenylene ligands significantly influences the resulting nanoparticle arrangement, allowing for tunable nanostructures. Hence, these functionalized ligands can guide the assembly of nanoparticles into well-defined architectures, making them highly promising for use in electronic and optical nanodevices.

Another triphenylene derivative, amphiphilic TP_{C10TEG} **195** have shown remarkable self-assembling and self-healing properties, particularly beneficial for developing nanostructured functional materials (Fig. 48).[183] Mesoporous silica/alumina hybrid nanocomposites were effectively created in the study by employing TP_{C10TEG} as a template in sol–gel synthesis. After the nanocomposites were drop-casted onto anodic aluminum oxide membrane (AAO), the hexagonal configurations were verified by X-ray diffraction examination and electron microscopy confirmed successful infiltration into the AAO channels, highlighting their potential for use in nanoelectronic and optoelectronic applications. For example, a study created a high-performance self-powered photodetector using nickel hexahydroxytriphenylene (Ni-CAT) grown in a composite structure.[184]

Researchers have explored the photoconductivity of both undoped and nanostructured hexaalkoxytriphenylene series (HAT4, HAT5, and HAT6) doped with gold chloride.[185] For HAT4 and HAT5, but not for HAT6, the photoconductivity improved by more than 10 times following doping with gold chloride. It is possible to explain the high photoconductivity in terms of core–core lengths, transition temperatures, and their side chains' length. The derivatives of hexa-alkoxytriphenylene doped with gold chloride exhibit photoconductivity in the range of 10^{-4}–10^{-5} S m^{-1}.which are five times more than the undoped value mixtures. This nanocomposite's strong NIR absorbance and photoconductivity make it a possible contender for use in organic solar cell technology.[185]

The increasing interest in chiral supramolecular nanostructures in p-conjugated supramolecular assemblies is a result of their possible uses in organic semiconductors. Using chiral limonene solution as the chiral source, a series of optically active triphenylene-based supramolecular gels were created.[186] These gels eventually form a heterochiral packing structure or a homochiral P- or M-type stacking. A detailed investigation was conducted into the effects of supramolecular packing on homochiral or heterochiral assemblies on their

mechanical and electrical properties. This could potentially establish a connection between a chiral supramolecular nanostructure and the mechanical strength and electrical performance of the final supramolecular physical gels. This work is important for the rational design of p-conjugated supramolecular nanostructure assemblies and for their possible use in optoelectronics and chiral organic electronics.[186]

Carbon nanotubes (CNTs), which are hollow cylinders composed completely of carbon, have been studied for their electrical, mechanical, and thermal properties.[187] To address the challenge of poor dispersibility in discotic liquid crystals, single-walled CNTs (SWNTs) were functionalized with triphenylene-based discotic mesogens. Hydroxylated triphenylene derivatives were synthesized and chemically grafted onto acid-purified SWNTs. The resulting nanocomposites, studied *via* differential scanning calorimetry and X-ray diffraction, revealed that the SWNTs were embedded within the columnar phase of the liquid crystal matrix. This highlights the potential of integrating π-conjugated mesogens with carbon nanostructures for advanced nanocomposite materials with tailored optical and electronic properties.

Lintang and coworkers have explored the mixture of thin film nanocomposites using functional amphiphilic organic moieties in mesoporous silicon channels.[183] Amphiphilic triphenylene derivatives have been utilized as self-assembling templates for the fabrication of mesostructured silica films. These derivatives enable the organization of silica precursors into well-defined nanostructures through their ability to form ordered assemblies in solution, providing a versatile approach for the development of functional silica-based materials with controlled porosity and morphology. However, these films depend on donor–acceptor systems and ethanol vapor-mediated maturing.

4. Structure–property relationship of triphenylene and its derivatives

Triphenylene, an incredibly symmetrically organized polycyclic aromatic hydrocarbon (PAH), has very strong and flat π-conjugated structure made up of four benzene rings fused together. The whole π-electron system being delocalized gives triphenylene very good optical, electronic, and thermal stability, which is the main reason for its widespread use in different areas like materials science and molecular electronics (Table 1).

Table 1 Summary of structure–property application relationships

Structural modification	Influenced property	Representative application
Long alkyl or alkoxy substituents	Promote columnar mesophases; enhance solubility	Discotic liquid crystals, organic semiconductors
Electron-donating groups ($-OR$, $-NR_2$)	Raise HOMO level; increase fluorescence efficiency	OLEDs, luminescent sensors
Electron-withdrawing groups ($-CN$, $-NO_2$, $-COOR$)	Lower LUMO level; improve electron transport	Organic photovoltaics, n-type materials
Heteroatom incorporation (N, S, O)	Modify electronic delocalization; introduce redox activity	Catalysts, coordination networks, COFs
Metal–triphenylene complexes	Enable charge–transfer transitions; enhance photostability	Photocatalysis, electrocatalysis
π-Extended frameworks (dimers, trimers, oligomers)	Increase conjugation length; broaden absorption	Photovoltaic and optoelectronic materials
Functional groups for sensing ($-COOH$, $-SH$, $-NH_2$)	Provide analyte recognition and binding sites	Chemical and biological sensors
Planar rigid cores with edge substitution	Improve molecular packing and mechanical integrity	COFs and nanostructured materials
Amphiphilic or hydrophilic side chains	Induce self-assembly in aqueous or hybrid media	Drug delivery, biofunctional materials

The flat molecular shape of triphenylene allows for very good π–π stacking interactions, which in turn helps with the movement of charge carriers and the transport of excitons – a necessity for high-performance optoelectronic devices. The triphenylene core can be significantly changed in terms of its physicochemical properties by substituents attached to its edges. When electron donating substituents like alkoxy, amino or alkyl groups are used, they create a higher electron density which, in turn, results in a smaller band gap and greater fluorescence quantum yield. On the other hand, if an electron withdrawing group is present (like cyano, carbonyl or nitro) the LUMO energy level will be lowered which will result in better electron transport and stabilization of the molecular orbitals for solar energy applications. The addition of flexible alkyl or alkoxy chains at the edge leads to the formation of columnar mesophase, a property of triphenylene-based discotic liquid crystals. These side chains help to dissolve and process the molecules while allowing molecular ordering that is beneficial for isotropic charge conduction over long distances. Meanwhile, the presence of a heteroatom or coordination with metal centers is another way to change the redox activity and catalytic potential through the alteration of the electronic distribution.

Thus, the structure–property relationship in triphenylene derivatives is governed by three main factors: (i) the degree of π-conjugation, (ii) the nature and position of substituents, and (iii) molecular packing in the solid state. Fine-tuning these parameters allows the rational design of triphenylene-based materials with tailored optical, electronic, and self-assembly characteristics.

5. Future perspectives

The future of triphenylene-based chemistry is poised for significant expansion as advances in molecular design, synthetic methodology, and materials engineering continue to converge. The intrinsic rigidity, planarity, and π-conjugation of the triphenylene framework render it an exceptional platform for developing multifunctional materials. However, despite notable progress, substantial opportunities remain for enhancing its performance, scalability, and integration into emerging technologies.

A primary direction for future research lies in the development of sustainable and atom-economical synthetic routes. Conventional methods for constructing the triphenylene core often rely on harsh reaction conditions, toxic reagents, or precious metal catalysts. To align with green chemistry principles, the focus should shift toward metal-free cyclization, photochemical, and electrochemical approaches, as well as flow-assisted synthesis for scalable production. These methodologies would not only reduce environmental impact but also improve reproducibility and yield, enabling the large-scale fabrication of substituted triphenylene derivatives with controlled functionalities.

Another promising avenue involves precise structure–property modulation through rational molecular engineering. Introducing heteroatoms, functional groups, or fused aromatic rings can fine-tune electronic structures, optimize HOMO–LUMO energy levels, and control molecular packing. The strategic design of asymmetric or donor–acceptor-type triphenylene systems could enable ambipolar charge transport and broaden absorption spectra, which are crucial for next-generation OLEDs, photovoltaic cells, and OFETs.

In the realm of functional materials, triphenylene-based covalent organic frameworks (COFs) and metal–organic frameworks (MOFs) present rapidly growing research frontiers. Their ordered π-stacked networks, chemical robustness, and large surface areas make them suitable for diverse applications, including gas adsorption, heterogeneous catalysis, ion conduction, and energy storage.

The incorporation of triphenylene derivatives into the fields of nanotechnology and hybrid materials is a very productive area of research. Nanoscale triphenylene-based architectures like nanoribbons, nanosheets, and 2D assemblies can exhibit outstanding properties regarding charge transport and light harvesting. The merger of such systems with graphene, transition-metal dichalcogenides, or conductive polymers could result in the invention of flexible, light-weight, and high-efficiency devices. In addition to material science, the biological and pharmaceutical possibilities of triphenylene derivatives are still mostly unexplored. Their flat aromatic cores and editable peripheries provide ways to create molecules that are bioactive and photoreactive for use in drug delivery, imaging, and photodynamic therapy.

6. Conclusions

Triphenylene derivatives represent an important class of polycyclic aromatic hydrocarbons that continue to gained considerable scientific attention owing to their rigid planar architecture and extensively delocalized π-conjugated system. These structural features impart remarkable thermal stability, high charge-carrier mobility, and the ability to form well-ordered self-assembled monolayers, establishing triphenylene-based systems as key building blocks in advanced organic materials. Their integration into OLEDs, OPVs, and OFETs has demonstrated their immense potential to enhance the efficiency and durability of next-generation electronic devices. The growing diversity of triphenylene derivatives, achieved through tailored functionalization and molecular engineering, has expanded their applicability across multiple disciplines, including nanotechnology, materials science, and pharmaceutical research. Progress in synthetic strategies—particularly the development of catalytic, photochemical, and green synthetic routes—has enabled the preparation of derivatives with fine-tuned electronic and optical properties suited for targeted applications. These advancements have positioned triphenylene-based materials as promising candidates for high-performance, sustainable, and versatile organic electronic systems. Beyond electronic applications, triphenylene and its derivatives have emerged as valuable components in nanostructured materials, catalysis, polymer science, and energy storage technologies. Their extended π-conjugation facilitates efficient charge transport and light absorption, characteristics essential for the advancement of next-generation solar energy conversion materials.

Conflicts of interest

Authors have no conflicts of interest to declare.

Data availability

No primary research results, software or code have been included and no new data were generated or analyzed as part of this review.

Acknowledgements

References

1 C. M. Buess and D. D. Lawson, *Chem. Rev.*, 1960, **60**, 313–330.

2 S. Banerjee and A. Guha, *Z. fur Krist.-Cryst. Mater.*, 1937, **96**, 107–110.

3 G. R. Desiraju and A. Gavezzotti, *Acta Crystallogr., Sect. B: Struct. Sci.*, 1989, **45**, 473–482.

4 K. P. Vijayalakshmi and C. H. Suresh, *New J. Chem.*, 2010, **34**, 2132–2138.

5 E. Clar and R. Schoental, *Polycyclic Hydrocarbons*, Springer, 1964.

6 M. Solà, *Front. Chem.*, 2013, **1**, 66422.

7 C. Tschierske, *J. Mater. Chem.*, 2001, **11**, 2647–2671.

8 S. Sergeyev, W. Pisula and Y. H. Geerts, *Chem. Soc. Rev.*, 2007, **36**, 1902–1929.

9 F. Ahmed and J. Trotter, *Acta Crystallogr.*, 1963, **16**, 503–508.

10 R. Wehlitz, T. Hartman and D. L. Huber, *J. Chem. Phys.*, 2021, **154**(4), 44304–44315.

11 J. W. Levell, A. Ruseckas, J. B. Henry, Y. Wang, A. D. Stretton, A. R. Mount, T. H. Galow and I. D. Samuel, *J. Phys. Chem. A*, 2010, **114**, 13291–13295.

12 A. Bayer, S. Zimmermann and J. Wendorff, *Mol. Cryst. Liq. Cryst.*, 2003, **396**, 1–22.

13 D. Markovitsi, I. Lécuyer, P. Lianos and J. Malthête, *J. Chem. Soc., Faraday Trans.*, 1991, **87**, 1785–1790.

14 S. Kumar, *Liq. Cryst.*, 2004, **31**, 1037–1059.

15 M. Gupta and S. K. Pal, *Langmuir*, 2016, **32**, 1120–1126.

16 A. Sugita, K. Suzuki and S. Tasaka, *Phys. Rev. B*, 2004, **69**, 212201.

17 J. De La Rie, M. Enache, Q. Wang, W. Lu, M. Kivala and M. Stöhr, *J. Phys. Chem. C*, 2022, **126**, 9855–9861.

18 M. Saleh, M. Baumgarten, A. Mavrinskiy, T. Schäfer and K. Müllen, *Macromolecules*, 2010, **43**, 137–143.

19 H. Kim, M. Park, S. Yang, D.-G. Kang, K.-U. Jeong and J.-H. Lee, *Liq. Cryst.*, 2015, **42**, 1779–1784.

20 S. Gonell, M. Poyatos and E. Peris, *Angew. Chem.*, 2013, **125**, 7147–7151.

21 V. Bhalla, H. Arora and M. Kumar, *Dalton Trans.*, 2013, **42**, 4450–4455.

22 W. Chen, H. Zhang, H. Zheng, H. Li, F. Guo, G. Ni, M. Ma, C. Shi, R. Ghadari and L. Hu, *Chem. Commun.*, 2020, **56**, 1879–1882.

23 Z. Yang, J. Luo, W. Zhang, J. Lei, C. Liu and Y. Li, *Org. Biomol. Chem.*, 2025, **23**, 323–327.

24 K. Dou, W. Zhao, C. Wang, Y. Fan, C. He, L. Zhang and S. Pang, *Chem. Eng. J.*, 2024, **501**, 157677.

25 X. Kong, H. Gong, P. Liu, W. Yao, Z. Liu, G. Wang, S. Zhang and Z. He, *New J. Chem.*, 2018, **42**, 3211–3221.

26 C. J. Lu, Q. Xu, J. Feng and R. R. Liu, *Angew. Chem., Int. Ed.*, 2023, **62**, e202216863.

27 D. Sonet and B. Bibal, *Tetrahedron Lett.*, 2019, **60**, 872–884.

28 Z. Qi, Z. An, B. Huang, M. Wu, Q. Wu and D. Jiang, *Org. Biomol. Chem.*, 2023, **21**, 6419–6423.

29 A. Mähringer, A. C. Jakowetz, J. M. Rotter, B. J. Bohn, J. K. Stolarczyk, J. Feldmann, T. Bein and D. D. Medina, *ACS Nano*, 2019, **13**, 6711–6719.

30 Y. Xue, Y. Li, F. Zhong, Z. Bai, P. Wang, K. Li, F. Lei, Z. He, Y. Yang and W. Feng, *Polym. Degrad. Stab.*, 2025, 111542.

31 A. Maczynski, M. Goral and B. Wisniewska-Goclowska, *IUPAC-NIST Solubility Data Series. 81. Hydrocarbons with Water and Seawater—Revised and Updated. Part 11. C13–C36 Hydrocarbons with Water*, 2006, vol. 35, p. 753.

32 Q. Ye, L. Li, J. Zhang, M. Teng, F. Wu and D. Han, *Appl. Organomet. Chem.*, 2025, **39**, e70374.

33 E. Wu, Y. Ma, Q. Tian, Z. Wang, Z. Song, S. Huo, F. Meng, Y. Xie and C. Pan, *ACS Nano*, 2025, **19**, 35701–35711.

34 Z. Chen, S. Zhang, Y. Zhao, Z. Wu, M. Chen, Y. Zeng, Z. Gao, Y. Wei, Z. Li and Z. Liang, *Laser Photonics Rev.*, 2025, **19**, 2401926.

35 J. A. Rego, S. Kumar and H. Ringsdorf, *Chem. Mater.*, 1996, **8**, 1402–1409.

36 S. K. Pal, S. Setia, B. Avinash and S. Kumar, *Liq. Cryst.*, 2013, **40**, 1769–1816.

37 N. Boden, R. J. Bushby, A. N. Cammidge and P. S. Martin, *J. Mater. Chem.*, 1995, **5**, 1857–1860.

38 G.-Y. Zhang, L.-L. Ma, E. Lin, Z.-Y. Wang, J.-T. Pan, J. Yang, M. Deng, Y. Wei, Y. Ye and N. Wang, *Nat. Commun.*, 2025, **16**, 9419.

39 S. Kumar and S. K. Varshney, *Mol. Cryst. Liq. Cryst.*, 2002, **378**, 59–64.

40 L. Zhang, C. Li and S. Pang, *Coord. Chem. Rev.*, 2026, **546**, 217081.

41 D. Pérez and E. Guitián, *Chem. Soc. Rev.*, 2004, **33**, 274–283.

42 H. C. Cheng, J. L. Ma, P. H. Guo and J. C. Shi, *Chem.–Asian J.*, 2025, **20**, e00809.

43 C. Mannich, *Ber. Dtsch. Chem. Ges.*, 1907, **40**, 153–158.

44 R. Freudenmann, B. Behnisch and M. Hanack, *J. Mater. Chem.*, 2001, **11**, 1618–1624.

45 R. J. Bushby and C. Hardy, *J. Chem. Soc., Perkin Trans. 1*, 1986, 721–723.

46 J. W. Goodby, M. Hird, K. J. Toyne and T. Watson, *J. Chem. Soc. Chem. Commun.*, 1994, 1701–1702.

47 M. Müller, J. Petersen, R. Strohmaier, C. Günther, N. Karl and K. Müllen, *Angew Chem. Int. Ed. Engl.*, 1996, **35**, 886–888.

48 N. Boden, R. J. Bushby and A. N. Cammidge, *J. Am. Chem. Soc.*, 1995, **117**, 924–927.

49 H. Naarmann, M. Hanack and R. Mattmer, *Synthesis*, 1994, 477–478.

50 S. R. Waldvogel, A. R. Wartini, P. H. Rasmussen and J. Rebek Jr, *Tetrahedron Lett.*, 1999, **40**, 3515–3518.

51 L. Zhai, R. Shukla, S. H. Wadumethrige and R. Rathore, *J. Org. Chem.*, 2010, **75**, 4748–4760.

52 S. M. Alhunayhin, R. J. Bushby, A. N. Cammidge and S. S. Samman, *Liq. Cryst.*, 2024, **51**, 1333–1344.

53 V. Bhalla, H. Singh and M. Kumar, *Org. Lett.*, 2010, **12**, 628–631.

54 V. Gupta, S. K. Pandey and R. P. Singh, *Org. Biomol. Chem.*, 2018, **16**, 7134–7138.

55 Z. Li, M. Powers, K. Ivey, S. Adas, B. Ellman, S. D. Bunge and R. J. Twieg, *Mater. Adv.*, 2022, **3**, 534–546.

56 Y. Zhang, S. H. Pun and Q. Miao, *Chem. Rev.*, 2022, **122**, 14554–14593.

57 M. Grzybowski, K. Skonieczny, H. Butenschön and D. T. Gryko, *Angew. Chem., Int. Ed.*, 2013, **52**, 9900–9930.

58 M. J. Rahman, J. Yamakawa, A. Matsumoto, H. Enozawa, T. Nishinaga, K. Kamada and M. Iyoda, *J. Org. Chem.*, 2008, **73**, 5542–5548.

59 Z. Sun, Z. Zeng and J. Wu, *Chem.–Asian J.*, 2013, **8**, 2894–2904.

60 M. A. Alsharif, Q. A. Raja, N. A. Majeed, R. S. Jassas, A. A. Alsimaree, A. Sadiq, N. Naeem, E. U. Mughal, R. I. Alsantali and Z. Moussa, *RSC Adv.*, 2021, **11**, 29826–29858.

61 R. S. Jassas, E. U. Mughal, A. Sadiq, R. I. Alsantali, M. M. Al-Rooqi, N. Naeem, Z. Moussa and S. A. Ahmed, *RSC Adv.*, 2021, **11**, 32158–32202.

62 M. K. Smith, N. E. Powers-Riggs and B. H. Northrop, *RSC Adv.*, 2014, **4**, 38281–38292.

63 F. B. Mallory, C. S. Wood and J. T. Gordon, *J. Am. Chem. Soc.*, 1964, **86**, 3094–3102.

64 T. Sato, S. Shimada and K. Hata, *Bull. Chem. Soc. Jpn.*, 1971, **44**, 2484–2490.

65 M. Daigle, A. Picard-Lafond, E. Soligo and J. F. Morin, *Angew. Chem.*, 2016, **128**, 2082–2087.

66 M. M. Zhou, J. He, H. M. Pan, Q. Zeng, H. Lin, K. Q. Zhao, P. Hu, B. Q. Wang and B. Donnio, *Chem.–Eur. J.*, 2023, **29**, e202301829.

67 S. Plaize and J.-F. Morin, *RSC Adv.*, 2024, **14**, 35227–35231.

68 K.-Q. Zhao, J.-Q. Du, X.-H. Long, M. Jing, B.-Q. Wang, P. Hu, H. Monobe, B. Henrich and B. Donnio, *Dyes Pigm.*, 2017, **143**, 252–260.

69 S. Pan, H. Jiang, Y. Zhang, D. Chen and Y. Zhang, *Org. Lett.*, 2016, **18**, 5192–5195.

70 Z. Liu, X. Zhang and R. C. Larock, *J. Am. Chem. Soc.*, 2005, **127**, 15716–15717.

71 M. Iwasaki, Y. Araki, S. Iino and Y. Nishihara, *J. Org. Chem.*, 2015, **80**, 9247–9263.

72 J. A. García-López and M. F. Greaney, Synthesis of biaryls using aryne intermediates, *Chem. Soc. Rev.*, 2016, **45**(24), 6766–6798.

73 B. P. Mathew, H. J. Yang, J. Kim, J. B. Lee, Y. T. Kim, S. Lee, C. Y. Lee, W. Choe, K. Myung and J. U. Park, *Angew. Chem., Int. Ed.*, 2017, **56**, 5007–5011.

74 D. Peña, S. Escudero, D. Pérez, E. Guitián and L. Castedo, *Angew. Chem., Int. Ed.*, 1998, **37**, 2659–2661.

75 J. B. Lee, M. H. Jeon, J. K. Seo, G. von Helden, J.-U. Rohde, B. S. Zhao, J. Seo and S. Y. Hong, *Org. Lett.*, 2019, **21**, 7004–7008.

76 Y. Yang, B. Zhou, X. Zhu, G. Deng, Y. Liang and Y. Yang, *Org. Lett.*, 2018, **20**, 5402–5405.

77 J. Tu, G. Li, X. Zhao and F. Xu, *Tetrahedron Lett.*, 2019, **60**, 44–47.

78 Y. Wu, W. Zhang, Q. Peng, C.-K. Ran, B.-Q. Wang, P. Hu, K.-Q. Zhao, C. Feng and S.-K. Xiang, *Org. Lett.*, 2018, **20**, 2278–2281.

79 C.-M. Qin, C.-Y. Zeng, W.-H. Yu, P. Hu, B.-Q. Wang, K.-Q. Zhao and B. Donnio, *Cryst. Growth Des.*, 2025, **25**, 9524–9535.

80 H.-M. Pan, J. He, W.-H. Yu, P. Hu, B.-Q. Wang, K.-Q. Zhao and B. Donnio, *J. Mater. Chem. C*, 2023, **11**, 14695–14704.

81 K. L. Zhang, W. H. Yu, K. Q. Zhao, P. Hu, B. Q. Wang and B. Donnio, *Chem.–Asian J.*, 2024, **19**, e202301080.

82 R. E. Yardley, J. A. Paquette, H. Taing, H. M. Gaebler, S. H. Eichhorn, I. P. Hamilton and K. E. Maly, *Org. Lett.*, 2019, **21**, 10102–10105.

83 J. Moursounidis and D. Wege, *Aust. J. Chem.*, 1988, **41**, 235–249.

84 E. Fischer, J. Larsen, J. B. Christensen, M. Fourmigué, H. G. Madsen and N. Harrit, *J. Org. Chem.*, 1996, **61**, 6997–7005.

85 K. B. Sukumaran and R. G. Harvey, *J. Org. Chem.*, 1981, **46**, 2740–2745.

86 C. Romero, D. Pena, D. Perez and E. Guitian, *J. Org. Chem.*, 2008, **73**, 7996–8000.

87 K. Fuchibe, M. Abe, H. Idate and J. Ichikawa, *Chem.–Asian J.*, 2020, **15**, 1384–1392.

88 D. Rodriguez-Lojo, D. Perez, D. Pena and E. Guitian, *Chem. Commun.*, 2013, **49**, 6274–6276.

89 M. G. Schwab, T. Qin, W. Pisula, A. Mavrinskiy, X. Feng, M. Baumgarten, H. Kim, F. Laquai, S. Schuh and R. Trattnig, *Chem.–Asian J.*, 2011, **6**, 3001–3010.

90 J. M. Alonso, A. E. Díaz-Álvarez, A. Criado, D. Pérez, D. Peña and E. Guitián, *Angew. Chem.*, 2011, **1**, 177–181.

91 R. C. Borner, N. Boden, R. J. Bushby, R. Borner, A. N. Cammidge, R. Bushby, A. Cammidge and M. Jesudason, *Liq. Cryst.*, 2006, **33**, 1439–1448.

92 Z.-h. Zhou and T. Yamamoto, *J. Organomet. Chem.*, 1991, **414**, 119–127.

93 H. Shirai, N. Amano, Y. Hashimoto, E. Fukui, Y. Ishii and M. Ogawa, *J. Org. Chem.*, 1991, **56**, 2253–2256.

94 Y. Wang, A. D. Stretton, M. C. McConnell, P. A. Wood, S. Parsons, J. B. Henry, A. R. Mount and T. H. Galow, *J. Am. Chem. Soc.*, 2007, **129**, 13193–13200.

95 Z. W. Schroeder, J. LeDrew, V. M. Selmani and K. E. Maly, *RSC Adv.*, 2021, **11**, 39564–39569.

96 E. C. Rüdiger, F. Rominger, L. Steuer and U. H. Bunz, *J. Org. Chem.*, 2016, **81**, 193–196.

97 E. J. Foster, R. B. Jones, C. Lavigueur and V. E. Williams, *J. Am. Chem. Soc.*, 2006, **128**, 8569–8574.

98 S. R. Waldvogel and D. Mirk, *Tetrahedron Lett.*, 2000, **41**, 4769–4772.

99 C. Regenbrecht and S. R. Waldvogel, *Beilstein J. Org. Chem.*, 2012, **8**, 1721–1724.

100 J. Yin, H. Qu, K. Zhang, J. Luo, X. Zhang, C. Chi and J. Wu, *Org. Lett.*, 2009, **11**, 3028–3031.

101 T. Osawa, T. Kajitani, D. Hashizume, H. Ohsumi, S. Sasaki, M. Takata, Y. Koizumi, A. Saeki, S. Seki and T. Fukushima, *Angew. Chem., Int. Ed.*, 2012, **51**, 7990–7993.

102 J. He, Y. Chen, P. Hu, B.-Q. Wang, K.-Q. Zhao and B. Donnio, *J. Mol. Liq.*, 2024, **414**, 126218.

103 Y. Chen, J. He, H. Lin, H.-F. Wang, P. Hu, B.-Q. Wang, K.-Q. Zhao and B. Donnio, *Beilstein J. Org. Chem.*, 2024, **20**, 3263–3273.

104 T. Wöhrle, I. Wurzbach, J. Kirres, A. Kostidou, N. Kapernaum, J. Litterscheidt, J. C. Haenle, P. Staffeld, A. Baro and F. Giesselmann, *Chem. Rev.*, 2016, **116**, 1139–1241.

105 M. A. Alam, J. Motoyanagi, Y. Yamamoto, T. Fukushima, J. Kim, K. Kato, M. Takata, A. Saeki, S. Seki and S. Tagawa, *J. Am. Chem. Soc.*, 2009, **131**, 17722–17723.

106 Z. Ke-Qing, W. Bi-Qin, H. Ping, L. Quan and Z. Liang-Fu, *Chin. J. Chem.*, 2005, **23**, 767–774.

107 H.-M. Chen, K.-Q. Zhao, L. Wang, P. Hu and B.-Q. Wang, *Soft Mater.*, 2011, **9**, 359–381.

108 P. Guragain, M. Powers, B. Ellman and R. J. Twieg, *Mater. Adv.*, 2024, **5**, 9032–9040.

109 T.-R. Zhang, Y.-P. Fan, W.-H. Yu, Q.-G. Li, Y. Shi, S.-K. Xiang, K.-Q. Zhao, B.-Q. Wang and C. Feng, *J. Mol. Liq.*, 2024, **408**, 125399.

110 S. K. Varshney, *Liq. Cryst.*, 2013, **40**, 1477–1486.

111 I. Paraschiv, M. Giesbers, B. van Lagen, F. C. Grozema, R. D. Abellon, L. D. Siebbeles, A. T. Marcelis, H. Zuilhof and E. J. Sudhölter, *Chem. Mater.*, 2006, **18**, 968–974.

112 A. El Mansoury, R. J. Bushby and N. Karodia, *Liq. Cryst.*, 2012, **39**, 1222–1230.

113 L. Tao, Y. Xie, K.-X. Zhao, P. Hu, B.-Q. Wang, K.-Q. Zhao and X.-Y. Bai, *New J. Chem.*, 2024, **48**, 12006–12014.

114 F. Yang, J. Xie, H. Guo, B. Xu and C. Li, *Liq. Cryst.*, 2012, **39**, 1368–1374.

115 K. Zhang, Y. Bai, C. Feng, G. Ning, H. Ni, W. Yu, K. Zhao, B. Wang and P. Hu, *New J. Chem.*, 2018, **42**, 272–280.

116 K.-Q. Zhao, X.-Y. Bai, X. Xiao, Y. Gao, P. Hu, B.-Q. Wang, Q.-D. Zeng, C. Wang, B. Heinrich and B. Donnio, *J. Mater. Chem. C*, 2015, **3**, 11735–11746.

117 J. Bi, H. Wu, Z. Zhang, A. Zhang, H. Yang, Y. Feng, Y. Fang, L. Zhang, Z. Wang and W. Qu, *J. Mater. Chem. C*, 2019, **7**, 12463–12469.

118 H. Lin, K.-X. Zhao, M. Jing, X.-H. Long, K.-Q. Zhao, P. Hu, B.-Q. Wang, P. Lei, Q.-D. Zeng and B. Donnio, *J. Mater. Chem. C*, 2022, **10**, 14453–14470.

119 H. Gopee, X. Kong, Z. He, I. Chambrier, D. L. Hughes, G. J. Tizzard, S. J. Coles and A. N. Cammidge, *J. Org. Chem.*, 2013, **78**, 9505–9511.

120 S. Chen, F. S. Raad, M. Ahmida, B. R. Kaafarani and S. H. Eichhorn, *Org. Lett.*, 2013, **15**, 558–561.

121 P. Staffeld, M. Kaller, P. Ehni, M. Ebert, S. Laschat and F. Giesselmann, *Crystals*, 2019, **9**, 74.

122 J. Kirres, F. Knecht, P. Seubert, A. Baro and S. Laschat, *ChemPhysChem*, 2016, **17**, 1159–1165.

123 J. F. Hang, H. Lin, K. Q. Zhao, P. Hu, B. Q. Wang, H. Monobe, C. Zhu and B. Donnio, *Eur. J. Org Chem.*, 2021, **2021**, 1989–2002.

124 W.-J. Deng, S. Liu, H. Lin, K.-X. Zhao, X.-Y. Bai, K.-Q. Zhao, P. Hu, B.-Q. Wang, H. Monobe and B. Donnio, *New J. Chem.*, 2022, **46**, 7936–7949.

125 Q. Zeng, S. Liu, H. Lin, K.-X. Zhao, X.-Y. Bai, K.-Q. Zhao, P. Hu, B.-Q. Wang and B. Donnio, *Molecules*, 2023, **28**, 1721.

126 A. O. Alsahli and A. N. Cammidge, *Eur. J. Org Chem.*, 2022, **2022**, e202200990.

127 Z. Chongyang, H. Ping, W. Biqin, F. Wenyan, Z. Keqing, D. Bertrand and B. Donnio, *Acta Chim. Sin.*, 2023, **81**, 469.

128 H. Lin, K.-X. Zhao, B.-Q. Wang, P. Hu, K.-Q. Zhao and B. Donnio, *Giant*, 2025, 100362.

129 X. Wu, H. Lin, X.-Y. Bai, P. Hu, B.-Q. Wang, K.-Q. Zhao and B. Donnio, *J. Mater. Chem. C*, 2025, **13**, 7678–7685.

130 T. Lorenzetto, G. Berton, F. Castellini, G. Casson, A. Scarso and F. Fabris, *Chem.–Eur. J.*, 2024, **30**, e202402348.

131 Y. Li, Y.-X. Wang, X.-K. Ren and L. Chen, *Mater. Chem. Front.*, 2017, **1**, 2599–2605.

132 V. Percec, M. R. Imam, M. Peterca, D. A. Wilson, R. Graf, H. W. Spiess, V. S. Balagurusamy and P. A. Heiney, *J. Am. Chem. Soc.*, 2009, **131**, 7662–7677.

133 V. Conejo-Rodríguez, B. Donnio, B. Heinrich, R. Termine, A. Golemme and P. Espinet, *J. Mater. Chem. C*, 2023, **11**, 1435–1447.

134 E. de Domingo, C. L. Folcia, J. Ortega, J. Etxebarria, R. Termine, A. Golemme, S. Coco and P. Espinet, *Inorg. Chem.*, 2020, **59**, 10482–10491.

135 S. Cobos, G. García, C. L. Folcia, J. Ortega, J. Etxebarria, G. López-Peña, D. H. Ortgies, E. M. Rodriguez and S. Coco, *J. Mater. Chem. C*, 2024, **12**, 12332–12340.

136 S. Chen, H. Taing, M. Ahmida, H. Y. He, A. Carr, H. M. Muchall and S. H. Eichhorn, *Soft Matter*, 2024, **20**, 7854–7864.

137 S. Ibáñez, M. Poyatos and E. Peris, *Chem. Commun.*, 2017, **53**, 3733–3736.

138 Y. Fan, J. Wang, Z. Zhang, X. Ma and M. Zhao, *ACS Appl. Nano Mater.*, 2023, **6**, 13037–13047.

139 S. Qi, Y. Fan, W. Li and M. Zhao, *Phys. Chem. Chem. Phys.*, 2020, **22**, 20061–20068.

140 K. Yu, J. Zhang, Y. Hu, L. Wang, X. Zhang and B. Zhao, *Catalysts*, 2024, **14**, 184.

141 R. Matsuoka, R. Toyoda, R. Shiotsuki, N. Fukui, K. Wada, H. Maeda, R. Sakamoto, S. Sasaki, H. Masunaga and K. Nagashio, *ACS Appl. Mater. Interfaces*, 2018, **11**, 2730–2733.

142 E. Peris, *Chem. Commun.*, 2016, **52**, 5777–5787.

143 S. Gonell, R. G. Alabau, M. Poyatos and E. Peris, *Chem. Commun.*, 2013, **49**, 7126–7128.

144 T. Mandal, T. K. Dutta, S. Mohanty and J. Choudhury, *Chem. Commun.*, 2021, **57**, 10182–10185.

145 S. Gonell, M. Poyatos and E. Peris, *Chem.–Eur. J.*, 2014, **20**, 5746–5751.

146 K. E. Shelar, N. Le, K. M. Mukeba, S. Dey, B. Farajidizaji, S. Athukorale, C. U. Pittman, C. E. Webster, B. Donnadieu and E. Caldona, *Mater. Chem. Front.*, 2022, **6**, 1391–1404.

147 M. Saleh, Y. S. Park, M. Baumgarten, J. J. Kim and K. Müllen, *Macromol. Rapid Commun.*, 2009, **30**, 1279–1283.

148 Y. Wang, M. Zhu, J. Deng, G. Xie and E. Baranoff, *New J. Chem.*, 2017, **41**, 1773–1780.

149 I. Bala, W.-Y. Yang, S. P. Gupta, J. De, R. A. K. Yadav, D. P. Singh, D. K. Dubey, J.-H. Jou, R. Douali and S. K. Pal, *J. Mater. Chem. C*, 2019, **7**, 5724–5738.

150 J.-Y. Park, J. M. Kim, H. Lee, K.-Y. Ko, K. S. Yook, J. Y. Lee and Y. G. Baek, *Thin Solid Films*, 2011, **519**, 5917–5923.

151 S. Kumar, D. Kumar, Y. Patil and S. Patil, *J. Mater. Chem. C*, 2016, **4**, 193–200.

152 S. N. Park, H. W. Lee, Y. S. Kim, J. Kim, S. E. Lee, H. W. Lee, Y. K. Kim and S. S. Yoon, *Synth. Met.*, 2015, **206**, 124–130.

153 V. Bhalla, H. Arora, H. Singh and M. Kumar, *Dalton Trans.*, 2013, **42**, 969–974.

154 N. Contreras-Pereda, S. Pané, J. Puigmartí-Luis and D. Ruiz-Molina, *Coord. Chem. Rev.*, 2022, **460**, 214459.

155 V. Bhalla, H. Singh, H. Arora and M. Kumar, *Sens. Actuators, B*, 2012, **171**, 1007–1012.

156 V. Bhalla, H. Singh and M. Kumar, *Dalton Trans.*, 2012, **41**, 11413–11418.

157 S. Kandel, V. Sathish, L. Mathivathanan, A. N. Morozov, A. M. Mebel and R. G. Raptis, *New J. Chem.*, 2019, **43**, 7251–7258.

158 H. Arora, V. Bhalla and M. Kumar, *RSC Adv.*, 2015, **5**, 32637–32642.

159 S.-Y. Ding and W. Wang, *Chem. Soc. Rev.*, 2013, **42**, 548–568.

160 D. Sonet and B. Bibal, Triphenylene: A versatile molecular receptor, *Tetrahedron Lett.*, 2019, **60**(12), 872–884.

161 A. P. Cote, A. I. Benin, N. W. Ockwig, M. O'Keeffe, A. J. Matzger and O. M. Yaghi, *science*, 2005, **310**, 1166–1170.

162 M. Dogru, M. Handloser, F. Auras, T. Kunz, D. Medina, A. Hartschuh, P. Knochel and T. Bein, *Angew. Chem. Int. Ed*, 2013, **52**, 2920–2924.

163 F. Haase and B. V. Lotsch, *Chem. Soc. Rev.*, 2020, **49**, 8469–8500.

164 S. Wan, J. Guo, J. Kim, H. Ihee and D. Jiang, *Angew. Chem. Int. Ed*, 2008, **47**, 8826–8830.

165 A. K. Mandal, J. Mahmood and J. B. Baek, *ChemNanoMat*, 2017, **3**, 373–391.

166 C. Du, W. Na, M. Shao, S. Shang, Y. Liu and J. Chen, *Chem. Mater.*, 2023, **35**, 1395–1403.

167 K. Wang, Z. Zhang, L. Lin, K. Hao, J. Chen, H. Tian and X. Chen, *ACS Appl. Mater. Interfaces*, 2019, **11**, 39503–39512.

168 K. Wang, Z. Zhang, L. Lin, J. Chen, K. Hao, H. Tian and X. Chen, *Chem. Mater.*, 2019, **31**, 3313–3323.

169 X. Ding, L. Chen, Y. Honsho, X. Feng, O. Saengsawang, J. Guo, A. Saeki, S. Seki, S. Irle and S. Nagase, *J. Am. Chem. Soc.*, 2011, **133**, 14510–14513.

170 M. Calik, F. Auras, L. M. Salonen, K. Bader, I. Grill, M. Handloser, D. D. Medina, M. Dogru, F. Löbermann and D. Trauner, *J. Am. Chem. Soc.*, 2014, **136**, 17802–17807.

171 K. Ashwini Kumar, K. L. Reddy, S. Vidhisha and S. Satyanarayana, *Appl. Organomet. Chem.*, 2009, **23**, 409–420.

172 C. Du, W. Na, M. Shao, S. Shang, Y. Liu and J. Chen, Self-templated synthesis of triphenylene-based uniform hollow spherical two-dimensional covalent organic frameworks for drug delivery, *Chem. Mater.*, 2023, **35**(3), 1395–1403.

173 H. Srinivasa and S. Hariprasad, *ChemistrySelect*, 2022, **7**, e202200783.

174 A. Ané, G. Prestat, G. Manh, M. Thiam, S. Josse, M. Pipelier, J. Lebreton, J. Pradère and D. Dubreuil, *Pure Appl. Chem.*, 2001, **73**, 1189–1196.

175 M. Montembault, G. Vo-Thanh, A. Deyine, V. Fargeas, M. Villiéras, A. Adjou, D. Dubreuil, D. Esquieu, C. Grégoire and S. Opi, *Bioorg. Med. Chem. Lett.*, 2004, **14**, 1543–1546.

176 K. P. Naidek, C. R. Zuconelli, O. M. Cruz, R. Ribeiro, S. M. Winnischofer and H. Winnischofer, *Biochem. Cell Biol.*, 2016, **94**, 205–211.

177 A. Das, N. L. Banik and S. K. Ray, *Cancer*, 2010, **116**, 164–176.

178 O. Hayashida, T. Matsuo, K. Nakamura and S. Kusano, *J. Org. Chem.*, 2016, **81**, 4196–4201.

179 C. Givelet and B. Bibal, *Org. Biomol. Chem.*, 2011, **9**, 7457–7460.

180 I. López-Tocón, J. C. Otero, J. F. Arenas, J. V. García-Ramos and S. Sánchez-Cortés, *Langmuir*, 2010, **26**, 6977–6981.

181 S. Kumar, S. K. Pal, P. S. Kumar and V. Lakshminarayanan, *Soft Matter*, 2007, **3**, 896–900.

182 Z. Shen, M. Yamada and M. Miyake, *J. Am. Chem. Soc.*, 2007, **129**, 14271–14280.

183 H. O. Lintang, M. A. Jalani, L. Yuliati and M. M. Salleh, Fabrication of mesoporous silica/alumina hybrid membrane film nanocomposites using template sol-gel synthesis of amphiphilic triphenylene, *IOP Conf. Ser.: Mater. Sci. Eng.*, 2017, **202**(1), 012003.

184 Y. Wang, L. Liu, Y. Shi, S. Li, F. Sun, Q. Lu, Y. Shen, S. Feng and S. Qin, *ACS Appl. Mater. Interfaces*, 2023, **15**, 18236–18243.

185 C. Kavitha, B. Avinash, S. Kumar and V. Lakshminarayanan, *Mater. Chem. Phys.*, 2012, **133**, 635–641.

186 H. Zhang, J. Cheng, Q. Zhou, Q. Zhang and G. Zou, *Soft Matter*, 2020, **16**, 5203–5209.

187 S. Kumar and H. K. Bisoyi, *Angew. Chem., Int. Ed. Engl.*, 2007, **46**, 1501.